University of Alberta

Oxidative Denitrogenation of Coal Liquids

by

Sepideh Mirshamsi

A thesis submitted to the Faculty of Graduate Studies and Research
in partial fulfillment of the requirements for the degree of

Master of Science
in
Chemical Engineering

Chemical and Materials Engineering Department

Abstract

The oxidative denitrogenation of quinoline (as a model compound representing the nitrogen containing structure of coal liquids) has been investigated in two steps: oxidation by perdecanoic acid at 50 ℃ to produce quinoline N-oxide in order to weaken the nitrogen-carbon bond; thermal decomposition of quinoline N-oxide to remove nitrogen as its respective oxides. Quinoline is successfully converted to quinoline N-oxide in the oxidation step. Thermal decomposition of quinoline N-oxide at 400 ℃ and 600 kPa of N_2 produces 52-wt% quinoline, 22-wt% a condensed polymeric compound and 26-wt% gaseous mixture of CO_2, CO and O_2. Almost all the nitrogen content of quinoline N-oxide has remained in the residue of decomposition reaction. This confirms that thermal decomposition not only fails to remove nitrogen from structure of the oxidized molecule, but it also leads to production of a more complex aromatic structure with 10.4-wt% nitrogen content, compared to 10.6-wt% nitrogen content of quinoline.

Acknowledgement

I would like to express the deepest appreciation to my principal supervisor, Dr. Arno de Klerk, whom without his guidance and persistent help this thesis would not have been possible.

Additionally, I would like to thank my second supervisor, Dr. Rajender Gupta, for his kind support and contributions to this project.

I am most grateful to Dr. Moshfiqur Rahman for his good advice and help on both academic and personal level. Many thanks go to all the other colleagues who helped me in many ways.

This work is enabled by the generous support of Sherritt Technologies. I particularly thank Ray Abbaslou, Ali Abbaspour and Iftikhar Huq for their advice during development of this project.

I also would like to acknowledge the support of administrative staff of Chemical & Materials Engineering Department at University of Alberta, especially, beautiful Lily Laser for her kindness and endless help. I also appreciate the support of Financial Aid Office at University of Alberta.

Last, but by no means least, I would like to thank my family and friends. Above all, endless gratitude and love to my dearest family, Mahnaz, Sahar, Peyman and my forever role model in life, Rouhallah. Many thanks go to my friends, Arvind, Azadeh and Morvarid for being there for me during the good times and hard times.

Table of Contents

Chapter 3: Oxidation of Quinoline by Perdecanoic Acid

Chapter 4: Thermal Behavior of Quinoline N-oxide Hydrate

Chapter 5: Thermodynamic Study

Chapter 6: Conclusion and Future Work

List of Tables   Page

List of Figures   Pages

Chapter 1

Introduction

1- Background and project proposal

Coal contains some heteroatoms, such as N, O and S and their amount depends on the coal rank. Nitrogen content of coal is usually less than 1.5-wt% and it is mostly available in organic forms [1]. The amount of sulfur usually varies from 1.0-wt% to 4.0-wt% and it exists in both organic and inorganic forms. The ratio of inorganic to organic sulfur is typically around 2:1[2].

Coal combustion is widely used for power and heat generation. Due to the presence of heteroatoms in coal, its combustion produces SOx, NOx and particulate matter that are emitted to the atmosphere causing environmental problems such as acid rain and ground level ozone (smog). Furthermore, in the presence of sunlight, NOx reacts with reactive VOCs to form photochemical oxidants [3]. The emitted gases will eventually fall in the ocean/ground with precipitation. Over geological time, they enter into the landmass, fossil fuels and minerals that humans extract and use [4]. During coal liquefaction, most of the nitrogen [1] and some sulfur containing compounds [5] remain in the liquid products, causing the same environmental issues when using coal liquids. The inhibition of catalyst activity during processing of coal-derived products (like coal liquids) is another problem associated with the high content of heteroatoms in coal. The basic nitrogen compounds can inhibit the activity of acidic catalysts during coal liquids refining [6]. Therefore, some regulations are established worldwide on the permissible amount of heteroatoms in coal and a number

of investigations are directed toward finding effective heteroatom removal methods in clean coal technology.

The following methods can be used to control the emission of SOx and NOx gases [7]:

- Limiting coal usage only to the coals with low heteroatom content
- Heteroatom removal by pre-treatment of coal or coal-derived products
- Heteroatom retention during usage of coal or coal-derived products
- SOx and NOx removal by flue gas treatment

The coal mines containing low amounts of heteroatoms are limited and restricted to specific locations. The sulfur retention methods are currently being developed. Flue gas treatment is currently the most widely adopted method to control sulfur emissions. But the necessity of using two or three flue gas scrubbers in series increases the equipment cost of establishing a coal-fired power station [7].

The remaining option is the pre-treatment methods. Physical cleaning techniques are able to remove mineral matter and 30-90% of pyritic sulfur associated to mineral compounds in coal. But it is possible to lose as much as 60% of coal during the process. Moreover, about 50 % of sulfur might be connected to the organic structure of coal and therefore, not removable by physical methods. Since both organic sulfur and nitrogen compounds are chemically bonded to the coal matrix, chemical methods must be used to selectively destroy the carbon-heteroatom bonds of organic compounds to eliminate the heteroatoms from the coal [7].

In all the chemical coal cleaning methods, the following important criteria must be considered [8]:

1. The reagent for heteroatom removal must selectively react either with organic sulfur compounds, pyritic content of coal or nitrogen compounds (or all of them), which means it must not significantly affect other coal components.

2. In order to reduce process cost, the reagent should be regenerable.

3. In both the reacted and unreacted forms, the reagent must be either volatile or soluble so that it can be recovered from the other components.

4. Since a portion of the reagent will be lost, by irreversible sorption or consumption in other ways, it must be inexpensive.

5. From a pollution control standpoint, the whole heteroatom removal process should not result in a new pollution problem.

Oxidative heteroatom removal is one of the suggested chemical cleaning methods that can remove heteroatoms to some extent and it also benefits from low reaction temperature, low reaction pressure and no hydrogen requirement. In this method, the heteroatom in organic structure transforms to its oxidized form so that the polarity of compound increases to facilitate selective extraction or absorption. Also, it is known that the valence shell of a heteroatom is expanded by oxidation and as a result, the bonding between carbon and heteroatom is weakened. For example, in the oxidation of aliphatic sulfides to sulphones, the C-S bond energy is reduced by 5.2 kcal/mole while the amount of the reduction is 11.8 kcal/mole for aromatic sulfides and thiophenes. Thus, the cleavage of carbon-heteroatom bond may become easier [9]. Therefore, the heteroatom removal methods (such as thermal decomposition, solvent extraction, etc.) are more effective on the partially oxidized heteroatom structures compared to their primary forms. In this research, thermal decomposition is used as the denitrogenation method for the partially oxidized nitrogen compounds. The N-oxide compound is exposed to a thermal zone to study the possibility of nitrogen removal as its respective oxides during thermal decomposition of the nitrogen compound.

In oxidative heteroatom removal, the reagent used is inexpensive, it is in the gas phase in both reacted and non-reacted forms and it does not result in any new air pollution problem. However, using this method, the heteroatom structure still transforms to the environmentally harmful oxide form. But it is much easier to capture these produced gases in a large-scale pre-treatment plant than it is to distribute a high heteroatom containing coal (or coal-derived products) to a wide range of smaller-scale consumer plants and then, trying to treat the produced flu gas.

In terms of selectively removing the heteroatom structure, it is highly possible that oxidative methods also oxidize some parts of carbon structure along with heteroatoms present in coal. Therefore, it is necessary to study the degree of heating value loss caused by oxidation and also, to optimize the oxidation method to be more selective towards heteroatom removal.

Nitrogen is the least studied element in coal cleaning and consequently, there is a little literature available on oxidative denitrogenation (ODN) methods, while more research is done on oxidative desulfurization (ODS) technology. This work provides a study on oxidative nitrogen removal of model nitrogen compounds available in coal liquids (coal liquefaction products). It must be noted that:

1-   This study is mostly a fundamental research on the nature of reactions happening and the possibility of nitrogen removal with use of oxidizing agents. So no attempt is made to improve the rate of reactions, the degree of denitrogenation or the selectivity towards nitrogen removal.
2-   No work is done on actual coal liquid mixtures. The compounds studied are the model nitrogen compounds present in the structure of coal and coal liquids.

Although there is not enough literature available on oxidative nitrogen removal techniques, some studies are done on oxidation of heterocyclic

nitrogen containing compounds to produce N-oxide compounds that can be useful in investigating the oxidation step. The literature will be reviewed in the chapter 2. This chapter also presents a background on coal composition, coal liquefaction process and work done on oxidative desulfurization of coal. Chapter 3 presents the experimental procedure, results, discussions and conclusions for oxidation of quinoline as a model nitrogen compound present in coal liquids. Chapter 4 studies the thermal behavior of commercially available quinoline N-oxide hydrate. Chapter 5 discusses the general conclusion of all work performed and also, presents the possible pathways for future work.

2- References

[1] Davidson, R. M. *Nitrogen in coal*; IEA Coal Research: London, 1994; pp 3-6.

[2] Attar, A.; Corcoran, W. H. Sulfur Compounds in Coal, *Industrial & Engineering Chemistry Product Research and Development* **1977**, *16*, 168–170.

[3] Cooper, C. D.; Alley F. C. *Air Pollution Control- A Design Approach,* 3rd ed.; Waveland Press Inc.: Illinois, 2002; pp 2-3 & 51-52.

[4] Nevers, N. D. *Air Pollution Control Engineering*, 2nd ed.; McGraw-Hill higher Education: Boston, 2000; pp 397-398.

[5] Winans, R. E.; Joseph, J. T.; Fisher, R. B. Changes in Organic Sulfur Compounds in Coal Macerals during Liquefaction, *ACS Division of Fuel Chemistry Preprints* **1994**, *39 (2)*, 434-437.

[6] de Klerk, A. *Refining and Refineries at a Glance,* in *Fischer-Tropsch Refining* [Online]; Wiley-VCH Verlag GmbH & Co: Germany, 2011; pp 25. http://onlinelibrary.wiley.com/doi/10.1002/9783527635603.ch2/summary (accessed May 2013)

[7] *Reviews in Coal Science: The Problems of Sulfur*; IEA Coal Research: London, 1989; pp 3.

[8] Meyers, R.A. *Coal Desulfurization*; Marcel Dekker Inc.: New York, 1977; pp 55.

[9] Borah D.; Baruah M. I. Oxidation of High Sulphur Coal. 3. Desulfurization of Organic Sulphur by Peroxyacetic Acid (Produced in situ) in Presence of Metal Ions, *Fuel Processing Technology* **2005**, *86*, 959-976.

Chapter 2

Literature Review

1- Introduction

Necessity of heteroatom removal from the structure of coal and coal-derived products, the possible approaches to this problem and the advantage of chemical cleaning methods are explained in the previous chapter. Chemical cleaning processes are promising sulfur removal methods by which almost all the inorganic sulfur can be eliminated from coal. However, organic sulfur removal is achieved only to some extent by chemical desulfurization methods. Complex reaction networks and uncharacterized structure of these compounds are the main reasons behind the failure of complete organic sulfur removal [1]. The same reason stands for the removal of nitrogen compounds, which are mostly bonded to the organic structure of coal. Solvent partition, thermal decomposition, acid-base neutralization, reduction, oxidation and nucleophilic displacement are suggested methods for removal of the organic sulfur from the coal matrix. Oxidation and displacement reactions form the major current studies on coal desulfurization [2].

This chapter is a review on the oxidation methods studied to remove the organic heteroatoms present in coal and coal liquids. To study heteroatom removal from coal liquids, it is essential to truly understand the composition and properties of coal, the chemistry of liquefaction process, the structure of heteroatom compounds existing in coal and the change in the structure of heteroatom compounds during liquefaction. All these topics are discussed in this chapter in the first 2 sections. The last section discusses the current oxidative heteroatom removal techniques.

2- Coal, its composition and properties

Coal is the most abundant and widely distributed fossil fuel resource of the world. In order to study coal technologies, such as liquefaction, desulfurization and denitrogenation, coal properties should be studied first. The following topics are discussed in this section: physical and chemical composition of coal, coal rank and changes in coal structure by rank.

2-1- Coal Composition

Considering the microscopic level, coal is composed of organic grains named macerals. Macerals can be categorized into 3 groups based on their grayness [3]:

- Dark gray: Liptinite, which is made of hydrogen-rich hydrocarbons coming from spores, pollens, cuticles and resins of the plant material.
- Medium to light gray: Vitrinite, which has less hydrogen content compared to liptinite and it is derived from "gelified" wood, bark, and roots.
- White and very bright: Inertinite, which has higher carbon content compared to liptinite or vitrinite since it is mainly made of oxidation products of other macerals. This maceral comes from ancient peat fires.

The chemical composition of coal can be defined in two ways: 1) proximate analysis with parameters such as: ash content, moisture content, volatile matter and fixed carbon; 2) elemental analysis for the main elements like carbon, hydrogen, nitrogen, sulfur, oxygen [4] as well as many measurements of the minor elements such as metals (Fe, Na, K, Ca, Hg and so on). Many coal chemists have attempted to use the resulting information to draw model molecules to represent what a "typical" molecule in the coal might look like. Two models are shown in Figure 2-1 and 2-2 [5].
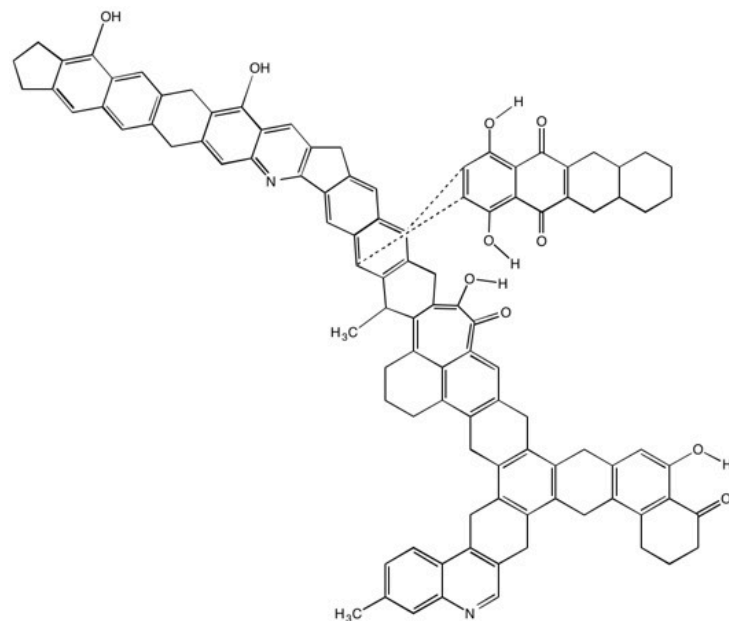
Figure 2-1- Given's model of a typical coal molecule [5]
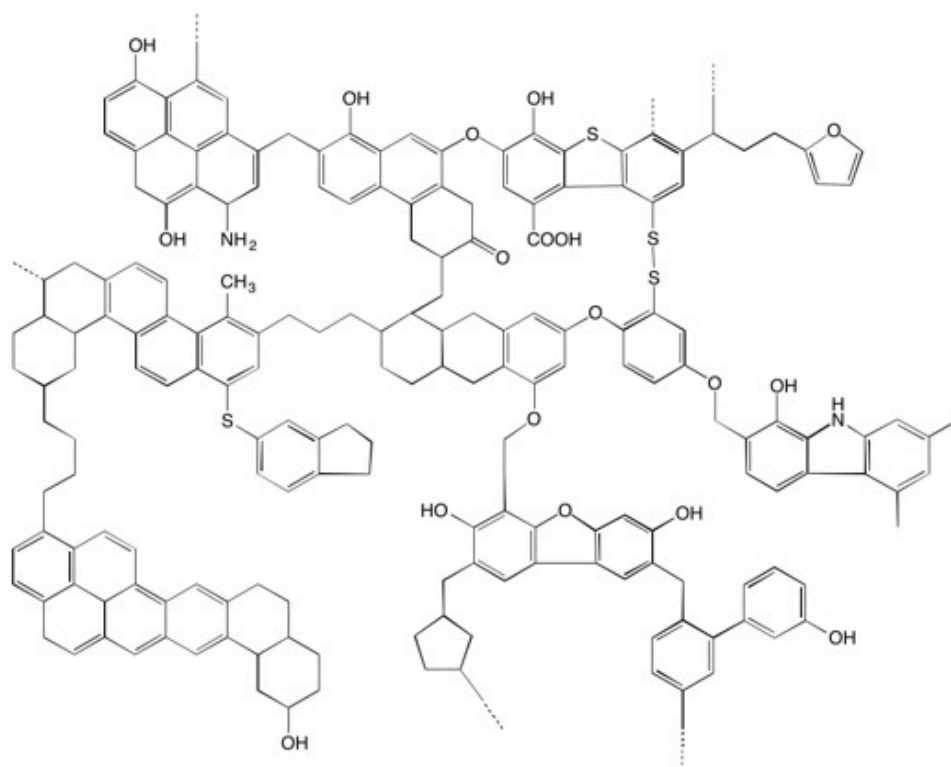
Figure 2-2- Wiser's Model of a typical coal molecule [5]

Coal seems to be made of parallel layers of lamellae in a structure similar to graphite. When considering a single aromatic cluster, the chemical bonds seem to be only in a two dimensional plane. In other words, the individual clusters appear to be joined together in one layer by various chemical bonds such as short aliphatic bridges (e.g. methylene), ether linkage, sulfide or disulfide linkages, and perhaps biphenyl linkages. But, the minimum distance observed in the 3rd dimension is about 3.44 angstroms. This amount is too long for a chemical bond. Thus, physical interactions such as hydrogen bonding or Van der Waal's forces should be holding layers of clusters together [6].

2-2- Coal Rank

Rank is a qualitative measure for carbon content of different coals. It has the same meaning as degree of maturation. Regardless of the origin, age and/or type, all coals can be classified based on their carbon contents in 6 different categories: Peat, lignite, subbituminous coal, bituminous coal, anthracite and graphite. Lignite and subbituminous coals are usually classified as low-rank coals, whereas bituminous and anthracite coals are referred as high-rank coals [4]. Figure 2-3 shows the relation between coal rank and carbon content [7].
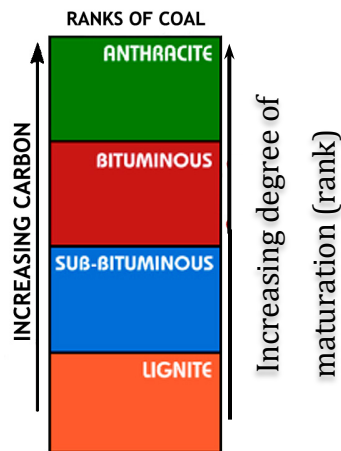
Figure 2-3- relation between coal rank and carbon content [7]

In addition to carbon, coal is composed of hydrogen, oxygen, nitrogen and sulfur. High-rank coals have high carbon content and therefore, high heating values, but they are low in hydrogen and oxygen content. Low-rank coals contain low amounts of carbon but are high in hydrogen and oxygen [7]. The properties of coal depend on its rank; the approximate values of some important properties are shown in Table 2-1 [6].

Table 2-1- Some properties of coal for different coal ranks [6]

Properties	Lignite	Subbituminous	Bituminous			Medium Volatile	Low Volatile	Anthracite
			High Volatile					
			A	B	C			
C (mineral matter free) (%)	65 - 72	72-76	76-78	78-80	80-87	89	90	93
O (%)	30	18	13	10	10-4	3-4	3	2
O as COOH (%)	13-10	5-2	0	0	0	0	0	0
O as OH (%)	15-10	12-10	9	-	7-3	1-2	0-1	0
Aromatic C atoms, Total C (%)	50	65	-	-	75	80-85	85-90	90-92
Av. number benzene rings/ cluster	1-2	2-3					5	>25
Volatile matter (%)	40-50	35-50	35-45	-	31-40	31-20	20-10	<10
Density	increases →							

2-3- Heteroatoms in coal

2-3-1- Sulfur

The sulfur content of different coal types vary from 0.2 to 10 -wt%, but for the most samples, it is within 1.0 to 4.0-wt%. The sulfur compounds can be

classified in two groups: inorganic compounds and organic compounds. The ratio of inorganic to organic sulfur is usually close to 2:1, but it may vary from 4:1 to 1:3.

Inorganic sulfur usually appears the forms of sulfates or disulfides (pyrite and marcasite). The amount of sulfate compounds increases with the length of coal exposure to the air and they can appear as iron, calcium and barium sulfates. The inorganic disulfides are in the form of Iron disulfide and they can be present in crystalline forms of pyrite (a cubic crystal structure) or marcasite (rhombic structure). [8]

Organic sulfur containing compounds are classified based on the type of functional group in their structure, namely sulfides, disulfides, thiols, thiophenes and compounds containing thiophene rings. Figure 2-4 shows the structure of these organic compounds [9].

| Sulfides | Disulfides | Thiols | Thiophenes |
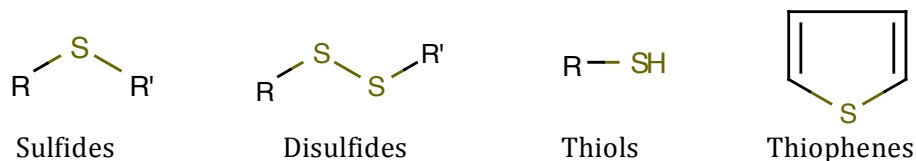
Figure 2-4- The structure of major organic sulfur functional groups of coal [9]

2-3-2- Nitrogen

The total amount of nitrogen varies from 0.4 to 2-wt% by coal rank as it is shown in Figure 2-5. Nitrogen amount increases from lignite to subbituminous stages and then, decreases during the bituminous stage [10].
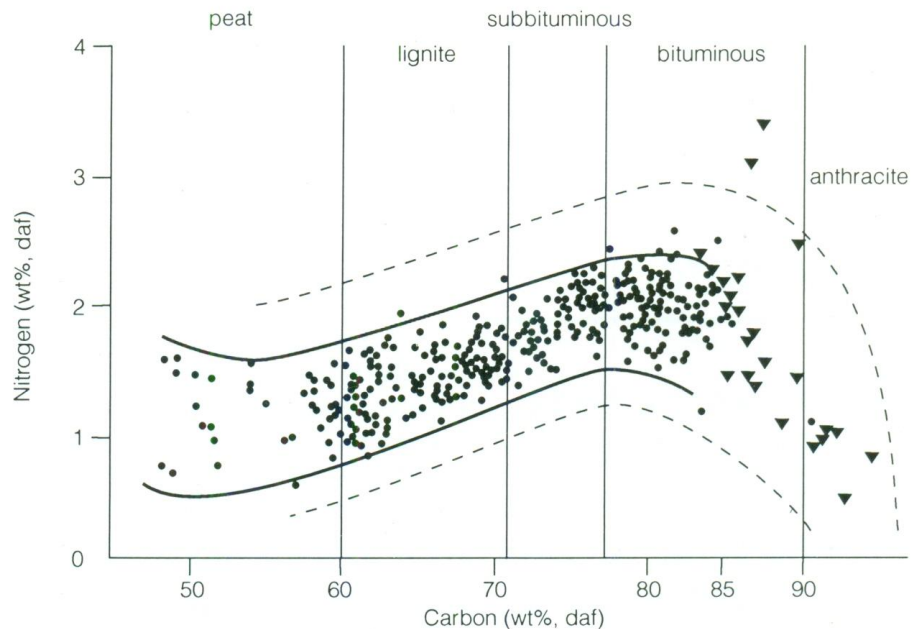
Figure 2-5- The relation between nitrogen content and rank of coal [10]

It is generally accepted that all the nitrogen compounds in coal exist in organic forms. For higher rank coals with carbon content from 87-wt% to over 96-wt%, ammonium rich Illite is also found beside the organic nitrogen compounds [10].

Studies on solid coal structure (such as XPS, XANES and NMR) suggest that pyrrolic-type nitrogen is the most abundant nitrogen functionality in solid coal, while the pyridinic-type nitrogen increases with coal rank. In some studies a significant presence of quaternary nitrogen species were also found in low rank coals. It is suggested that the quaternary nitrogen may be the product of pyridinic compounds oxidation [10].

Studies on coal-derived products can also provide some useful information on the nature of nitrogen compounds in parent coal and it benefits from ease of examination due to material solubility. Analysis of coal oxidation products shows the presence of pyrroles and heteroaromatic compounds such as carbazoles, quinolines, pyridines and acridines. Analysis of solvent refined coal indicates the presence of indoles, carbazoles, amines,

15

anilines, quinolines, aza compounds and aminoquinolines in coal liquids. However, the amines and anilines existing in coal-derived products might be produced by hydrogenation of heterocyclic forms, therefore, the evidence for the presence of these compounds in parent coals is less certain [10].

Figure 2-6 shows the structure of the common heterocyclic nitrogen compounds found in coal and coal-derived products [10].

| Pyrrole | Pyridine | Indole |

| Quinoline | Carbazole | Acridine |
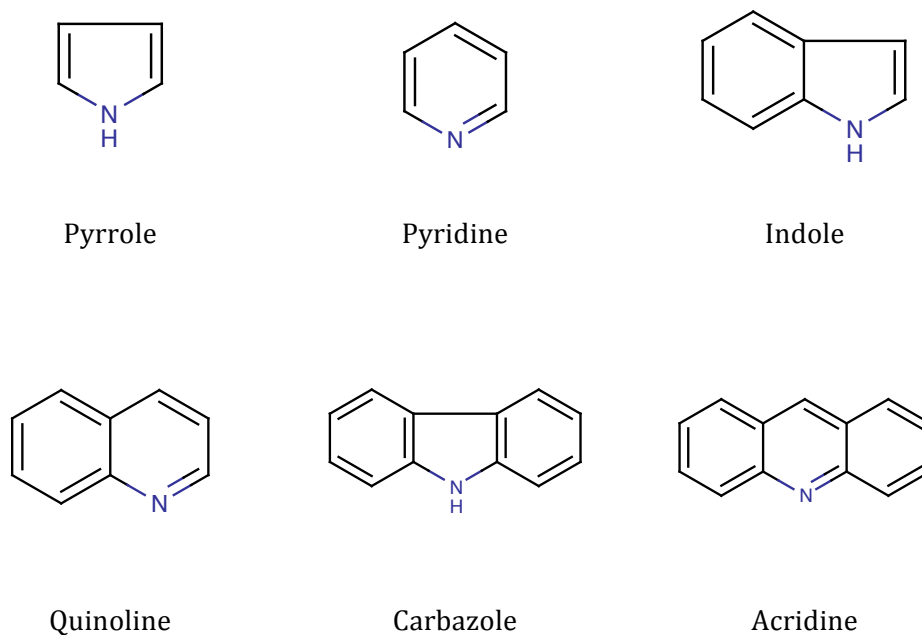
Figure 2-6- Some cyclic nitrogen functional groups of coal [10]

3- Coal Liquefaction

3-1- Coal liquefaction technologies

The purpose of coal liquefaction is to manufacture synthetic transportation fuels, like gasoline, diesel fuel, and aviation fuels using a continuous hydrogenation process [4].

Coal liquefaction technologies use two basic approaches: indirect coal liquefaction (ICL) and direct coal liquefaction (DCL) [11].

In ICL, coal is completely broken down into syngas by gasification. Later, the syngas is modified to the desired balance of carbon monoxide and hydrogen, then it is cleaned (removing sulfur and other impurities) and finally, it is reacted over a catalyst to produce desired products by Fischer-Tropsch reaction (FT). In general, two types of FT synthesis exist: the first one uses high-temperature version to produce gasoline-like fuel and the second one uses low-temperature version to produce diesel-like fuel [11].

DCL is the process based on the Berguis reaction (Formula 2-1) [11]:

$$nC + (n + 1)H_2 \rightarrow C_nH_{2n+2} \qquad (2\text{-}1)$$
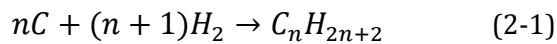
Coal is dissolved in a solvent at high temperature, pressure and under hydrogen atmosphere (either in form of hydrogen gas or a hydrogen-donor solvent) [11]. Figure 2-7 shows the block flow diagram for a typical DCL plant [12].
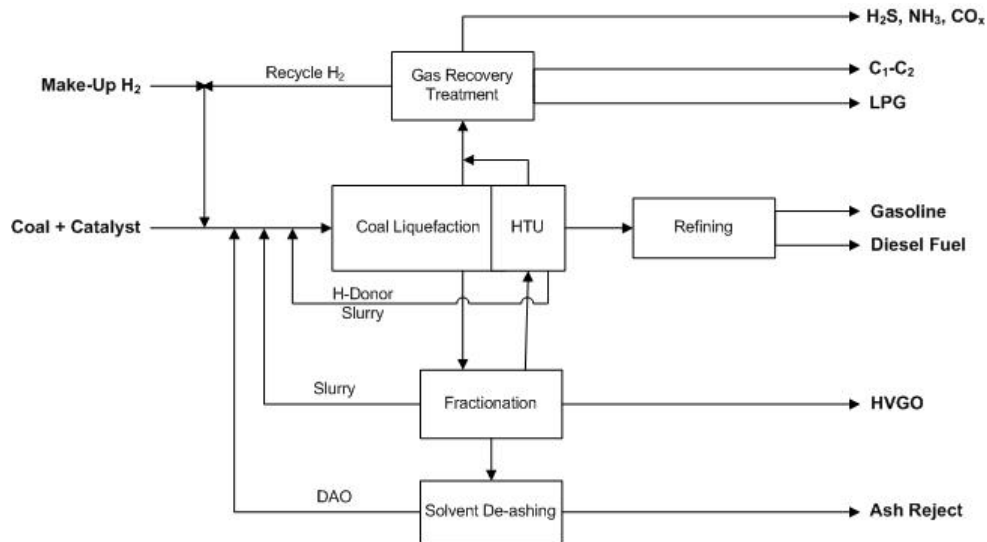
Figure 2-7- The block flow diagram of a typical DCL plant [12]

The process can convert long carbon chains into shorter ones by hydrocracking. As a result, the H/C ratio of product is improved [11]. Coal particle size, its rank, solvent to coal ratio, temperature, pressure, heating rate, residence time, presence of hydrogen environment and catalyst all play

a significant role in production yield [6]. The overall thermal efficiency is about 60-70% and liquid yield can be about 70% of the dry weight coal. These coal liquids can be used directly as a synthetic crude oil or in power generation. However, further refining is needed in order to use them as transport fuels [11].

Primary coal liquids consist of solubilized materials extracted by the solvent. Based on the amount of coal hydrogenation, these materials can vary from low-melting solids to non-distillable liquids. Consequently, product composition is a function of process conditions. Increase in depth of hydrogenation always increases H/C ratio, and consequently reduces molecular weight, boiling range and viscosity. Since the aliphatic fraction of coal can be easily hydrocracked to hydrocarbon gases and also, since the naphthenic solvent acts as a hydrogen donor material, the liquefaction products are richer in aromatic compounds compared to the parent coal from which they are produced [4]. Liquefaction products can be easily extracted with hexane, toluene and tetrahydrofuran (THF). The hexane soluble fraction with light gases is called oils and gases. Hexane insoluble-toluene soluble fraction is called asphaltenes, and toluene insoluble-THF soluble fraction is called preasphaltenes [13].

3-2- Change in heteroatom compounds during liquefaction process

In order to study the heteroatom removal of coal liquids, it is necessary to understand thoroughly the changes in structure of the heteroatoms during the liquefaction process.

As it is stated in section 2-3-2, one of the methods to study the structure of nitrogen in coal is to liquefy the coal structure and then study the produced coal liquids. This is due to the fact that, for most of the nitrogen compounds, the structure does not change during liquefaction process. However, in cases

that amines or anilines are found in coal-liquified products, it is possible that they have been produced by hydrogenation of heterocyclic forms during liquefaction [10].

Unlike the nitrogen compounds, the sulfur structure changes significantly during the coal liquefaction process. Since different coal macerals have different liquefaction behavior, it is more meaningful to analyze the behavior of sulfur compounds in each maceral separately than studying the whole coal. For each studied maceral, the sulfur analysis of the asphaltene fractions shows that the aliphatic sulfur compounds are in very low abundance while larger polycyclic aromatic sulfur compounds are in significant abundance. What is striking is the dominance of molecules containing two sulfur atoms. These species are similar across all three maceral groups as is demonstrated in Figure 2-8 [13].
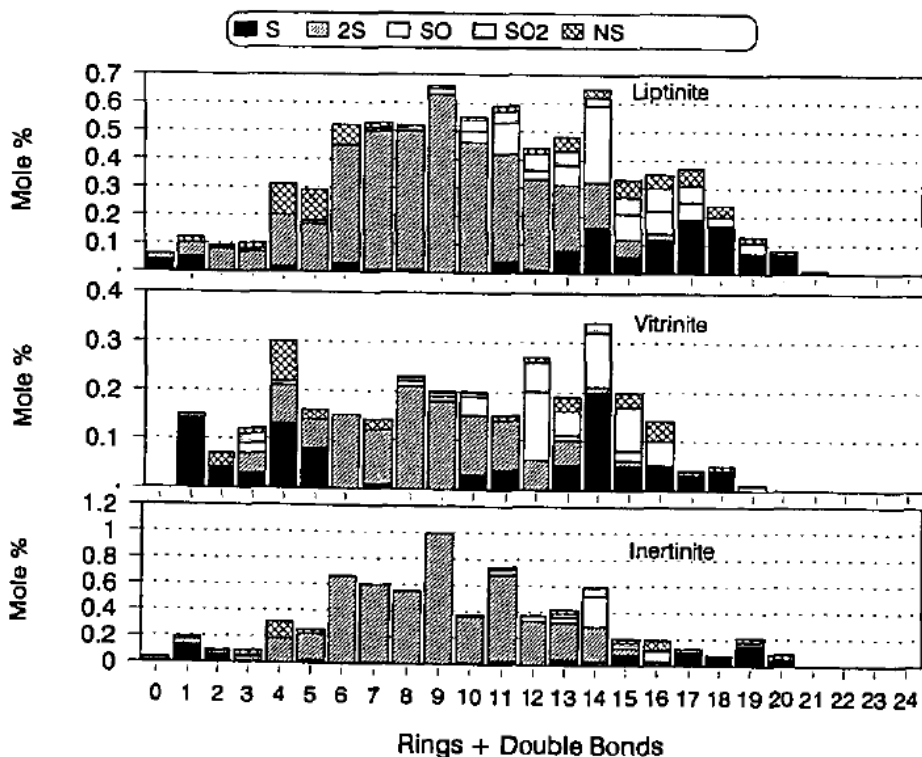
Figure 2-8- Sulfur compounds of the asphaltene fraction in different macerals [13]

If the result for the asphaltene is adjusted for the yields, one can directly compare products with the starting material. This is done for the liptinite and the result is shown in Figure 2-9 in comparison with the unreacted maceral. For the single sulfur compounds the aliphatics are gone and large polycyclic aromatics were formed. However, the overall abundance decreased. The total yields of compounds with two sulfur atoms are very similar but there is a different mix of molecules with the same general trend observed for the single sulfur. The *S+O* species shifted to more polycyclic aromatics in the products. Compounds with both N and S must be very reactive under these liquefaction conditions since they are not present in the coal liquid products [13].
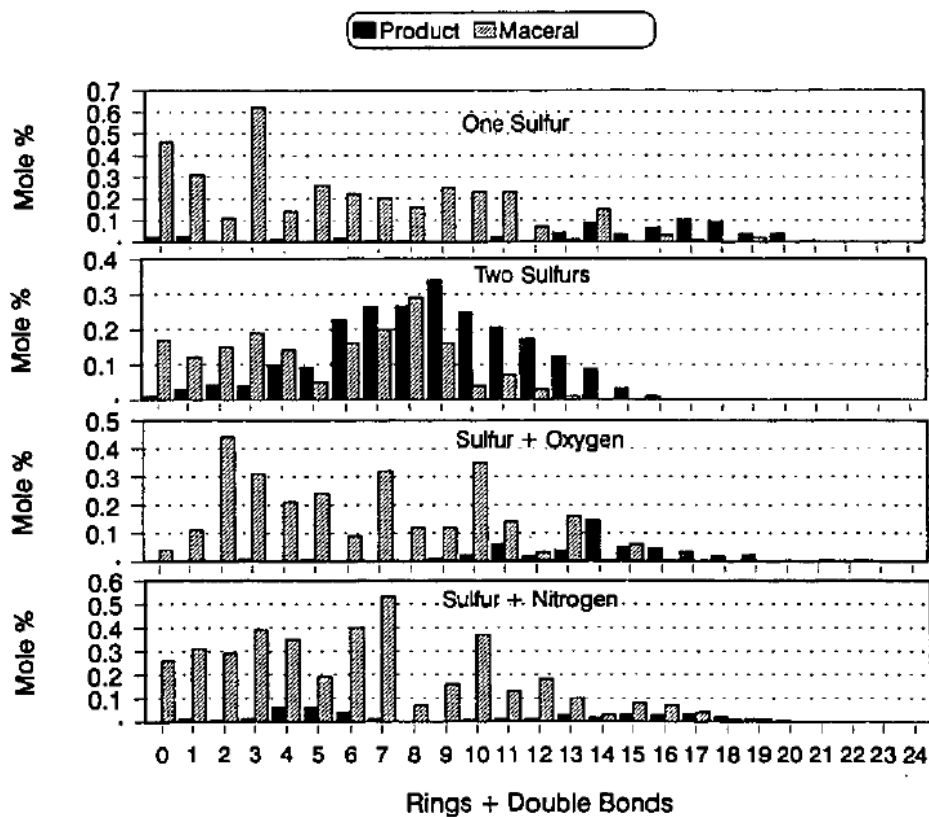
Figure 2-9- Comparison of sulfur types from the whole maceral and from the asphaltene product of liptinite [13]

3-3- Current nitrogen removal methods

Hydrodenitrogenation (HDN) is currently the most extensively used nitrogen removal method. In this process, the nitrogen-containing compounds are exposed to hydrogen in presence of a catalyst and the nitrogen content is removed as NH_3 [14]. The nitrogen compounds are adsorbed on the active catalyst sites. The C-H and C-N bonds of these adsorbed species may be broken resulting in splitting reactions, and/or they can react with the adsorbed hydrogen to form compounds that desorb from the catalyst sites. When dehydrogenation does not happen, the adsorbed compounds may react with each other to form condensed products on the catalyst [15].

In order to remove nitrogen atom through hydrogenation, the hydrogenation of nitrogen-containing aromatic ring must occur first. Then, the nitrogen atom can be removed by cleavage of C-N bond. As an example, the reaction scheme for hydrodenitrogenation of quinoline is shown in figure 2-10 [14].
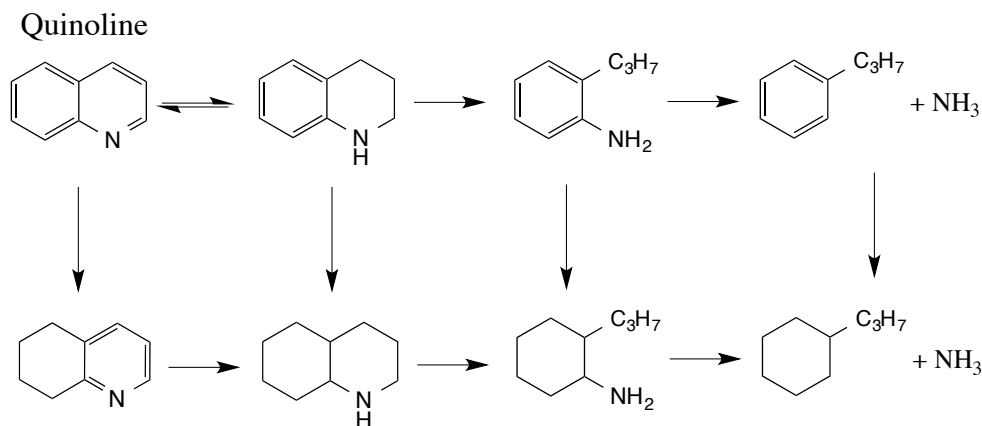
Figure 2-10- Reaction scheme for hydro-denitrogenation of quinoline [14]

Ion-exchange resins or adsorbents were also used to remove nitrogen from coal-liquids. The organic resins - like sulfonic acids on a styrene-divinyl-

benzene backbone – has shown a larger denitrogenation capacity compared to inorganic adsorbents – such as basic or neutral alumina [14].

Solvent extraction is another method studied for denitrogenation of coal liquids. Ionic liquids, such as tetrafluoroborate or hexafluorophosphate, were reported to be able to extract nitrogen from transportation fuels [14]. In another study, nitrogen compounds were separated from coal liquids by extraction into a methanol-water layer [16]. Supercritical water was also used to remove the nitrogen content of coal liquids [14].

Oxidative removal methods have also been studied to remove heteroatoms from of coal liquids. These methods are discussed in detail in the following section.

4- Oxidative Removal of Heteroatoms in Coal Structure

The strong nucleophiclic nature of heteroatoms (like sulfur and nitrogen) is the reason behind their oxidation. The overlap of highest occupied molecular orbital of the heteroatom center with the lowest occupied molecular orbital of the O—O causes the electrophilic oxygen attack to the nucleophiclic heteroatom center [17].

Nitrogen is the least studied element in coal and consequently, there is little literature available on oxidative Nitrogen removal, while more research is done on oxidative desulfurization (ODS) technology. A review of available literature on oxidative desulfurization of coal can help in finding suitable oxidative methods to remove the nitrogen structure. This is discussed in the section 4-1. The section 4-2 studies the works done on oxidation of pure organic nitrogen compounds to produce N-oxides.

4-1- Oxidative Desulfurization of Coal

Pyrite (FeS_2) naturally oxidizes to sulfates when coal is exposed to air. The generated sulfates can be leached by water using the acid mine drainage process. All the pyrite removal investigations are attempts to elevate this natural oxidation process. Different oxidants such as metal ions (Fe^{3+}, Hg^{2+}, Ag^{2+}), strong acids (HNO_3, $HClO_4$) and also, O_2, Cl_2, SO_2 and H_2O_2 have enough oxidation capability to convert pyrite [1].

Several attempts were made to remove the organic sulfur structure of coal using oxidative methods. Usually, the coal samples were treated prior to oxidation to remove inorganic sulfur compounds. The oxidation of organic sulfur compounds such as thiols, sulfides, disulfides and thiophenes usually leads to formation of sulphoxides or sulfones. There's a large difference in the boiling point and polarity between these compounds and the original sulfur-containing compounds of coal. Therefore, it is possible to separate the sulfur-oxide forms from the coal structure by ordinary purification procedures such as distillation, solvent extraction and chromatographic adsorption [18]. The studied oxidative desulfurization methods for organic structure are categorized based on the oxidizing agents in the following sections.

4-1-1- Oxidative desulfurization of coal using air/oxygen

Air oxidation has been tried on Indian coal (sulfur content: 3.6-wt%) in a non-isothermal slow heating system. The effect of pre-treatment of coal samples with $HgCl_2$ was studied as well. Coal samples were treated with dilute HCl and dilute HNO_3 to remove inorganic sulfur compounds prior to oxidation. To prepare Hg-treated samples, the inorganic-sulfur free coal was dissolved in a 3% $HgCl_2$ and the solution was stirred for 1 hour at room temperature. The oxidation experiment then was performed on both inorganic-sulfur free feed coal and Hg-treated coal (10 g) in an oven under air atmosphere with 2 $Kmin^{-1}$ heating rate till temperature reaches 150 °C. The

amount of desulfurization observed was 14.53-wt% for Hg-treated coal and 10.9-wt% for feed coal. The treatment with $HgCl_2$ was reported to weaken the C-S bond due to formation of strong Hg-S bond, leasing to a higher degree of desulfurization [19].

In another study, alkali treatment was combined with air oxidation to remove both the organic and inorganic sulfur structures at the same time. 21 g of coal sample (total sulfur content: 3.15-wt%, inorganic sulfur: 2.36-wt%, organic sulfur: 0.79-wt%) was treated in 500 mL of NaOH solution (0.25 M) at 90°C while atmospheric air was passing on them for 4 hours. The results indicated 66% organic sulfur removal and 15% pyritic sulfur removal. The alkali solution was reported to make the C-S bond unstable and therefore, easier to break. Organic sulfur reduction was reported to be mainly because of the removal of thiols present in coal. The C-S bond of thiols, which is weakened by alkali treatment, can easily break due to oxidation and convert to disulfides. Further oxidation of organic disulfides produces a number of stable intermediates, which finally forms sulphonic acid at the end, as shown in formula 2-2. The amount of thiophenic sulfur was also decreased using the proposed method [20].

$$\hspace{10cm} (2\text{-}2)$$
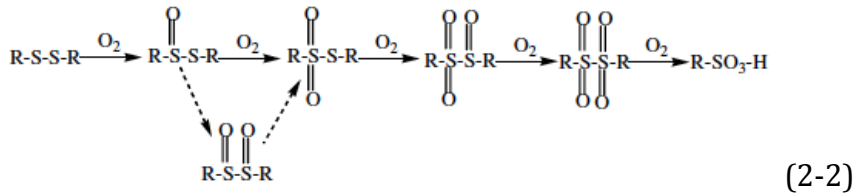
The effect of further treatment with HCl solution was also studied. The oxidation experiment was performed using the same method indicated above and then, PH was adjusted to 1 with HCl and samples were kept in the solution for another hour. 73% organic sulfur removal and 84% pyritic sulfur removal was removed. The further adjusting of PH to acidic condition increases the amount of inorganic sulfur removal, following the formula 2-3 [20].

$$FeS_2 + 2H^+ + O_2 \rightarrow Fe^{2+} + H_2S + SO_2 \qquad (2\text{-}3)$$
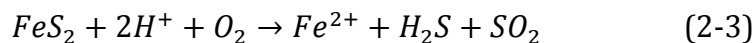
The Pyrolysis of treated coal samples (using TGA) indicated that there was just a slight change in burning quality and the heat value of coal by treatment. This could be due to oxidation of some carbon-carbon bonds or dissolution of some organic compounds in the solvents [20].

4-1-2- Oxidative desulfurization of coal using hydrogen peroxide

Hydrogen peroxide (30%) was reported to be able to oxidize the sulfur structure of coal. An Indian coal with 3.6-wt% sulfur content was used for the experiments. At first, coal was treated by dilute HCL and dilute HNO_3 to remove most of inorganic sulfur. Then, the inorganic sulfur free coal (2 g) was reacted with hydrogen peroxide (30 mL of 30% H_2O_2) at 25°C and the products were analyzed after 1, 2, 3, 4 and 24 hours. The results indicate that sulfur is removed from 3.70-wt% after 1 hour, 6.25-wt% after 4 hours and 9.24-wt% after 24 hours. The low level of desulfurization indicated that hydrogen peroxide was not strong enough to break down all the C-S and S-S bonds. Since hydrogen peroxide preferentially oxidizes amines, alcohols and organic sulfur compounds over ethers and benzenes, the properties of parent coals were retained using the proposed desulfurization method [21].

The desulfurization experiment was also performed on pure model compounds to understand which type of organic sulfur compounds could be removed. 2 types of model sulfur compounds were studied: a) an aliphatic compound (methionine) and b) an aromatic compound (dibenzothiophene). The result indicated that, while the aliphatic compound participated in desulfurization reaction, hydrogen peroxide was unable to oxidize the aromatic sulfur compound. This is because of the high stability of dibenzothiophene and its resistance towards cleavage of C-S bond [21].

Pure organic sulfur compounds (like thiols, disulfides and sulfides) react with hydrogen peroxide to produce sulphonic acids as shown in equations 2-4 and 2-5 [21].

$$R\text{-}SH \xrightarrow{H_2O_2} R\text{-}S\text{-}S\text{-}R \xrightarrow{H_2O_2} R\text{-}\overset{OO}{\underset{}{S}}\text{-}S\text{-}R \longrightarrow R\text{-}\overset{OO}{\underset{O}{S}}\text{-}S\text{-}R \xrightarrow{H_2O} R\text{-}SO_3H \qquad (2\text{-}4)$$

$$R_2S \xrightarrow{H_2O_2} R_2SO \xrightarrow{H_2O_2} R_2SO_2 \xrightarrow{H_2O} RSO_3H \qquad (2\text{-}5)$$
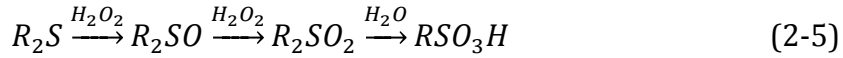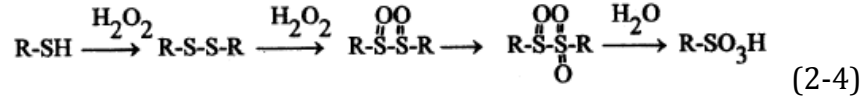
The present leached Fe, which was originally bonded to organic structure of coal, was reported to enhance the oxidation with hydrogen peroxide by catalyzing H_2O_2 decomposition (Fenton type reaction) as shown in formula 2-6 – 2-9. Produced OH· could contribute in the oxidation reaction as shown in formula 2-10 [21].

$$Fe^{2+} + H_2O_2 \rightarrow Fe^{3+} + OH\cdot + OH^- \qquad (2\text{-}6)$$

$$Fe^{2+} + OH\cdot \rightarrow Fe^{3+} + OH^- \qquad (2\text{-}7)$$

$$Fe^{3+} + H_2O_2 \rightarrow Fe^{2+} + HO\cdot_2 + H^+ \qquad (2\text{-}8)$$

$$Fe^{3+} + HO_2^\cdot \rightarrow Fe^{2+} + H^+ + O_2 \qquad (2\text{-}9)$$

$$R\text{-}S\text{-}R + OH^\cdot \rightarrow R\text{-}\overset{O\text{-}H}{\underset{-H^+}{S}}\text{-}R \xrightarrow{} R\text{-}\overset{O}{\underset{}{S}}\text{-}R \xrightarrow{OH^\cdot} R\text{-}\overset{O}{\underset{O\text{-}H}{S}}\text{-}R \xrightarrow{-H^+} R\text{-}\overset{O}{\underset{O}{S}}\text{-}R \xrightarrow{H_2O} R\text{-}SO_3H \qquad (2\text{-}10)$$
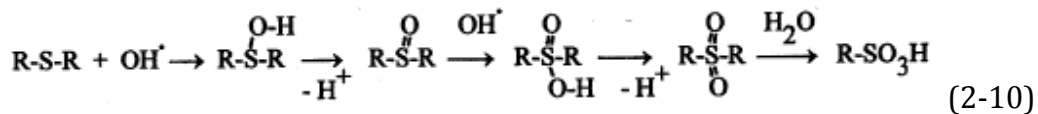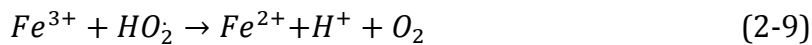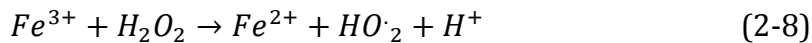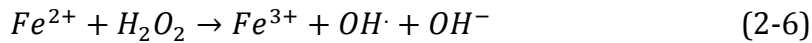
Since Fe could enhance desulfurization reaction, the effect of externally addition of some metal ions (Ni^{2+}, Cu^+, Co^{2+}, Sn^{2+}, Sb^{3+} and Pd^{2+}) on the degree of desulfurization was also studied. 0.2 mL of the metal chloride solution (0.001 M) was added to the reaction flask and the oxidation experiment was performed by hydrogen peroxide using the same method explained before. It was reported that, in some cases, the added ion could remarkably increase the rate and also, the degree of desulfurization. The highest desulfurization degree (31.12-wt%) was obtained by using Sb^{3+} after 24 hours [21].

26

4-1-3- Oxidative desulfurizaion of coal using peroxyacetic acid

Peroxyacetic acid was reported to be able to oxidize the organic sulfur compounds of coal to some extent at room temperature. The same reaction conditions for oxidation by hydrogen peroxide have been used. At first, coal (Indian coal, sulfur content: 3.6-wt%) was treated with HCl and HNO_3 to obtain an inorganic sulfur free coal. Then, 2 g of mineral free coal sample was reacted with the peroxyacetic acid, which was prepared in situ by reaction of hydrogen peroxide (30 mL of 30% H_2O_2) and glacial acetic acid (30 mL) according to the formula 2-11. In case of studying the metal ion influence (Ni^{2+}, Cu^+, Co^{2+}, Sn^{2+}, Sb^{3+} and Pd^{2+}), a metal chloride solution (0.2 ml, 1 M) was also added to the reaction flask. The products were analyzed after 1, 2, 3, 4 and 24 hours treatment [17].

$$CH_3CO_2H + H_2O_2 \rightarrow CH_3CO_3H + H_2O \qquad\qquad (2\text{-}11)$$
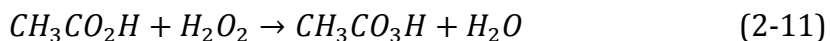
The sulfur removal was achieved to the extent of 6.92-wt% after 1 hour, 10.02-wt% after 4 hours and 13.41-wt% after 24 hours treatment. The optimum desulfurization is achieved using Pb^{2+} ion at 4 hours (32.32-wt%). The degree of desulfurization observed by peroxyacetic acid was higher than what was observed for hydrogen peroxide (using the same coal sample and the same reaction conditions). It was concluded that peroxyacetic acid is a stronger oxidizer for organic sulfur compounds compared to hydrogen peroxide. This was reported to be due to the stronger polarization of dissymmetric O-O bond in the structure of peroxyacetic acid compared to the symmetric O-O bond in the structure of hydrogen peroxide [17].

The oxidation of thiols, sulfides and disulfides was reported to lead to production of sulphonic acid by forming a number of intermediates, following the same reaction pathways shown earlier in formulas 2-2, 2-4 and 2-5. The mechanism of monosulphoxide formation is shown in formula 2-12 [17].

$$(2\text{-}12)$$
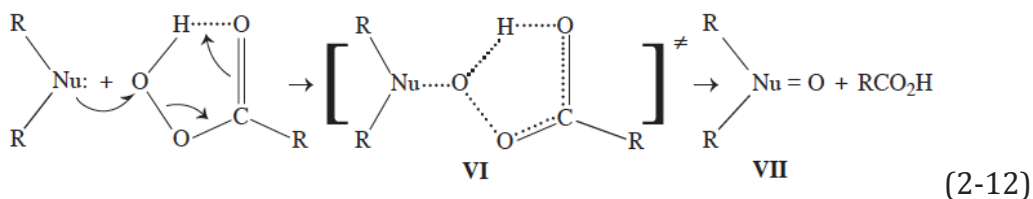
Although desulfurization predominantly is due to the oxidation of aliphatic sulfur compounds, peroxyacetic acid is able to oxidize thiophenes to some extent to produce sulphoxide (VIII) and sulphone (IX), which can combine together to form dimeric sesquioxide (X or XI) according to formula 2-13 [17].

$$(2\text{-}13)$$
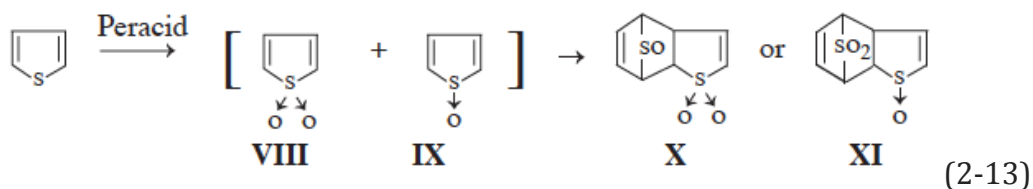
The dimerization of IX may also happen resulting in release of SO_2 as shown in formula 2-14 [17].

$$(2\text{-}14)$$
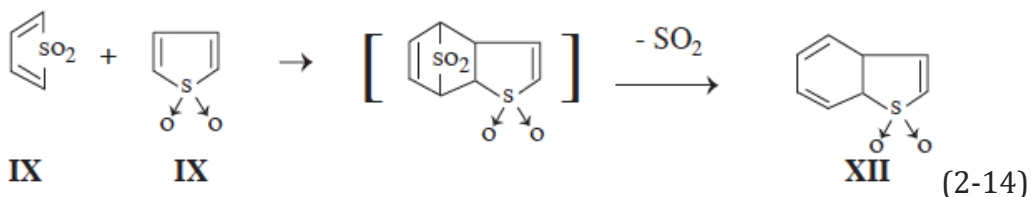
4-1-4- Oxidative desulfurizaion of coal using potassium permanganate

The use of potassium permanganate in coal desulfurization is also reported. First, coal (Pittsburgh No. 8) was pre-cleaned using 1,1,1-trichloroethane by heavy liquid separation. 20 g of pre-cleaned coal was mixed with different concentration of potassium permanganate (2, 4, 6, 8 and 10-wt%) in coal and stirred for 1 hour at room temperature. Then, the solution was washed with warm water at 80 °C for 1 hour. The amount of desulfurization in each step is shown in table 2-2 [22].

Table 2-2- The degree of desulfurization after heavy liquid separation and $KMnO_4$ oxidation on the studied Pittsburgh coal [22]

Sample	Total S (wt%)	Pyritic S (wt%)	Sulfate S (wt%)	Organic S (wt%)
Raw coal	3.58	2.82	0.02	0.74
Pre-cleaned coal	1.78	1.04	0.02	0.72
$KMnO_4$ (10%) oxidation products	0.98	0.32	0.32	0.34

52-wt% of organic sulfur could be removed using 10-wt% potassium permanganate. The oxidation pathways for sulfides, mercaptanes and thiophenes were reported to be the same as what's been suggested in previous sections, i.e. formation of sulphoxides and sulphones from the parent sulfur compounds. A major disadvantage was reported for the proposed procedure: possible deposition of manganese dioxide, produced from decomposition of potassium permanganate, on the coal matrix. Extensive acid treatment was required to remove the deposited chemicals, which could destroy the coal properties [22].

4-2- Oxidation of organic nitrogen compounds present in coal

Although there is little information available on oxidative nitrogen removal techniques, some studies are done on oxidation of pure organic nitrogen compounds for applications other than coal denitrogenation. Due to the usefulness of heterocyclic N-oxides, there is some literature available on their production from the corresponding heterocyclic nitrogen compounds by different oxidation methods [23]. Also, because of very slow biodegradation of quinolines, some studies were done on their degradation to corresponding N-oxides in order to enhance wastewater treatment [24]. Moreover, some of the nitrogen compounds available in coal also exist in petroleum fuel and therefore, their oxidation behavior were studied as the model compounds representing petroleum nitrogen content [25].

As it is discussed earlier, cleavage of C-N bond by producing N-oxides is a necessary step for a successful oxidative denitrogenation process. Therefore, the study of literature available on oxidation of nitrogen compounds, although following other applications, can be helpful in designing a pathway for oxidative denitrogenation of coal or coal liquids.

Quinoline is one of the major nitrogen compounds available in coal liquids and also, its basic nature causes the inhibition of acidic catalysts during processing of coal liquids [26]. Therefore, in this research, quinoline is chosen as the model compound representing the pyridinic nitrogen structure of coal liquids. Hence, only the literature involving quinoline oxidation is studied in this section.

Practically all the attempts in producing heteroaromatic N-oxides can be classified in three major groups: (a) N-oxidation of the corresponding nitrogen structure, (b) cyclization reaction to form the ring that carries the N-oxide group and (c) chemical modification of a commercially available N-oxide in a way that the N-O function would be preserved. Only the first category is related to the first step of oxidative denitrogenation methods, i.e. oxidation of nitrogen structure. Percarboxylic acids are mostly used as the oxidizing agent for direct N-oxidation of heterocyclic nitrogen compounds [27]. The quinoline N-oxides were first produced by oxidation of quinoline using perbenzoic acid. Relatively few N-oxides were synthesized until 1940s [28]. In some cases hydrogen peroxide or other oxidants have shown promising oxidation results as well [27]. The following sections are a review on some of the recent work done on oxidation of nitrogen compounds (categorized based on the oxidizing agent).

4-2-1- Non-catalytic oxidation using organic peroxides

Organic Peroxides were extensively used as oxidizers particularly for the oxidation of olefins, sulfur-containing and nitrogen-containing compounds. Perdecanoic acid was reported to be able to oxidize some aromatic nitrogen

compounds (pyridine, quinoline and acridine). The oxidation reaction was performed for 20-30 minutes in a glass reactor under argon atmosphere at a temperature range of 30-55 ℃. The interaction between a compound containing tertiary nitrogen and perdecanoic acid was reported to produce N-oxide and decanoic acid in 2 stages: The first stage involved the formation of an intermediate N-containing component, which at the second stage, decomposed and produced reaction products. The influence of solvent on the oxidation was studied, too. The degree of oxidation in benzene was reported to be appreciably higher compared to acetone. It seems that while the solvent electrophilicity and polarizability did not influence the rate of reaction, solvent basicity and polarity had a decisive effect on reaction rate. The trend of reaction rate in both acetone and benzene followed the series of acridine>quinoline>pyridine. No information was provided on the yield of the products [29].

In another study, organic N-oxides have been prepared with use of urea-hydrogen peroxide. Trifloroperacetic acid was produced by the reaction of trifluoroacetic anhydride with urea-hydrogen peroxide. This synthesized mixture was able to oxidize pyridine, quinoline and pyrimidine substrates. Formulas 2-15 – 2-18 show the mechanism of this process [30].
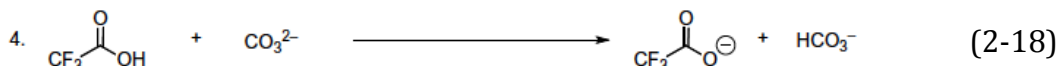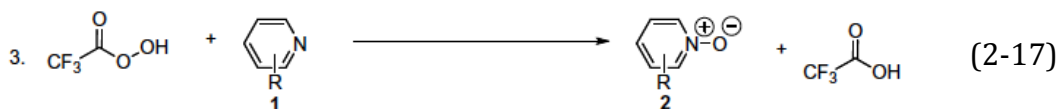
Since all the reagents and by-products were soluble in water, the products were isolated from other materials by partition between an organic solvent and water [30].

31

4-2-2- Catalytic oxidation using hydrogen peroxide

The oxidation of some nitrogen compounds with use of aqueous hydrogen peroxide was reported in the presence of silica-supported vanadium as catalyst. 1 mmol of nitrogen compound, 10 mg of catalyst and 3 mmol of hydrogen peroxide (30%) were dissolved in 2 mL of acetonitrile at 80 ℃. The mixture was stirred for the appropriate time. Table 2-3 shows the structure of produced N-oxides and the yield of the reaction. This procedure was reported to benefit from low cost of oxidizing agent, generating water as the only by-product and catalyst recyclability [23].

Table 2-3- The oxidation results of different nitrogen compounds using hydrogen peroxide in presence of silica-supported vanadium [23]
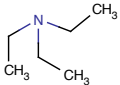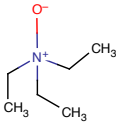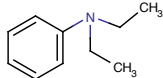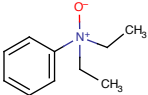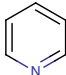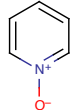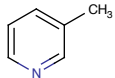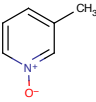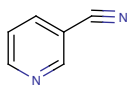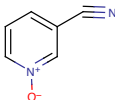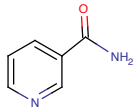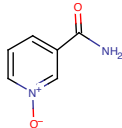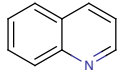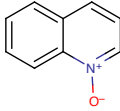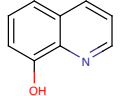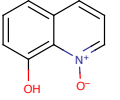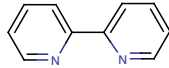
Entry	Substrate	Time (h)	Product	Yield (%)
1		4		99
2		3		89
3		10		79
4		12		45
5		3		99
6		3		98

Table 2-3- *continued*

7		8		71
8		8		92
9		4		97

4-2-3- Non-catalytic and catalytic oxidation using other oxidants

The use of dimethyldioxirane was reported in oxidizing a series of 2-substituted pyridines, quinolines and isoquinolines in dried acetic acid at 23 ˚C without using any catalyst. Formula 2-19 shows oxidation reaction of studied components [31].

(2-19)
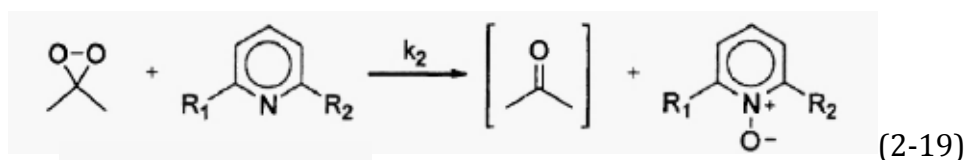
In another study, the oxidation of tertiary nitrogen components to N-oxides has been tried by sodium percarbonate using various Rhenium-based catalysts in presence of acetic acid at 50 ˚C. High oxidation yield was found using this method and metyltrioxorhenium was the most effective catalyst among various catalysts studied. Presence of acetic acid was reported to be necessary because it helped in releasing hydrogen peroxide from sodium percarbonate. The produced hydrogen peroxide then would react with nitrogen compounds to produce N-oxides. The result of sodium percarbonate oxidation was compared to hydrogen peroxide oxidation. The results showed a better yield using sodium percarbonate as oxidizer due to catalyst deactivation during hydrogen peroxide oxidation because of the presence of

water. Sodium perborate was found to be unable to oxidize nitrogen compounds [32].

Anhydrous tetra-butyl hydroperoxide (TBHP) was also used as an oxidizer to produce N-oxides from tertiary nitrogen compounds at 110 ℃ in presence of alumina supported MoO_3 as the catalyst. Aliphatic tertiary amines were reported to be the most reactive components while substituted anilines were more reactive compared to pyridines. The catalyst was reported to be reusable and recyclable [33].

5- Summary

The sulfur content of most coal types varies from 1.0 to 4.0-wt% and it can be classified in two groups: inorganic compounds and organic compounds. Inorganic sulfur usually appears the forms of sulfates or disulfides (pyrite and marcasite). Organic sulfur containing compounds are classified based on the type of functional group in their structure, namely sulfides, disulfides, thiols, thiophenes and compounds containing thiophene ring [9]. The total amount of nitrogen varies from 0.4 to 2-wt% and it is mostly available in organic form. Pyrrolic-type nitrogen is the most abundant nitrogen functionality in solid coal, while the pyridinic-type nitrogen increases with coal rank [10].

During the coal liquefaction process, the structure of nitrogen compounds does not change significantly [10]. However, the overall abundance of sulfur compounds decreases and the structure of these compounds shifts to more polycyclic aromatic forms [13].

Oxidative heteroatom removal is one of the chemical cleaning processes that can reduce the organic heteroatom content of coal to some extent. Different oxidizing agents have been used to remove the organic sulfur of coal such as air [15, 16], hydrogen peroxide [21], percarboxylic acids [17], etc. The studied methods are found to be able to remove the aliphatic sulfur

compounds in significant amount, while most of them are unable to remove the heterocyclic compounds. However, peracetic acid is reported to remove a part of the thiophinic structure along with aliphatic types [17]. In most of the studied methods, the oxidative desulfurization process does not significantly affect the burning quality and heat value of coal.

There is a few literature available on oxidative Nitrogen removal methods, while more research is done on oxidative desulfurization. However, there are some investigations available on the oxidation of nitrogen compounds for applications other than coal cleaning. These investigations can help in finding a suitable method to oxidize the nitrogen compounds available in coal and coal liquids. Several oxidizing agents are used to produce N-oxides by oxidation of the parent nitrogen compound using both catalytic and non-catalytic methods. Percarboxylic acids are the most used oxidizing agent for direct N-oxidation of heterocyclic nitrogen compounds at low temperatures [27]. In cases that hydrogen peroxide is used as the oxidizing agent, the use of a catalyst seems to be necessary [23].

6- References

[1] *Reviews in Coal Science: The Problems of Sulfur*; IEA Coal Research: London, 1989; pp 3, 11-13, 34-35.

[2] Kawatra, S.K.; Eisele ,T. C. *Coal Desulfurization - High efficiency Preparation Methods*, Taylor & Francis Inc.: New York, 2001; p 321.

[3] Kentucky Geological Survey, http://www.uky.edu/KGS/coal/coalcomp.htm, (accessed May, 2012).

[4] Berkowitz, N*. An Introduction to Coal Technology,* 2nd ed.; Academic Press. Inc.: San Diego, 1994; pp 13, 32, 346, 362-363.

[5] http://www.coalscience.com/cc.htm (accessed May, 2012)

[6] Fischer-Tropsch Archive, The Chemistry of Coal Liquefaction, http://www.fischer-tropsch.org/DOE/DOE_reports/12163/fe12163-C.pdf, (accessed May 2012).

[7] Vogler, L. *Canadian Coal Deposits* [Online]; Technische Universität Bergakademie Freiberg: Germany; pp 3-4. http://www.geo.tu-freiberg.de/oberseminar/os06_07/Canadian%20Coal%20Deposits%20-%20Luise%20Vogler.pdf (accessed May 2012).

[8] Attar, A.; Corcoran, W. H. Sulfur Compounds in Coal, *Industrial & Engineering Chemistry Product Research and Development* **1977**, *16*, 168–170.

[9] Davidson R.M. *Organic Sulphur in Coal;* IEA Coal Research: London, 1993; p 30.

[10] Davidson, R. M. *Nitrogen in Coal*; IEA Coal Research: London, 1994; pp 3-6.

[11] Höök M.; Aleklett K. A Review on Coal-to-Liquid Fuels and Its Coal Consumption, *International Journal of Energy Research* **2010**, *34*, 848–864.

[12] National Energy Technology Laboratory (NETL), Direct Liquefaction Processes, http://www.netl.doe.gov/technologies/coalpower/gasification/gasifipedia/6-apps/6-3-2_direct-liquefaction.html, (accessed May 2013)

[13] Winans, R. E.; Joseph, J. T.; Fisher, R. B. Changes in Organic Sulfur Compounds in Coal Macerals during Liquefaction, *ACS Division of Fuel Chemistry Preprints* **1994**, *39 (2)*, 434-437.

[14] Ogunsola, O. M. *Removal of Nitrogen from Liquid Fuels by Supercritical Fluid* in *Ultraclean Transportation Fuels* [Online], American Chemical Society: Washington, 2007, pp 160-164. http://pubs.acs.org/doi/abs/10.1021/bk-2007-0959.ch012 (accessed June 2013)

[15] Mezey, E. J.; Singh, S.; Hissong, D. W. *Fuel Caotaminants, Volume 2: Removal Technology Evaluation* [Online], Industrial Environmental Research Laboratory: North Carolina, 1976; pp 95. http://nepis.epa.gov (accessed June 2013)

[16] Kodera, Y.; Ukegawa, K.; Mito, Y.; Komoto, M.; Ishikawa, E.; Nakayama, T. Solvent Extraction of Nitrogen Compounds from Coal Liquids, *Fuel* **1991**, *70 (6)*, 765-769.

[17] Borah, D.; Baruah M. I. Oxidation of High Sulphur Coal. 3. Desulfurization of Organic Sulphur by Peroxyacetic Acid (Produced In Situ) in Presence of Metal Ions, *Fuel Processing Technology* **2005**, *86*, 959-976.

[18] Aida, T.; Yamamoto, D. Oxidative Desulfurisation of Liquid Fuels, *ACS Division of Fuel Chemistry Preprints* **1994**, *39 (2)*, 623-626.

[19] Borah, D.; Baruah M. K. Kinetic and Thermodynamic Studies on Oxidative Desulphurisation of Organic Sulphur from Indian Coal at 50-150 °C, *Fuel Processing* Technology **2001**, *72*, 83-101.

[20] Liu, K.; Yang, J.; Jia, J.; Wang, Y. Desulphurization of Coal via Low Temperature Atmospheric Alkaline Oxidation, *Chemosphere* **2008**, *71*, 183-188.

[21] Borah, D.; Baruah, M.; Haque, I. Oxidation of High Sulphur Coal, Part 2. Desulphurisation of Organic Sulphur by Hydrogen Peroxide in Presence of Metal Ions, *Fuel* **2001**, *80*, 1475-1488.

[22] Attia, Y.; Lei, W. Processing and Utilization of High Sulfur Coals, *Elsevier* **1987**, *2*, 202-212.

[23] Rout, L.; Punniyamurthy, T. Silica-Supported Vanadium-Catalyzed N-Oxidation of Tertiary Amines with Aqueous Hydrogen Peroxide, *Advanced Synthesis & Catalysis* **2005**, *347*, 1958–1960.

[24] Thomson, A.B. Degradation of Quinoline by Wet Oxidation – Kinetics Aspects and Reaction Mechanisms, *Water Research* **1998**, *32*, 136-146.

[25] De Souza, W. F.; Guimarãesb, I. R.; Guerreiro, M.C.; Oliveira, C. A. Catalytic Oxidation of Sulfur and Nitrogen Compounds from Diesel Fuel, *Applied Catalysis A: General* **2009**, *360*, 205-209.

[26] de Klerk, A. *Refining and Refineries at a Glance,* in *Fischer-Tropsch Refining* [Online]; Wiley-VCH Verlag GmbH & Co: Germany, 2011; pp 25. http://onlinelibrary.wiley.com/doi/10.1002/9783527635603.ch2/summary (accessed May 2013)

[27] *Organic Chemistry: Chemistry of the Heterocyclic N-oxides;* Katritzky, A. R.; Lagowski, J. M.; Academic Press: London, 1971; Vol 19, pp 21-22.

[28] *The Chemistry of Heterocyclic Compounds: Quinolines, Part II;* Jones, G.; John Wiley and Sons Ltd: New York, 1982; Vol. 32, p 379.

[29] Dutka, V.S.; Matsyuk, N.V.; Dutka, Yu.V. Influence of a Reaction Medium on the Oxidation of Aromatic Nitrogen-Containing Compounds by Peroxyacids, *Russian Journal of Physical Chemistry A* **2011**, *85*, 45-50.

[30] Rong, D.; Phillips, V.; Rubio, R.; Castro, M. A.; Wheelhouse, R. A Safe, Convenient and Efficient Method for the Preparation of Heterocyclic N-oxides Using Urea Hydrogen Peroxide, *Tetrahedron Letters* **2008**, *49*, 6933–6935.

[31] Winkeljohn W.R.; Leggett-Robinson, P.; Peets, M.R.; Strekowski, L.; Vasquez, P. C.; Baumstark, A.L. N-Oxidation of 2-Sunstituted Pyridines and Quinolines by Dimethyldioxirane: Kinetics and Steric Effects, *Heterocyclic Communications* **2011**, *13*, 25–28.

[32] Suman, J.; Jomy, K.; Bir, S. Rhenium-Catalyzed Highly Efficient Oxidations of Tertiary Nitrogen Compounds to N-Oxides Using Sodium Percarbonate as Oxygen Source, *ChemInform* **2007**, *38*, 2661-2663.

[33] Suman, J.; Jomy, K.; Bir, S. Alumina Supported MoO3: an Efficient and Recyclable Catalyst for Selective Oxidation of Tertiary Nitrogen Compounds to N-oxides Using Anhydrous TBHP as Oxidant under Mild Reaction Conditions, *Catalysis Letters* **2007**, *115*, 8-12.

Chapter 3

Oxidation of Quinoline by Perdecanoic Acid

1- Introduction

The first step in oxidative denitrogenation methods involves the transformation of nitrogen atom to its oxidized form in order to expand the valence shell of nitrogen and decrease the N-C bond strength. Quinoline is one of the major pyridinic nitrogen compounds in coal and coal liquids, and also, it contributes to inhibition of acidic catalysts due to its basic nature. Therefore, it has been selected as a model compound representing the nitrogen structure of coal liquids.

Amongst all the studied oxidation methods to produce N-oxides (presented in chapter 2, section 4-2), the oxidation of nitrogen containing compounds by perdecanoic acid has the most economical reaction conditions such as: low reaction temperature (30-55 ℃), low reaction time (20-30 minutes), atmospheric pressure (argon atmosphere) and no need of catalyst [1]. Also, the chemicals required to synthesize perdecanoic acid are readily available commercially. Therefore, the oxidation of quinoline is studied following this procedure. Perdecanoic acid was synthesized using the reaction of hydrogen peroxide with decanoic acid. The synthesized mixture then was used as an oxidizer to produce quinoline N-oxide. The only alteration to the experimental procedure is use of atmospheric air instead of an inert environment for oxidation experiments, since the oxygen in air might actually help the oxidation reaction. The experimental procedures, structure of oxidation products, conversion and mass balance data are discussed in this chapter.

2- Experimental

2-1- Materials

- Quinoline

  Make: Sigma Aldrich
  CAS number: 91-22-5
  Purity: 98%
  Molecular weight: 129.16
  Melting point: -17 - -13 ℃
  Boiling point: 237 ℃
  Color: light yellow
  Form: clear, liquid

- Quinoline N-oxide hydrate

  Make: Sigma Aldrich
  CAS number: 64201-64-5
  Purity: 97%
  Molecular weight: 145.16 (anhydrous basis)
  Melting point: 52-55 ℃
  Water content: 1.91 mole/mole of quinoline N-oxide hydrate
  Color: yellow to brown
  Form: powder

- Acetone

  Make: Caledon
  CAS number: 67-64-1
  Purity: 99.5%
  Molecular weight: 58.08
  Freezing point: -94.6 ℃
  Boiling point: 56.2 ℃
  Color: colorless
  Odor: sweet
  Form: liquid

- Distilled water

  Resistivity @ 25 °C: 15 MΩ•cm
  Molecular weight: 18.02
  Freezing point: 0 ℃

Boiling point: 99.98 ℃
Color: colorless
Odor: odorless
Form: liquid

- Decanoic Acid

  Make: Sigma Aldrich
  CAS number: 334-48-5
  Purity: ≥ 98.0%
  Molecular weight: 172.26 $g/_{mole}$
  Melting point: 27-32 ℃
  Boiling point: 268-270 ℃
  Color: white
  Form: crystalline

- Hydrogen Peroxide

  Make: Fisher Scientific
  CAS number: Hydrogen peroxide: 7722-84-1
  　　　　　　Water: 7732-18-5
  Purity: 50.3 %
  Molecular weight: 34.01 $g/_{mole}$
  Melting point: -52 ℃
  Boiling point: 114 ℃
  Color: colorless
  Form: liquid

- Sulfuric acid

  Make: Fischer Scientific
  CAS number:　　*water:* 7732-18-5
  　　　　　　Sulfuric acid: 7664-93-9
  Purity: ≥95%
  Molecular weight: 98.08 $g/_{mole}$
  Melting point: 10 ℃
  Boiling point: 290-338 ℃
  Color: clear, colorless to brown
  Form: liquid

- Diethyl ether

  Make: Sigma Aldrich
  CAS number: 60-29-7

Purity: ≥ 99.0 %

Molecular weight: 74.12 $g/_{mole}$

Melting point: -116 ℃

Boiling point: 34.6 ℃

Color: colorless

Form: liquid

- Chloroform (stabilized with ethanol)

  Make: Fischer Scientific

  CAS number: *Chloroform:* 67-66-3

                  Ethyl alcohol: 64-17-5

  Purity: 99.9% (HPLC grade)

  Composition: 99% chloroform, 1% ethyl alcohol

  Molecular weight: 119.38 $g/_{mole}$

  Melting point: -63 ℃

  Boiling point: 60.5-61.5 ℃

  Color: colorless

  Form: liquid

- Acetic acid

  Make: Sigma Aldrich

  CAS number: 64-19-7

  Purity: ≥99.7%

  Molecular weight: 60.05 $g/_{mole}$

  Melting point: 16.2 ℃

  Boiling point: 117-118 ℃

  Color: colorless

  Form: liquid

- Sodium thiosulfate Pentahydrate Solution (0.1N)

  Make: Fischer Scientific

  CAS number: *water:* 7732-18-5

                  Sodium thiosulfate Pentahydrate: 10102-17-7

  Melting point: 0 ℃

  Boiling point: 100 ℃

  Color: colorless

  Form: liquid

- Potassium iodide

  Make: Fischer Scientific

CAS number: 7681-11-0

Purity: ≥ 99.0%

Molecular weight: 166.00 $g/_{mole}$

Melting point: 680 ℃

Boiling point: 1330 ℃

Color: white

Form: solid

- Starch

Make: Fischer Scientific

CAS number: 9005-84-9

Purity: 100%

Molecular weight: 162.01 $g/_{mole}$

Melting point: 256-258 ℃

Color: white

Form: powder solid

2-2- Equipment

- Thermogravimetric Analyzed (TGA)

Make: Mettler Toledo

Model: TGA/DSC 1

Pans: 70 µL Alumina crucibles with lid

Carrier gas: Nitrogen

Temperature Program: initial T =40 ℃, ramp= 20 ℃/min, final T= 150 ℃, hold 20 min

- Infrared Spectroscopy

Make: ABB

Model: MB3000

Attachment: MIRacle™ ATR for FTIR spectrometers (make: PIKE technologies)

KBr: PIKE Technologies, product NO: 160-8010

Manual KBR pellet press: PIKE technologies, product NO.: 161-1100, 161-1627

Resolution: 2 wavenumbers

Spectra: 100 scans

Software: Horizon MB

- Gas Chromatography-Mass Spectrometry (GC-MS)

Make: Varian Inc.
Model: Saturn 2200 (GC model: CP 3800)
Carrier gas: Helium 1 mL/min
Auto injector: Varian CP-8410
GC Column: Make: Varian Inc., Model: CP7430 (30 m ×0.25mm i.d.)
GC Temperature program: initial T =50 ℃, hold 10 min; ramp= 10 ℃/min, final T= 320 ℃, hold 10 min; inj. T= 320 ℃, FID T= 320 ℃, TCD T= 220 ℃
GC Detectors: FID/TCD
MS mass range: 50-350 m/z
MS ionization mode: starts at 3.5 min

- Rotary Evaporator (Rota-vap)

  Make: Heidolph Instruments
  Model: Hei-Vap Advantage
  Vacuum pump model: Rotavap Vario
  Temperature: 60 ℃
  Vacuum pressure: chosen based on the required vacuum for the solvent to boil at 40 ℃

- Fluidized Sand bath

  Make: Omega
  Model: FSB-3
  Temperature range: 50-600 ℃

- UV-Vis Spectrometer

  Make: Shimadzu Corporation
  Model: UV-2700
  Wavelength range: 185-800 nm
  Resolution: 1 nm
  Cell: rectangular quartz cells (make=Mandel Scientific Inc., model=Sn-1/Q/10)
  Software: UVProbe

- High-Performance Liquid Chromatography (HPLC)

  Make: Waters Corporation
  Model: Alliance (e2695 separation module)
  Column: 3 series of μBondapak Amino (NH2) column, 125Å, 10 μm, 3.9 mm X 300 mm, 1/pkg (model= WAT084040)
  Method: solvent= Chloroform (flow: 1 mL/min), column T= 35±5 ℃, pressure high   limit= 4000 psi, sample volume= $1\mu L$
  Detectors: 1- Waters 2998 Photodiode Array (PDA): wavelength range= 210-400 nm, resolution= 1.2 nm, sampling rate= 10 points/sec

- Refrigerated/Heating Circulator

  Make: Julabo USA Inc.
  Model: F25-HE
  Bath Fluid: Julabo Thermal C10 (chemical= polydimethylsiloxane, CAS#=63148-62-9, working range=-20-160 ℃)
  Working Temperature Range: -28 – 200 ℃
  Temperature Stability: ±0.01
  Pump Capacity Flow: 22.26 L/min

2-3- Procedures

As it's earlier discussed in chapter 2, section 4-2-1, peracids are able to oxidize heterocyclic nitrogen compounds at low temperature and pressure without using a catalyst. The longer chain peroxy carboxylic acids are stronger oxidizers compared to the shorter chain ones. Perdecanoic acid has been reported to successfully oxidize the heterocyclic nitrogen structures including quinoline at 30-55 ℃ [1]. Therefore, in this research, the oxidation experiments were performed using perdecanoic acid as the oxidizing agent at 50 ℃. The procedures for synthesis of perdecanoic acid, testing the peroxide content of synthesized mixture and the oxidation of quinoline using this mixture are explained in the following sections.

2-3-1- Synthesis of perdecanoic acid

17.2 g (0.1 mole) of decanoic acid was dissolved in 30 g. of sulfuric acid with efficient agitation. This solution was cooled to 10 ℃ in the internal bath of a refrigerated circulator. Then, using a burette, 10.2 g. (0.15 mole) of hydrogen peroxide (50%) was slowly added drop-wise to the solution, while stirring and the temperature was maintained between 20-30 ℃. After addition of hydrogen peroxide over the period of 20 minutes, the mixture was stirred for another 40 minutes (total reaction time equals to 1 hour). 100 mL of water was added slowly to the reaction mixture to precipitate perdecanoic acid. Then, the reaction mixture was extracted with diethyl ether

and then, the ether phase was separated and washed with water several times until free of sulfuric acid and hydrogen peroxide. Then, it was dried over anhydrous sodium sulfate followed by filtration using a filter paper [2]. Finally, diethyl ether was evaporated using a rotary evaporator (T=40 ℃, P= 600 mbar, drying time= 3 hours). The block diagram of this procedure is shown in Figure 3-1.
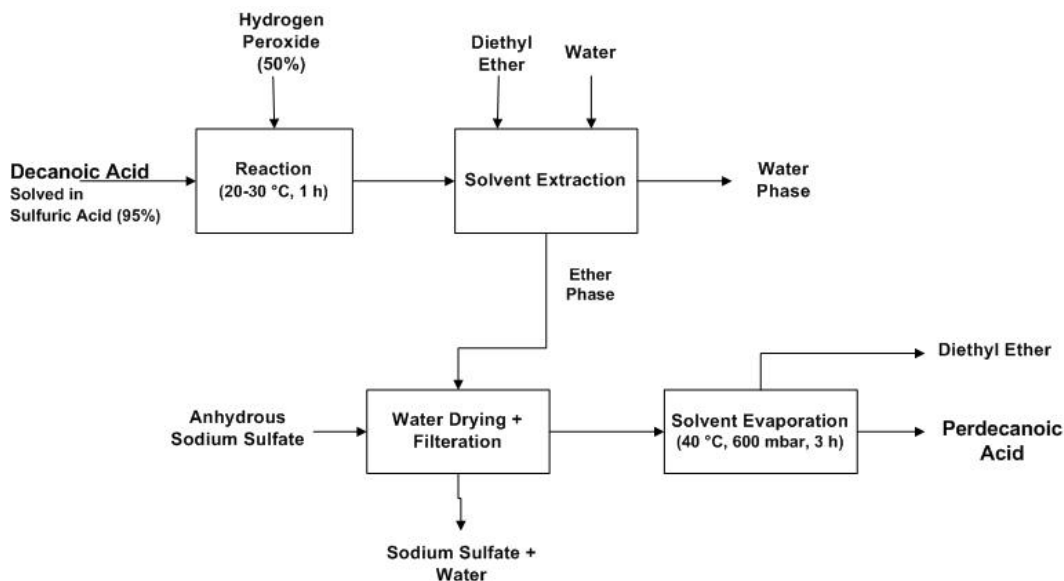
Figure 3-1- Block diagram for synthesis procedure of perdecanoic acid

The produced material was analyzed by IR spectroscopy to check the structure. The decomposition of long-chain peracids happens at a slow but significant rate at room temperature [2]. Therefore, the synthesized perdecanoic acid was stored in a freezer and the mixture was tested for peroxide content right before performing each oxidation experiment.

2-3-2- Peroxide content

The typical method suggested for determination of rancidity in oils has been used to determine the peroxide content of the synthesized perdecanoic acid mixture [3]. The sample was dissolved in a mixture of solvents (30 mL of acetic acid, 20 mL of chloroform). 1 mL of saturated potassium iodide solution (1.4 g potassium iodide in 1 mL of distilled water) was added to the

mixture and exactly one minute later, 100 mL of water was added to the solution. Standard sodium thiosulfate solution (0.1 N) was used to titrate the liberated iodine using starch as an indicator. Toward the last, vigorous shaking was required to titrate the last amount of iodine in the chloroform phase. The results can be expressed as grams of peroxide per 100 g of sample, i.e. weight percentage, calculated using the formula 3-1 [3].

$$Peroxide\ content\ (wt\%) = \frac{0.5 \times V \times N \times M}{10 \times m} \quad (3\text{-}1)$$

$V = volume\ of\ used\ thiosulfate\ (mL), \qquad N = normality\ of\ thiosulfate$

$m = weight\ of\ sample\ (g), \quad M = molecular\ weight\ of\ peroxide\ (^g/_{mole})$

The block diagram of this method is shown in Figure 3-2. Also, a blank is carried out using the same method explained above.
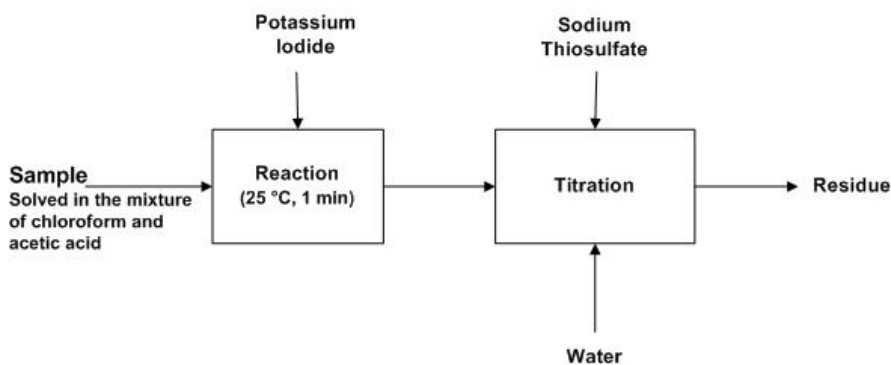
Figure 3-2– Block diagram of peroxide content test

2-3-3- Oxidation of quinoline using perdecanoic acid

The micro-reactor setup (material: Stainless steel, micro-reactor volume: 15 mL, setup total volume: 25 mL) was washed with acetone prior to experiment and then, dried using airflow. In the micro-reactor setup, quinoline and synthesized perdecanoic acid mixture were dissolved in chloroform and then, immediately the setup was heated to 50 ˚C using a sand bath. Excess amount of perdecanoic acid was used for the oxidation reaction

49

(calculated based on the peroxide content of the synthesized perdecanoic acid mixture). The exact weight of used materials is presented for each individual experiment in Table 3-2 in section 3-3. Temperature and pressure of set up were recorded every minute during the experiment. After 30 minutes of reaction time, the set up was cooled down to room temperature using airflow. The product was weighed and analyzed by UV spectroscopy, HPLC, IR spectroscopy and GC-MS right away. It has also been tested for peroxide content. Then, it was stored in a freezer to avoid decomposition. The product of the oxidation experiment was also tested (by UV spectroscopy) 2, 4 and 7 days after the date of performing the experiment. This helps to study the possible changes in the composition of products. Figure 3-3 shows the block diagram of the quinoline oxidation experiment.
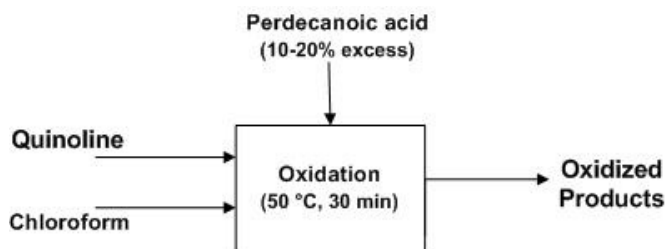
Figure 3-3– Block diagram of quinoline oxidation experiment

3- Result and Discussion

3-1- Synthesis of perdecanoic acid

The crude perdecanoic acid is a white solid at room temperature (melting point= 41 $^{\circ}$C) [2]; however, using the method explained in section 2-3-1, what's been produced was a mixture of solid and liquid phases at room temperature, almost like a pasty phase (phase of a material between solidus and liquidus temperatures). This indicates the presence of impurities in the produced perdecanoic acid. At the temperature of the freezer, the mixture completely crystallized to a white solid. The major impurities are either

decanoic acid or hydrogen peroxide. Crystallization of the synthesized mixture from petroleum naphtha (at -20 °C) or hexane can yield analytically pure perdecanoic acid [2]. However, the decanoic acid present in the synthesized mixture does not participate in the oxidation reaction and the present hydrogen peroxide might actually help in oxidizing quinoline. Therefore, the purity of oxidizing agent is not of significant importance in the studied oxidation experiments and the crude synthesized mixture was used without being recrystallized. Prior to performing each oxidation experiment, the crude perdecanoic acid mixture was tested for peroxide content using the method explained in section 2-3-2. This was necessary to calculate the correct weight required to have excess amount of perdecanoic acid available for oxidation of quinoline.

3-2- Peroxide content test

Most of the organic peroxides can be reduced by iodide ions in an acidic environment. The reaction is as follows:

$$ROOR' + 2I^- + 2H_2O \rightarrow I_2 + ROH + R'OH + 2OH^- \qquad (3\text{-}2)$$

Generally, the peroxide content test must be performed in the absence of oxygen, such as in nitrogen or carbon dioxide environment, to avoid the reaction of oxygen of air with iodide ions. Moreover, the present hydrogen peroxide in the synthesized mixture can also react with iodide ions. In mildly acidic condition and low reaction temperature (0-5 °C) the reaction of hydrogen peroxide is extremely slow [4]. However, this slow reaction still results in some error in the final peracid content data. Performing the titration at fixed time intervals and extrapolation of data to zero time can eliminate this error, giving the actual concentration of peracid in the sample. Afterwards, the rate of hydrogen peroxide reaction can be increased by addition of ammonium molybdate and continuing the titration gives the concentration of hydrogen peroxide [5]. These conditions give an accurate result but, on the other hand, complicate the experimental procedure. If there

is no need of high accuracy, the experiment can be rapidly performed under air and also, the hydrogen peroxide interference can be neglected. This simplifies the experimental procedure and also, gives good enough results for peracids since they react with iodide ion much faster than the oxygen of air and hydrogen peroxide in mild acidic conditions.

After completion of reaction, water is added to the solution and the liberated iodine is titrated with sodium thiosulfate according to the following reaction (formula 3-3) [4].

$$2S_2O_3^{--} + I_2 \rightarrow S_4O_6^{--} + 2I^- \qquad (3\text{-}3)$$
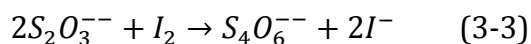
Usually aqueous acetic acid is used as the solvent for the above reaction, since the liberated iodine can be titrated with thiosulfate in one phase. But, because long chain peracids are not soluble in aqueous acetic acid, a mixture of chloroform and acetic acid has been chosen for determining the peracid content of the synthesized sample [4]. This is the same as the method suggested for determination of rancidity in oils [3]. The presence of chloroform results in a two-phase titration, which requires vigorous stirring; but it clearly shows the intense color of iodine.

The peroxide content test has been done the day before performing oxidation experiments. Table 3-1 shows the result of the three tests performed and also the mean and standard deviation (SD) of calculated peroxide content data.

<p style="text-align:center">Table 3-1- Results of three peroxide content tests performed on synthesized perdecanoic acid mixture</p>

Sample weight (g)	Consumed Sodium Thiosulfate (mL)	Peroxide content		
		Calculated amount (wt%)	Mean	SD
0.44	22.9	48.9		
0.41	21.5	49.3	49.2	0.23
0.40	21.0	49.3		

Although the peroxide content test proves the presence of about 49.2-wt% of peroxides in the synthesized mixture, it doesn't provide any information on the structure of the formed peroxide. If perdecanoic acid has been formed, its reaction with iodide ions (during the peroxide content test) must lead to formation of decanoic acid. In the residue of peroxide content test, the chloroform layer is the part containing the formed carboxylic acids and the water layer is the part containing iodine, potassium iodide, sodium thiosulfate, starch and acetic acid. Therefore, to confirm the formation of perdecanoic acid, the chloroform layer has been separated and washed with water several times and then, it was analyzed by GC-MS. The result confirms the presence of decanoic acid.

3-3- Oxidation of quinoline

The oxidation experiment was performed three times to check the repeatability of results. Table 3-2 shows the conditions of each experiment.

Table 3-2- Reaction conditions of three performed quinoline oxidation experiments using synthesized perdecanoic acid mixture and chloroform as the solvent

Test	Reactants weight (g)			Solvent weight (g)	Reaction temperature (°C)	Reaction time (min)
	Quinoline	Perdecanoic acid				
		Total (g)	excess (%)			
1	0.51	1.78	17.8	3.99	50	30
2	0.50	1.65	11.4	4.00	50	30
3	0.50	1.68	13.4	3.93	50	30

The product of each test was weighted after performing the experiment and then, stored in a freezer to avoid decomposition of the produced compounds. On the same day of performing the oxidation experiment, the products were analyzed by FTIR, UV Spectroscopy, HPLC and GC-MS to identify the new structures formed. The results are presented in the section 3-3-1. The products were also analyzed in 2, 4 and 7 days (after the date of performing oxidation experiment) by UV spectroscopy. Using the UV

spectroscopy results, the concentration of quinoline and quinoline N-oxide in the products were calculated on the same day, 2 days, 4 days and 7 days after performing the oxidation experiments. These data are discussed in section 3-3-2.

3-3-1- Structure of products

If the oxidation of quinoline leads to oxidation of nitrogen atom, it is expected to have both quinoline and quinoline N-oxide in the products (it is unlikely to have 100% conversion for the oxidation reaction). Also, since perdecanoic acid decomposes back to decanoic acid at 50-100 ℃ [6], the unreacted perdecanoic acid must be converted to decanoic acid during oxidation experiment. The peroxide content test on the oxidation products resulted in 0% peroxide content. This again shows that the perdecanoic has completely decomposed during the oxidation reaction. Therefore, the oxidation products must only consist of quinoline, quinoline N-oxide and decanoic acid (all dissolved in chloroform). A reference solution was made using these four compounds and it was analyzed along with oxidation products using the same spectroscopic and chromatographic methods. The results were compared for any difference.

Figure 3-4 shows the IR spectrum of the oxidation products in comparison with IR spectra of chloroform, quinoline, quinoline N-oxide hydrate, decanoic acid and the reference solution. Almost all the chloroform content of both products and reference solution was evaporated before IR spectroscopy analysis, because the high chloroform content of these two samples results in large absorption peaks, which may make the other peaks difficult to observe. As expected, the IR spectra of reference solution and oxidation products match with each other with no significant difference in Figure 3-4. In the IR spectrum of quinoline N-oxide (spectrum b, brown line), the four absorption peaks observed in the wavenumber range from 1190 to 1300 cm-1 are due to N-O group [7]. However, decanoic acid (spectrum f, gray line) also absorbs in

this region. Due to the overlapping of absorption peaks, the formation of N-O bond cannot be confirmed with IR spectroscopy.
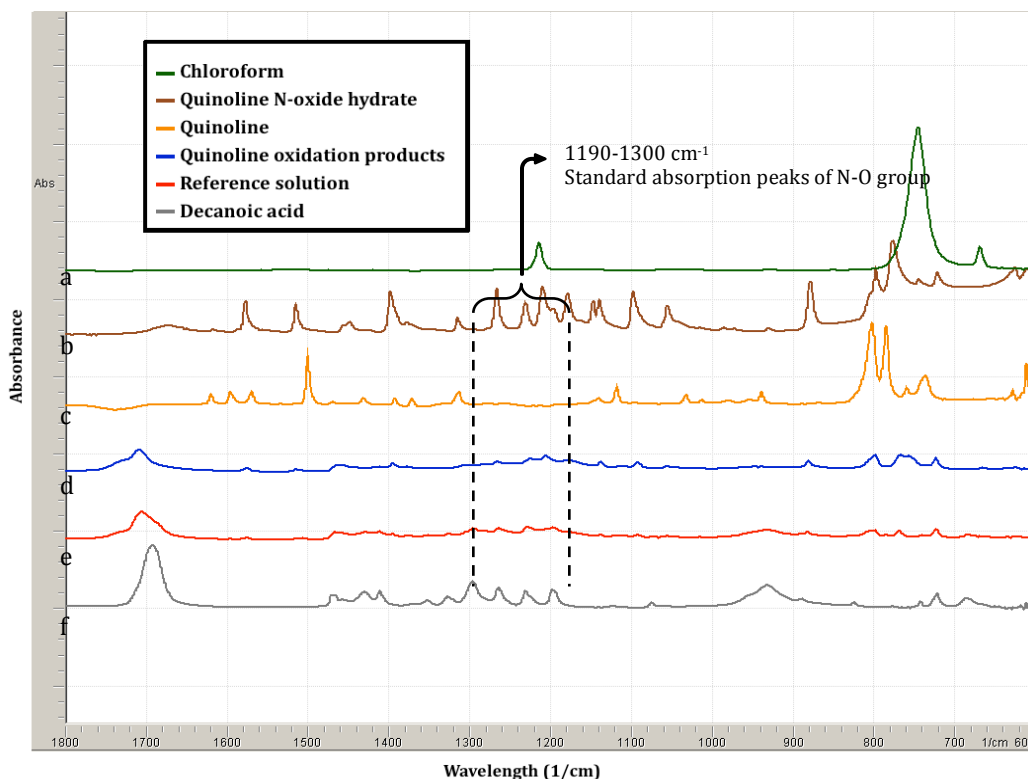
Figure 3-4- IR spectrum of a) green line – chloroform, b) brown line – quinoline N-oxide hydrate, c) yellow line – quinoline, d) blue line – reference solution, e) red line- quinoline oxidation products using perdecanoic acid at 50 °C and f) gray line- decanoic acid [using ATR attachment]

Figure 3-5 shows the UV spectra of oxidation products in comparison with quinoline, quinoline N-oxide and decanoic acid. All the four solutions were prepared by diluting the sample in chloroform. Chloroform was also used as the reference to eliminate absorption bands of solvent. The analysis was done in both ultraviolet and visible regions (185-800 nm). However, since no absorption was observed in the visible region, only the ultraviolet region is shown in Figure 3-5. It must be noted that the commercially available quinoline N-oxide is in the hydrate form and also, it easily absorbs water from environment. This water content might affect the UV spectra of samples. Therefore, prior to preparing the solutions, the quinoline N-oxide hydrate

was dried in TGA at 150 °C for 20 minutes. The dried sample was dissolved in a vial full of chloroform right away and then, it was immediately used for analysis by UV spectroscopy.
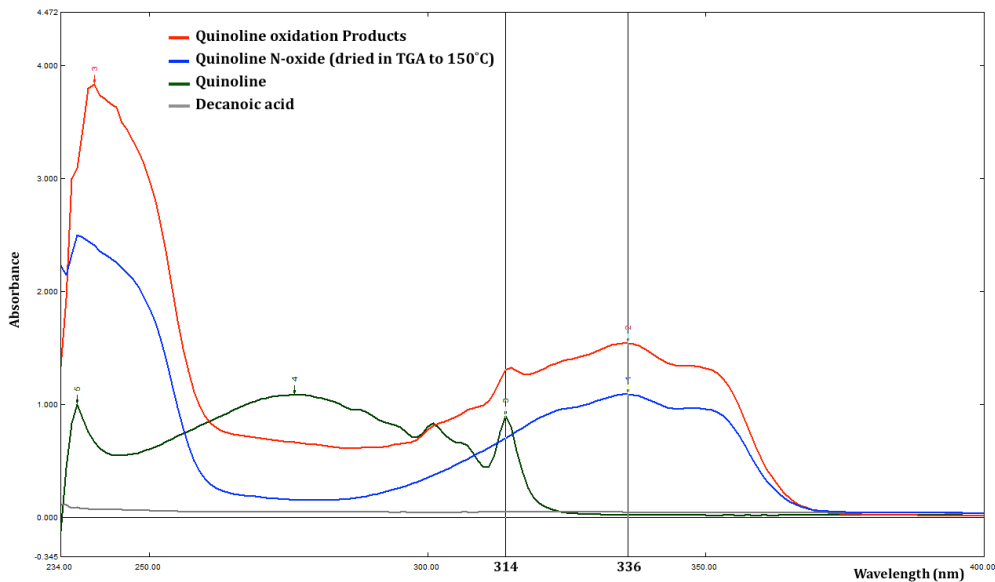
Figure 3-5- UV spectra of a) green line - quinoline, b) blue line - quinoline N-oxide (dried in TGA to 150 °C), c) gray line – decanoic acid and d) red line- quinoline oxidation products using perdecanoic acid at 50 °C

In Figure 3-5, the UV spectrum of oxidation products (red line) seems to be the sum of UV spectra of quinoline (green line) and quinoline N-oxide (blue line). No other absorption peaks seem to be present. This confirms the absence of any other compound that has significant absorption peaks in the ultraviolet and visible regions. The absorptions at wavenumbers 314 nm and 336 nm are used to determine the concentration of quinoline and quinoline N-oxide in the oxidation products. This is later discussed in detail in section 3-3-2.

No absorption band is observed for decanoic acid in the ultraviolet region. However, very high concentrations of decanoic acid can shift the baseline a little. The UV spectrum of perdecanoic acid is found to be the same as decanoic acid. In general, organic peroxides have very similar absorption bands with their corresponding non-peroxy analogues [4]. Therefore, even if

a trace amount of perdecanoic acid hasn't decomposed to decanoic acid during the oxidation experiment, it doesn't affect the UV spectrum of oxidation products.

Although the UV spectroscopy of oxidation products only shows the presence of quinoline and quinoline N-oxide, it is unable to reveal the presence of any other compound that do not absorb in the ultraviolet and visible regions. It is necessary to use a chromatographic method to properly separate and identify the compounds present in the oxidation products. Quinoline N-oxide is known to lose its oxygen in the heated inlet of an analyzing instrument [7] such as a gas chromatograph. For example, when commercially obtained 97% pure quinoline N-oxide hydrate is analyzed by GC-MS, not only does some of the quinoline N-oxide decompose to lose its oxygen, causing a big quinoline peak, but also some new compounds are formed (Figure 3-6). Therefore, a chromatographic method must be used that does not heat up the sample for analysis.
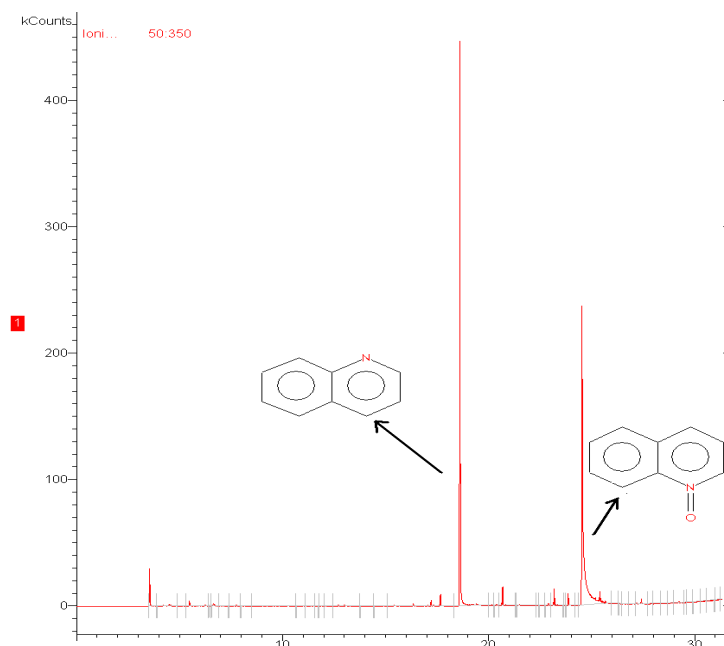
Figure 3-6- GC-MS analysis of quinoline N-oxide hydrate

HPLC analysis of the reference solution (diluted in chloroform) at low temperature (35 ℃) shows that, not only it does not decompose the sample,

but also it is able to properly separate and identify quinoline and quinoline N-oxide. This is shown in Figure 3-7.

(a)

(b)

(c)

(d)
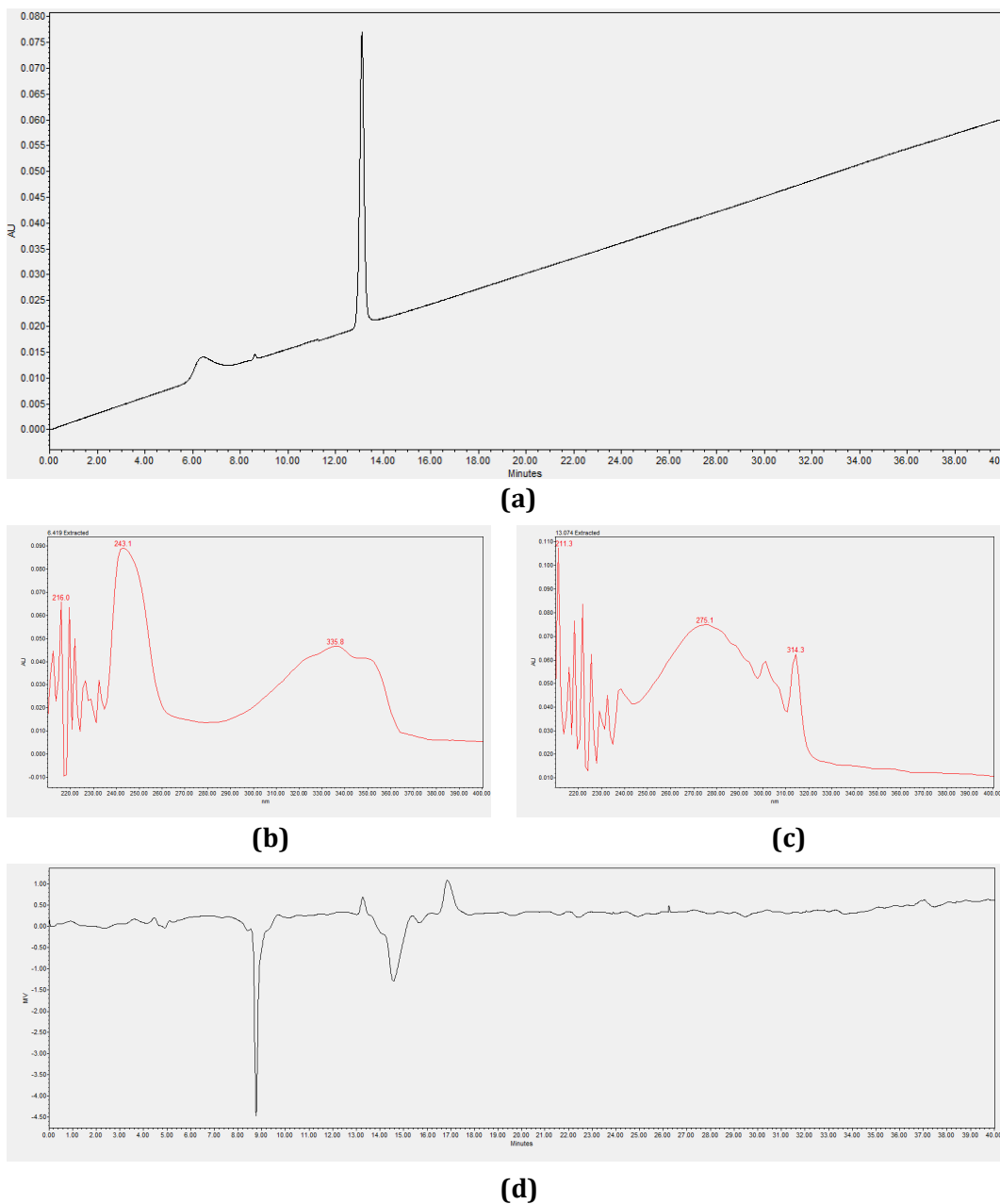
Figure 3-7- HPLC analysis of reference solution diluted in chloroform; a) extracted UV spectra at 275 nm, b) extracted UV spectra at retention time about 6.42 minutes, c) extracted UV spectra at retention time about 13.07 minutes and d) RI detector result

It must be noted that the UV detector of the HPLC provides a three-dimensional graph with retention time, wavelength and absorbance as the variables. Extracting this graph at a fixed wavelength gives a two-

dimensional chromatographic graph that shows any change in absorbance by retention time for that specific wavelength (Figure 3-7-a). This graph actually shows the presence of any new compound (beside the chemical used for stationary phase) that passes through the chromatography column, enters the sample cell of UV detector and absorbs light in the ultraviolet region. To properly identify each one of these detected compounds, the three-dimension UV graph must be extracted at the retention time corresponding to presence of that compound (Figures 3-7-b and 3-7-c) and then, the extracted graph must be compared with the UV spectra of pure compounds. The HPLC instrument also has a refractive index (RI) detector, which provides additional information on the presence of any other compounds that do not absorb in the ultraviolet region (Figure 3-8-d). It must be noted that there is about 0.25 minutes delay between RI detector and UV detector, causing 0.25 minutes difference in their retention times for the same compound.

In Figure 3-7, The UV graph extracted at retention time about 6.42 minutes (graph b) corresponds to UV spectrum of quinoline N-oxide shown in Figure 3-5 and the one extracted at retention time about 13.07 minutes (graph c) corresponds to UV spectroscopy of quinoline shown in Figure 3-5. It must further be noted that decanoic acid does not absorb in the ultraviolet region and therefore, the UV detector of HPLC is not able to detect it. The UV detector also shows the presence of another compound at retention time about 8.67 minutes. The extracted UV spectrum is shown in Figure 3-8. This peak is also observed in HPLC analysis of quinoline (diluted in chloroform), indicating that it must be an impurity of the quinoline used for oxidation experiment. The GC-MS analysis of quinoline sample, suggests that this impurity is iso-quinoline. The UV spectrum shown in Figure 3-8 also matches with UV spectrum of iso-quinoline [8].

Figure 3-8- Extracted UV spectra at retention time about 8.67 minutes in HPLC analysis of reference solution diluted in chloroform

Although the RI detector shows a lot of peaks (Figure 3-7-d), most of them are also available in the RI graph of a blank run, i.e. just chloroform (Figure 3-9). This proves the contamination of the column (which is mainly used for bitumen analyses) and therefore, all the RI results must be compared with the blank run to check whether RI detector has found a new compound in the sample. The only new peak in the RI graph of the reference solution (Figure 3-7-d) is observed at a retention time of about 13.25 minutes, which corresponds to quinoline present in the sample.
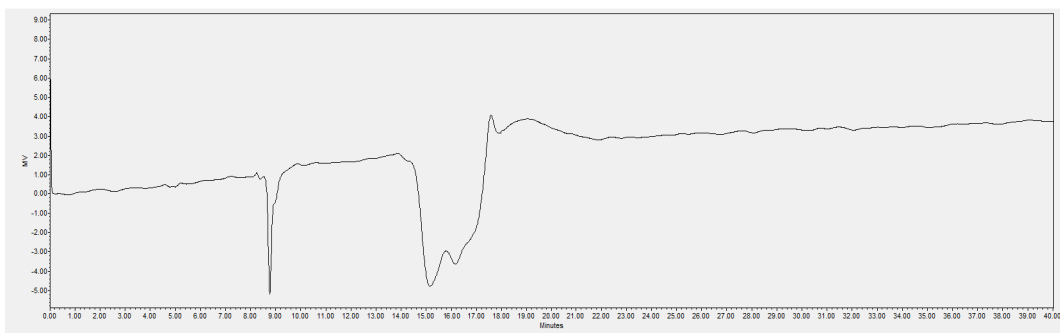
Figure 3-9- The RI detector result for HPLC analysis of a blank solution (just chloroform)

The RI detector is also unable to clearly indicate decanoic acid. This is due to the fact that chloroform is used as both the solvent and the stationary phase for HPLC analysis. The refractive indexes of chloroform and decanoic acid are too close to each other (chloroform= 1.44 at 30 °C, decanoic acid=

60

1.43 at 30 ℃ [9]). This makes the RI detector insensitive to decanoic acid in the mixture. Moreover, the RI detector does not show any peak for quinoline N-oxide. Thus, the refractive indexes of quinoline N-oxide and chloroform must be close to each other, too.

Figure 3-10 shows the HPLC analysis of quinoline oxidation products.

(a)

(b)

(c)

(d)
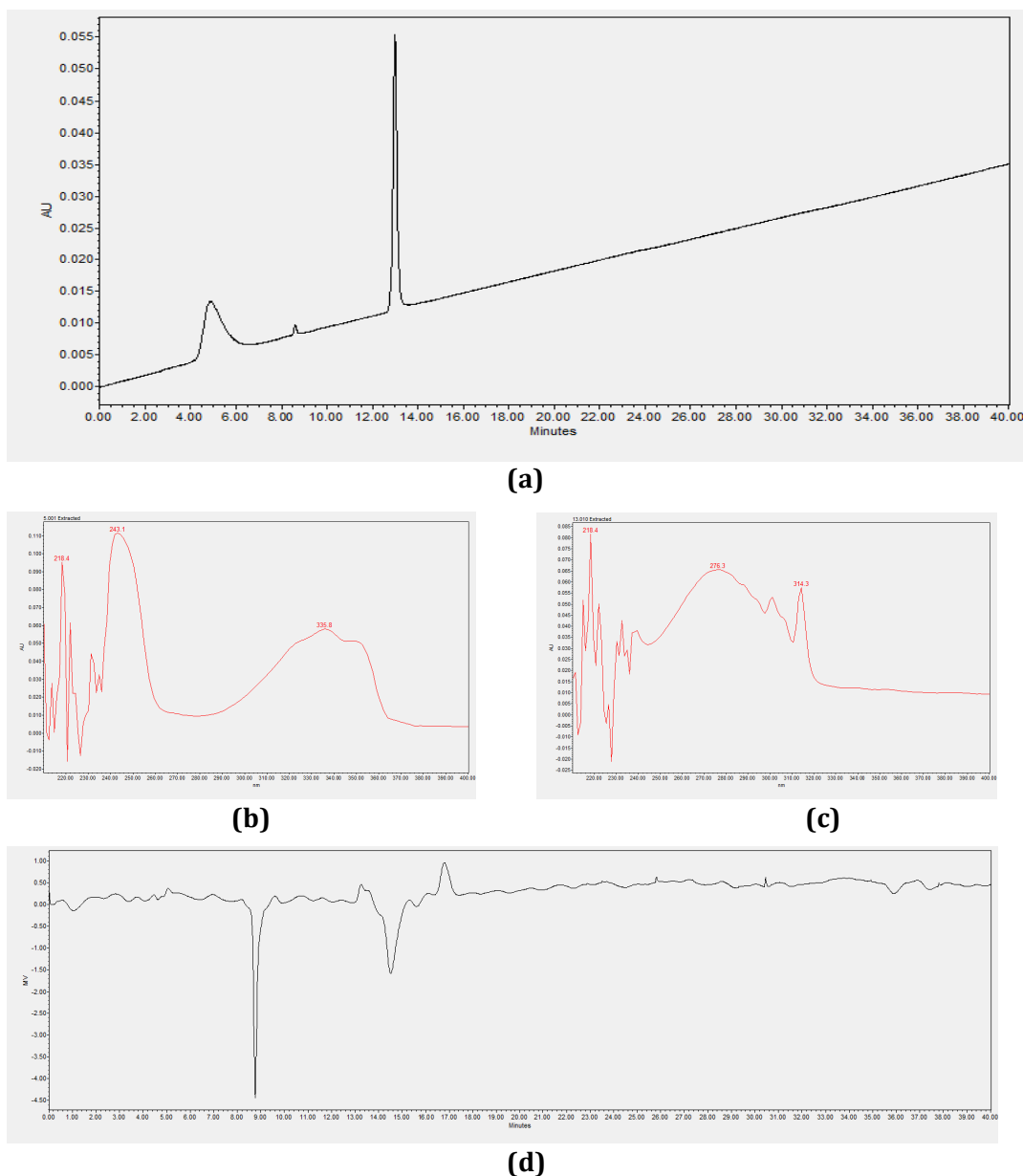
Figure 3-10- HPLC analysis of quinoline oxidation products using perdecanoic acid at 50 ℃ – diluted in chloroform; a) extracted UV spectra at 275 nm, b) extracted UV spectra at retention time about 5.00 minutes, c) extracted UV spectra at retention time about 13.01 minutes and c) RI detector result

61

In Figure 3-10, the extracted UV graphs (b) and (c) respectively matches with UV spectra of quinoline and quinoline N-oxide in Figures 3-5 and 3-7. This confirms the presence of these two compounds in the analyzed solution. The small peak corresponding to iso quinoline is also available in the analysis of oxidation products. The RI detector does not detect any compounds beside quinoline in the oxidation products.

From all mentioned in this section, it could be concluded that the oxidation of quinoline by perdecanoic acid has only led to formation of quinoline N-oxide and decanoic acid. The concentration of the products, conversion of oxidation reaction, mass balance data and change in composition of products by time are discussed in the following section.

3-3-2- Mass and molar concentration of products

UV spectroscopy can be used to determine the concentration of different species in a solution. Based on the Beer-Lambert law (formula 3-4), at a fixed wavelength, the amount of absorption for a solution only depends on the concentration of absorbing species. This can be used to determine the unknown concentration of compounds in a solution [10].

$$A = \epsilon . c . l \qquad (3\text{-}4)$$

Where, $A = absorbance$ $l = pathlength\ through\ the\ sample$
$c = concentration$ $\epsilon = molar\ absorptivity\ constant$

In Figure 3-5, the absorbance at wavelength 336 nm is only proportional to the quinoline N-oxide concentration. At wavelengths lower than 325 nm, the absorption is due to both quinoline and quinoline N-oxide. Any fixed wavelength at this region can be used to determine the concentration of quinoline in the sample. The absorbance at 314 nm is chosen for this matter. In order to calculate the concentration of quinoline and quinoline N-oxide in a sample, the calibration curves of absorbance based on the concentration of these compounds must be plotted at wavelengths 336 nm and 314 nm.

It must be noted that, for all the UV spectroscopy analysis done, the baseline is not always at 0 absorbance and it shifts to negative or positive numbers for some samples (even the blank runs). This is illustrated in Figure 3-11. The baseline shift impacts the amount of absorbance at all wavelengths, causing an error in the calculated concentrations. For a better accuracy, the baseline must be corrected for all the UV results. For all the UV calibrations done, the results are presented based on using both raw UV spectroscopy data and the baseline-corrected ones. At the end of this section, it is shown how the baseline correction improves the standard deviation of mass balance data.
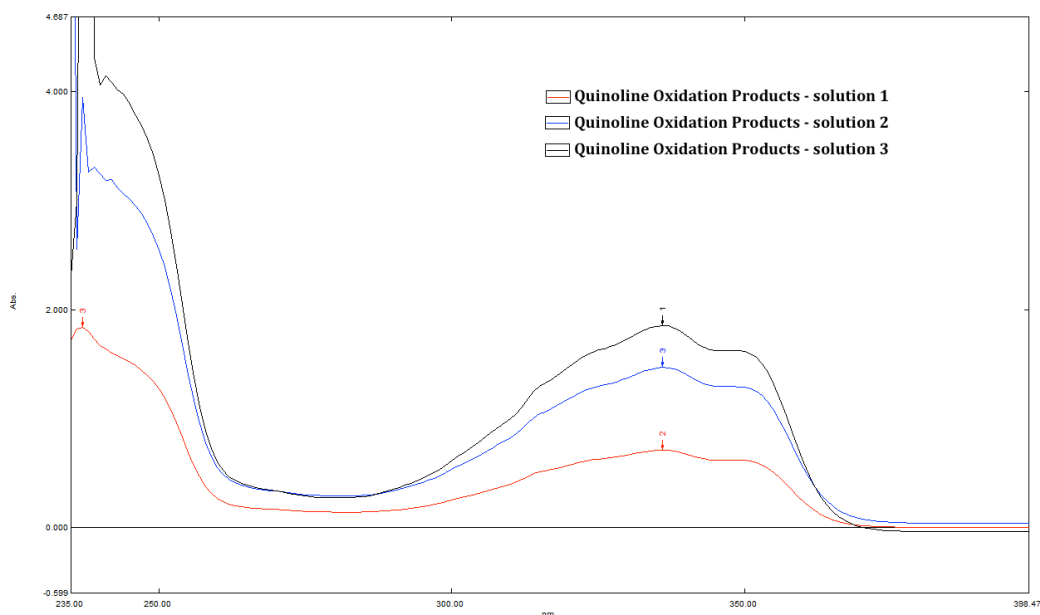
Figure 3-11- The baseline shift in UV spectroscopy analysis of three different solutions of quinoline oxidation products (using perdecanoic acid at 50 °C) in chloroform

Four different solutions of quinoline in chloroform (with known concentration) are prepared. The UV spectra of these solutions are presented in Figure 3-12. The calibration curve of absorbance at 314 nm is plotted against concentration of quinoline (mg/g of chloroform) in Figure 3-13 for a) raw data and b) baseline-corrected data. The linear trend line of data points

gives the equation of absorbance based on concentration at this wavelength. The trend line is forced to go to zero, since the amount of absorption must be zero for a blank solution without any quinoline.
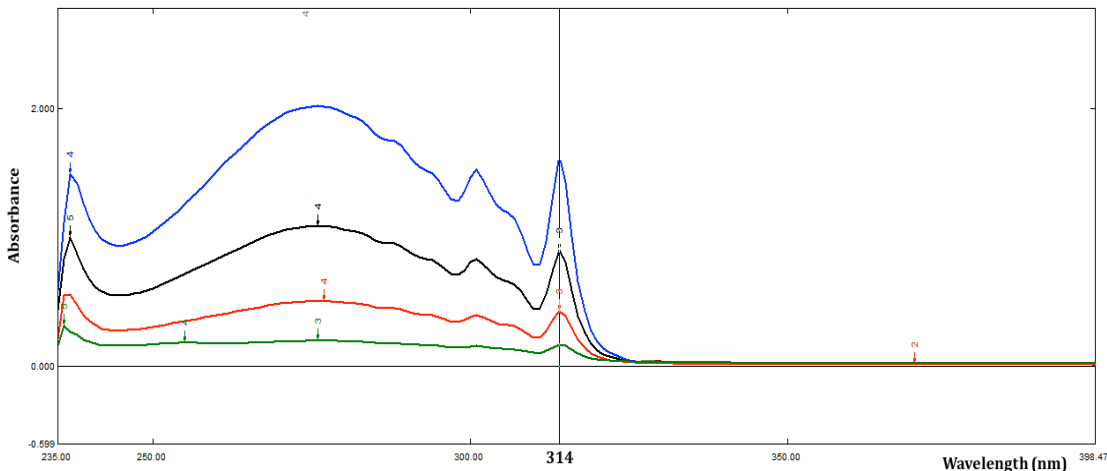
Figure 3-12- UV spectra of 4 different solutions of quinoline in chloroform with known concentrations
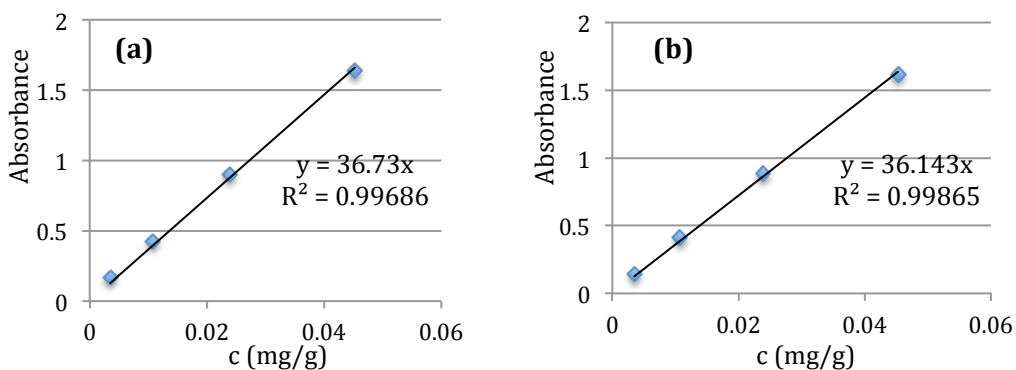
Figure 3-13- Calculated UV calibration curves for quinoline in chloroform at 314 nm using a) raw absorbance data and b) baseline-corrected absorbance data

The same procedure is done for six different solutions of quinoline N-oxide. The solutions are made by drying the quinoline N-oxide hydrate sample in TGA at 150 ℃ for 20 minutes, dissolving the dried sample in a vial full of chloroform and then, immediate preparation of different solutions and recording the UV spectra. The results are presented in Figure 3-14. Figure 3-15 shows the equations between concentration of quinoline N-oxide (mg/g of chloroform) and a) raw absorbance data at 314 nm, b) baseline-corrected

64

absorbance data at 314 nm, c) raw absorbance data at 336 nm and d) baseline-corrected absorbance data at 336 nm.
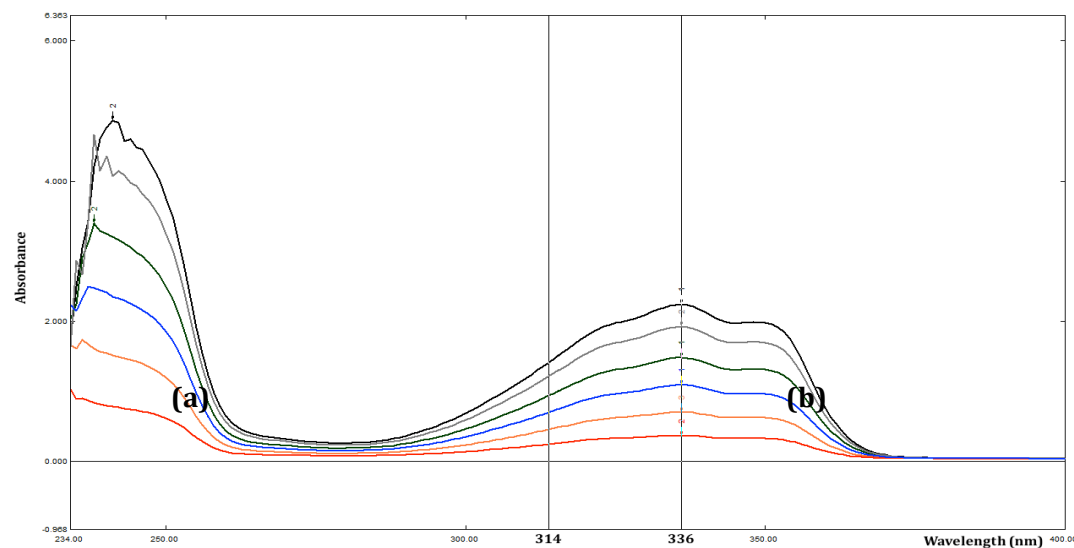
Figure 3-14- UV spectra of 6 different solutions of quinoline N-oxide (dried in TGA at 150 °C) in chloroform with known concentrations
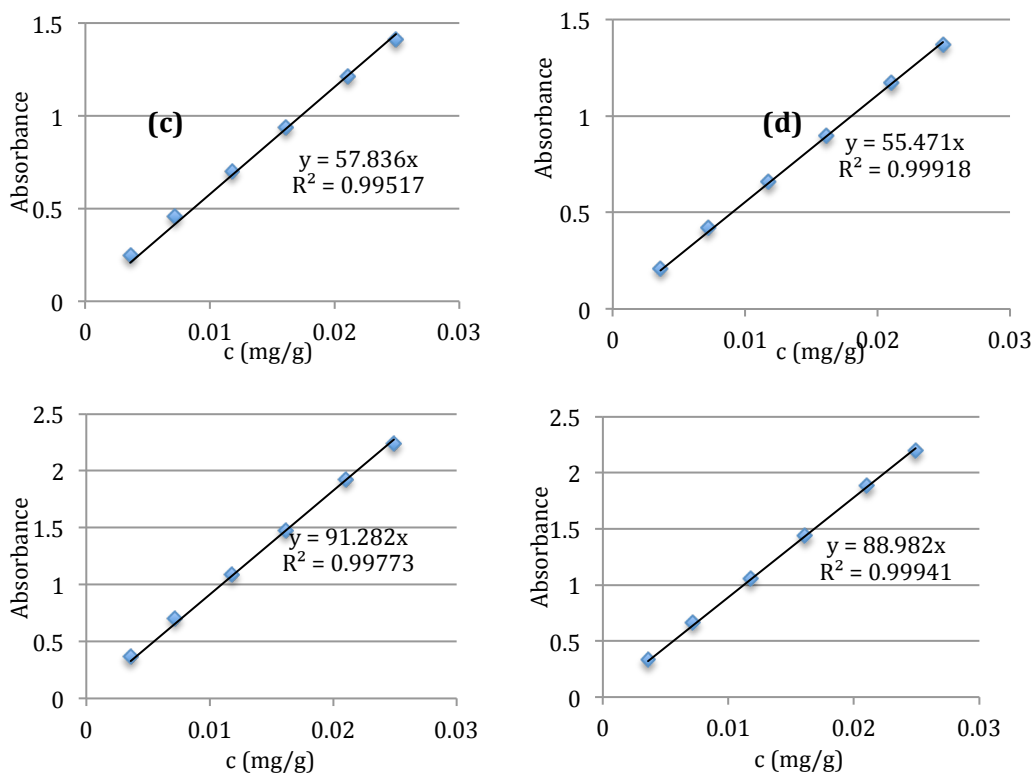
Figure 3-15- Calculated UV calibration curves for quinoline N-oxide in chloroform using a) raw absorbance data at 314 nm, b) baseline-corrected absorbance data at 314 nm, c) raw absorbance data at 336 nm and d) baseline-corrected absorbance data at 336 nm

65

Using the calibration equations shown in Figures 3-13 and 3-15, it is possible to calculate the concentration of quinoline and quinoline N-oxide in the oxidation products. This is done for all three oxidation tests performed (Table 3-2) using the baseline-corrected calibration curves. The product of each experiment is analyzed by UV-spectroscopy on the same day of performing the oxidation experiment and also, 2 days, 4 days and 7 days afterwards. Each UV analysis is repeated 3 times to check for repeatability of data. The calculated mass and mole data are presented in Table 3-3. It must be noted that all these data are calculated based on the baseline-corrected UV graphs. The average and standard deviation of the data points for same day, 2 days, 4 days and 7 days analysis are later presented in Table 3-4.

Table 3-3- Measured amount of reactants and calculated amounts of products (based on UV spectroscopy results and calibration curves obtained with baseline-corrected absorbance data shown in Figures 3-13 and 3-15) for three performed quinoline oxidation experiments using synthesized perdecanoic acid mixture and chloroform as the solvent

Test	Reactants		Products (calculated based on UV-Spectroscopy tests)*						
	Quinoline**		UV tests		Quinoline		Quinoline N-oxide		Total
	mg	millimole	Date	No.	mg	millimole	mg	millimole	millimoles of quinoline
1	510 ± 10	3.95 ± 0.08	Same day	1	94	0.73	500	3.45	4.17
				2	89	0.69	501	3.46	4.15
				3	92	0.71	485	3.35	4.06
			2 days after	1	103	0.80	515	3.56	4.35
				2	100	0.78	510	3.52	4.29
				3	100	0.77	509	3.51	4.28
			4 days after	1	113	0.88	471	3.25	4.12
				2	98	0.76	486	3.36	4.12
				3	80	0.62	488	3.36	3.98
			7 days after	1	94	0.73	494	3.41	4.14
				2	91	0.71	478	3.29	4.00
				3	90	0.70	468	3.23	3.92

Table 3-3- *continued*

Test	Reactants		UV tests		Products (calculated based on UV-Spectroscopy tests)*				
	Quinoline**				Quinoline		Quinoline N-oxide		Total
	mg	millimole	Date	No.	mg	millimole	mg	millimole	millimoles of quinoline
2	500 ± 10	3.88 ± 0.08	Same day	1	66	0.51	478	3.30	3.81
				2	78	0.60	473	3.26	3.86
				3	87	0.67	493	3.40	4.07
			2 days after	1	66	0.51	495	3.41	3.92
				2	91	0.71	494	3.41	4.12
				3	80	0.62	527	3.63	4.25
			4 days after	1	68	0.53	521	3.59	4.12
				2	89	0.69	491	3.39	4.08
				3	89	0.69	521	3.59	4.28
			7 days after	1	65	0.50	494	3.41	3.91
				2	84	0.65	460	3.17	3.82
				3	89	0.69	496	3.42	4.11
3	500 ± 10	3.88 ± 0.08	Same day	1	97	0.75	455	3.14	3.89
				2	101	0.78	457	3.15	3.93
				3	91	0.71	446	3.08	3.79
			2 days after	1	102	0.79	432	2.98	3.77
				2	122	0.95	452	3.12	4.07
				3	122	0.95	450	3.10	4.05
			4 days after	1	100	0.78	471	3.25	4.03
				2	126	0.98	483	3.33	4.31
				3	124	0.96	482	3.32	4.28
			7 days after	1	98	0.76	434	2.99	3.75
				2	124	0.96	442	3.05	4.01
				3	118	0.91	453	3.12	4.03

The average and standard deviation of the data points for same day, 2 days, 4 days and 7 days analysis are later presented in Table 3-4.

**The readability of the weight balance used to weigh the reactants is 0.01 g.*

a) *Mass balance data*

To check the mass balance of the oxidation experiment, the total mole of quinoline present in products (both as quinoline and quinoline N-oxide) can be compared with total mole of quinoline in the reactants in Table 3-3. It can be seen that, for most of the tests, there is a bias indicating 2-6 mole % more product than feed. This is either due to experimental errors or due to production of a heavier compound instead of quinoline N-oxide during oxidation experiment. All the analysis results presented in section 3-3-1 shows that oxidation of quinoline by perdecanoic acid has only led to production of quinoline N-oxide and decanoic acid. Therefore, experimental error is the only reason behind the imbalance of mass data. The fact that even, the UV analyses of the same sample do not lead to the same mass data emphasizes the existing experimental error.

A weight balance with readability of 0.01 g was used to measure the weight of the reactants for each oxidation experiment. But, in preparing the sample solutions of the oxidation products for UV spectroscopy analysis, a weight balance with readability of 0.001 g has been used, causing the calculated mass data for oxidation products to be 1 mg-accurate. Therefore, most of the bias observed in the mass balance can be explained by the difference in the accuracy of the data for the measured quinoline moles in the reactants and calculated quinoline moles in the products. Moreover, the impurities of the commercially available quinoline N-oxide hydrate and also, the hydrophilic nature of this nitrogen-containing compound can cause an error in the calculated mass of products using UV spectroscopy results.

b) *Change in the composition of products by time*

The comparison between data for same day, 2 days, 4 days and 7 days shows whether there is any change in the composition of products (like deoxygenation of the produced quinoline N-oxide) by time. Since both the oxidation experiment and the UV analysis are repeated 3 times, there are 9

data points available for each date of analysis. These data are normalized for 1 mole of quinoline present in the reactants (assuming that the readability of the data for reactants and products are the same); the mean and standard deviation (SD) of the data are calculated and presented in Table 3-4. The mean data are also presented in Figure 3-16 as a bar graph.

No significant difference has been observed between the data points for same day analysis and 7 days after analysis. However, Student t-Test can help to better see whether there is a significant difference in the means. The probability associated with a Student's paired t-Test, with a two-tailed distribution is calculated between the 2 sets of 9 data points for same day analyses and 7-day analyses (data available in Table 3-3). The result for millimoles of quinoline present as quinoline, quinoline N-oxide and in total is 0.10, 0.12 and 0.93 respectively. All these numbers are more than 0.05, showing that, with 95% possibility, the mole data calculated for same day analysis and 7 day analysis are the same. This confirms that the composition of products does not change in 1 week while the products are stored in a freezer.

Table 3-4- Millimoles of quinoline present in the products of quinoline oxidation as quinoline, quinoline N-oxide and in total at the same day of performing the experiment, in 2 days, in 4 days and in 7 days (the mean and standard deviation [SD] of 9 calculated data based on _baseline-corrected_ UV spectroscopy results and normalized for 1 mole of quinoline in the reactants)

Date	millimoles of quinoline present in products as:					
	Quinoline		Quinoline N-oxide		Total	
	Mean	SD	Mean	SD	Mean	SD
Same day	0.84	0.03	0.18	0.02	1.02	0.03
2 days after	0.86	0.06	0.20	0.04	1.06	0.04
4 days after	0.87	0.04	0.20	0.04	1.06	0.04
7 days after	0.83	0.04	0.19	0.04	1.02	0.03
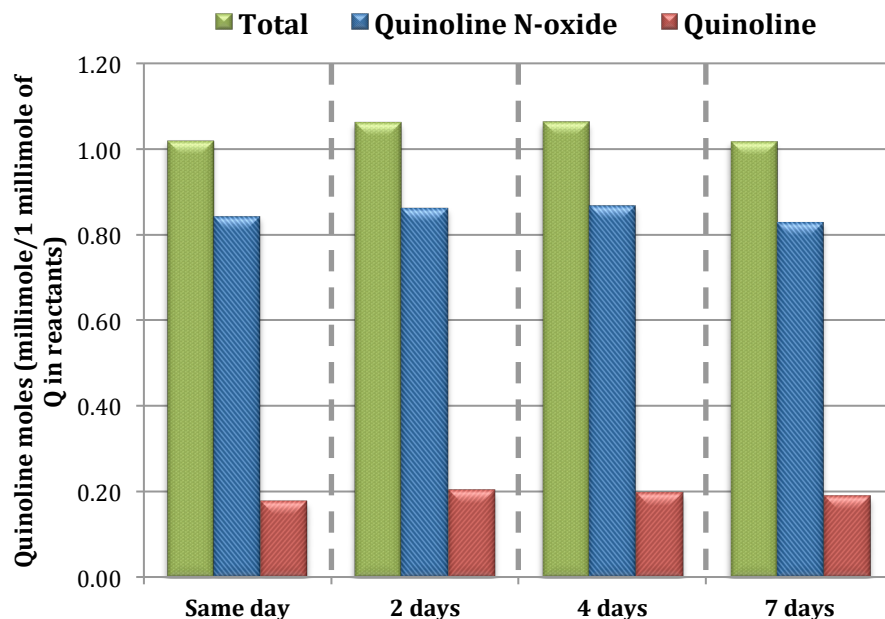
Figure 3-16- Moles of quinoline present in the products of quinoline oxidation as quinoline (red), quinoline N-oxide (blue) and in total (green) at the same day of performing the experiment, in 2 days, in 4 days and in 7 days (the mean of 9 calculated data based on _baseline-corrected_ UV spectroscopy results and normalized for 1 mole of quinoline in the reactants)

c) _The effect of baseline correction_

For each sample, the UV analysis is repeated 3 times, leading to 3 calculated mole balance data. For a better comparison, the mean of these 3 data is calculated and then, normalized for 1 millimole of quinoline in the reactants of each oxidation test. The calculations are done using both the raw UV spectroscopy data and also, the baseline-corrected ones. For the raw data, the results are presented in Table 3-5 and as a bar graph in Figure 3-17. For the baseline-corrected ones, the results are presented in Table 3-6 and also as a bar graph in Figure 3-18. Comparing the two bar graphs with each other, it can easily be seen that the baseline correction has improved the standard deviation between the calculated quinoline moles data. In other words, the correction of baseline of UV spectra, improves the repeatability of the oxidation tests performed.

Table 3-5- Moles of quinoline present in the products of three performed quinoline oxidation experiments as quinoline, quinoline N-oxide and in total (calculated based on _raw_ UV spectroscopy data and normalized for 1 mole of quinoline in the reactants)

Test	Date	millimoles of quinoline present in products as:		
		Quinoline	Quinoline N-oxide	Total
1	Same day	0.15	0.85	1.00
	2 days after	0.20	0.90	1.10
	4 days after	0.17	0.84	1.01
	7 days after	0.13	0.81	0.94
2	Same day	0.08	0.82	0.90
	2 days after	0.14	0.90	1.04
	4 days after	0.14	0.92	1.06
	7 days after	0.09	0.83	0.91
3	Same day	0.14	0.76	0.89
	2 days after	0.21	0.79	1.00
	4 days after	0.21	0.86	1.06
	7 days after	0.16	0.75	0.90

Table 3-6- Moles of quinoline present in the products of three performed quinoline oxidation experiments as quinoline, quinoline N-oxide and in total (calculated based on _baseline-corrected_ UV spectroscopy data and normalized for 1 mole of quinoline in the reactants)

Test	Date	millimoles of quinoline present in products as:		
		Quinoline	Quinoline N-oxide	Total
1	Same day	0.18	0.86	1.05
	2 days after	0.20	0.89	1.09
	4 days after	0.19	0.84	1.03
	7 days after	0.18	0.84	1.02
2	Same day	0.15	0.86	1.01
	2 days after	0.17	0.90	1.07
	4 days after	0.16	0.91	1.07
	7 days after	0.16	0.86	1.02
3	Same day	0.19	0.81	1.00
	2 days after	0.23	0.79	1.02
	4 days after	0.23	0.85	1.09
	7 days after	0.23	0.79	1.02
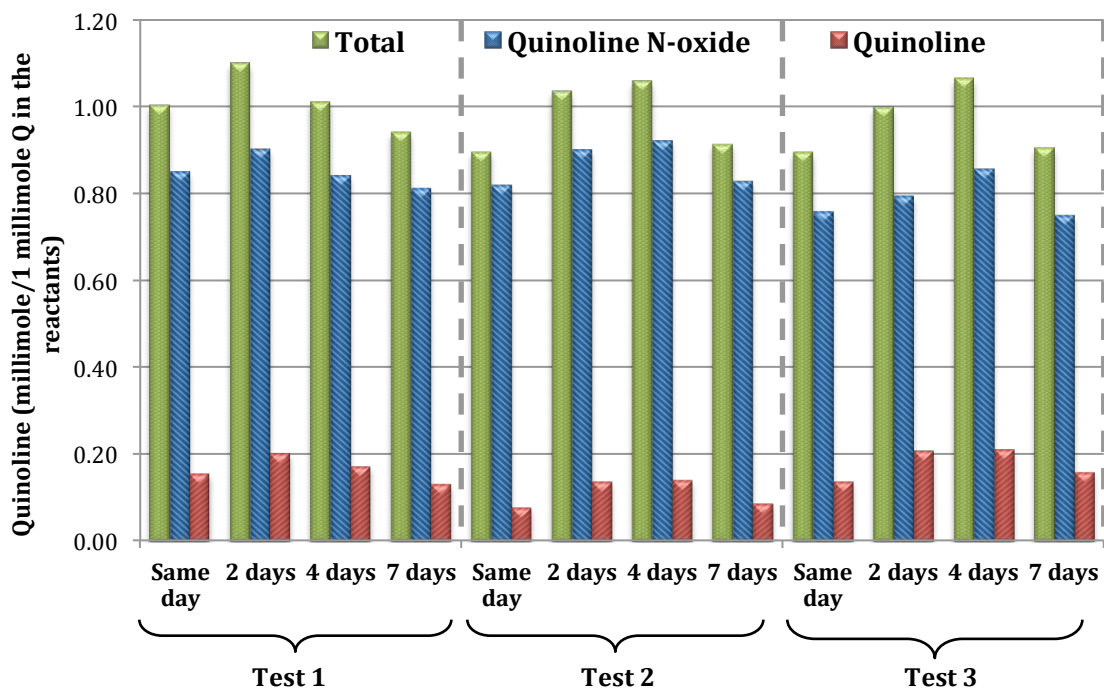
Figure 3-17- Moles of quinoline present in the products of three performed quinoline oxidation experiments as quinoline (red), quinoline N-oxide (blue) and in total (green) – calculated based on *raw* UV spectroscopy data and normalized for 1 mole of quinoline in the reactants
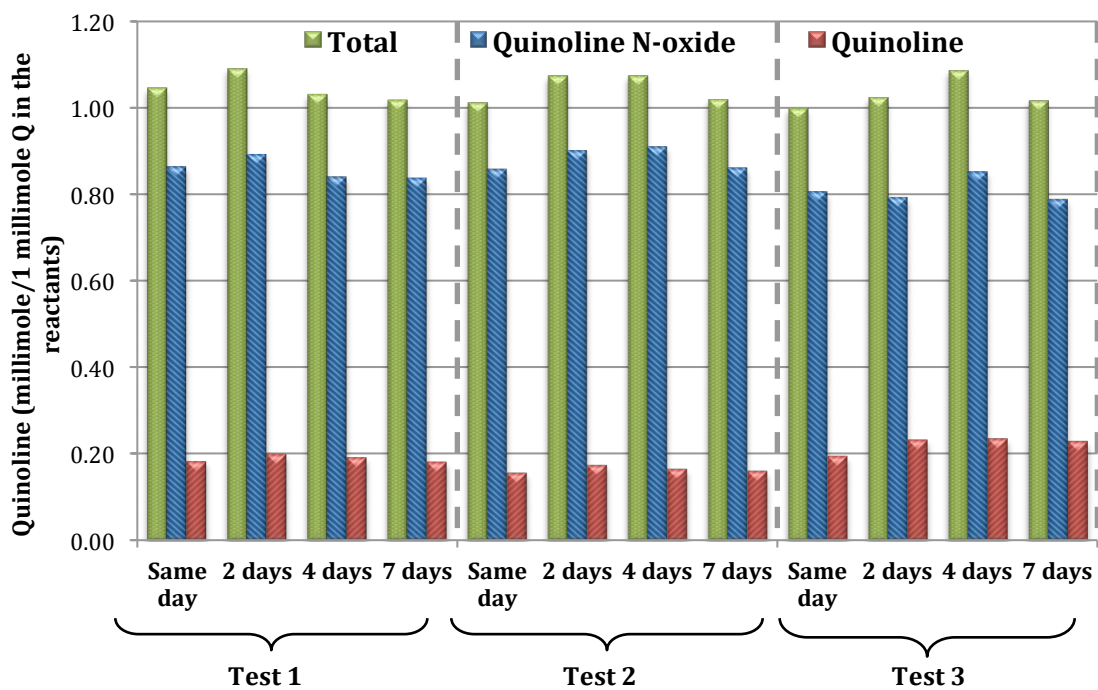
Figure 3-18- Moles of quinoline present in the products of three performed quinoline oxidation experiments as quinoline (red), quinoline N-oxide (blue) and in total (green) – calculated based on *baseline-corrected* UV spectroscopy data and normalized for 1 mole of quinoline in the reactants

72

4- Conclusion

The oxidation of quinoline by perdecanoic acid (10-20% excess) has been studied using chloroform as the solvent. The perdecanoic acid has been synthesized using the reaction of hydrogen peroxide (50%) with decanoic acid. The synthesized perdecanoic acid decomposed, even while kept in the freezer, to decanoic acid. Therefore, the peroxide content test was performed on the synthesized mixture prior to performing the oxidation experiment in order to calculate the required amount of the mixture. Using this synthesized mixture (10-20% excess), about 83 mole % of quinoline has been converted to quinoline N-oxide when the reaction is performed at 50 °C for 30 minutes. All the perdecanoic acid decomposed and turned to decanoic acid during the oxidation experiment. The produced quinoline N-oxide was stable while kept in the freezer for 1 week. The oxidation experiment has been repeated three times. The calculated weight and mole data were repeatable for the performed experiments. However, for each experiment, an error has been observed in the mass balance between the products and reactants.

5- References

[1] Dutka, V.S.; Matsyuk, N.V.; Dutka, Yu.V. Influence of a Reaction Medium on the Oxidation of Aromatic Nitrogen-Containing Compounds by Peroxyacids, *Russian Journal of Physical Chemistry A* **2011**, *85*, 45-50.

[2] Parker, W. E.; Riccuiti, C.; Ogg, C. L.; Swern D. Peroxides. II. Preparation, Characterization and Polarographic Behavior of Long-chain Aliphatic Peracids, *Journal of American Chemical Society* **1955**, *77*, 4037-4041.

[3] Wheeler, D. H. Peroxide Formation as a Measure of Autoxidative Deterioration, *Oil and Soap* **1939**, *9*, 4, 89-97.

[4] Johnson, R. M.; Siddiqi, I. W. *The Determination of Organic Peroxides;* Pergamon Press: London, 1970; pp 15-23 & 70-71.

[5] Sully, D.; Williams, P. L. The Analysis of Solutions of Per-acids and Hydrogen Peroxide, *Analyst* **1962**, *87*, 653-657.

[6] Dutka, V. S.; Zagorskaya, V. V.; Dutka, Yu. V.; Savitskaya, O. I. Thermal Decomposition of Aliphatic Peroxy Acids, *Kinetics and Catalysis* **2011**, *52*, 3, 353-357.

[7] *The Chemistry of Heterocyclic Compounds: Quinolines, Part II;* Jones, G.; John Wiley and Sons Ltd: New York, 1982; Vol. 32, pp 414 & 424.

[8] National Institute of Standards and Technology (NIST), http://webbook.nist.gov/cgi/cbook.cgi?ID=C119653&Mask=400, (accessed May, 2013).

[9] Reaxys, https://www.reaxys.com, (accessed May, 2013).

[10] Chemguide, Using UV-visible Absorption Spectra, http://www.chemguide.co.uk/analysis/uvvisible/analysis.html, (accessed May, 2013).

Chapter 4

Thermal Behavior of Quinoline N-oxide Hydrate

1- Introduction

In this research, quinoline has been chosen as a model compound representing the nitrogen containing structure of coal liquids. Synthesis of quinoline N-oxide by oxidation of quinoline using peracids has been investigated in the previous chapter. In this chapter, denitrogenation of quinoline N-oxide by means of thermal decomposition is studied. The commercially available quinoline N-oxide hydrate is exposed to a thermal zone to study the thermal behavior of this compound and the possibility of nitrogen removal as its respective nitrogen oxides during thermal decomposition of quinoline N-oxide.

2- Experimental

2-1- Materials

- Quinoline N-oxide hydrate, quinoline, acetone, distilled water: details are provided earlier in chapter 3, section 2-1

- Nitrogen

  Make: Praxair Inc*.*
  CAS number: 7727-37-9
  Purity: 99.998 % (O_2< 5 ppm, H_2O< 3 ppm)
  Molecular weight: 28.01
  Melting point: -210 ℃
  Boiling point: -195.80
  Color: colorless
  Odor: odorless
  Form: gas

2-2- Equipment

- Gas Chromatography-Mass Spectrometry (GC-MS), Infrared Spectroscopy, Rotary Evaporator (Rota-vap), Fluidized Sand bath: details are provided earlier in chapter 3, section 2-2

- Differential Scanning Calorimeter (DSC)

  Make: Mettler Toledo
  Model: DSC 1
  Sensor type: FRS5
  Pans: 40 µL Al pans with lid and without pin
        30 µL HP stainless crucibles with lid, gold-plated sealing and without pin
  Carrier gas: Nitrogen
  Temperature Program: specified for each sample in section 3

- Gas Chromatography (GC)

  Make: Agilent Technologies
  Model: 7890A
  Column 1: HayeSep R, mesh= 80/100
  Column 2: Molecular Sieve 13X, mesh=45/60
  Detectors: FID/TCD
  Carrier gas: Helium 28 mL/min
  Temperature program: Initial T =70 ℃, hold 7 min; Ramp= 10 ℃/min, Final T= 250 ℃, hold 2 min; Ramp= -30 ℃/min, Final T=70 ℃, hold 8 min; Inj. T= 100 ℃, FID T= 250 ℃, TCD T = 200 ℃

- Mass Spectrometry (MS)

  Make: Pfeiffer Vacuum
  Model: OmniStar™ GSD 320
  Capillary operating temperature: up to 350 ℃
  Sample gas pressure: up to 1000 mbar
  Detector: C-SEM/Faraday
  Mass range: 1-300 amu
  Software: Quadera™

- Elemental Analysis (CHNS)

  Make: Elementar

Model: vario MICRO cube
Carrier gas: Helium (200 mL/min)
Program: Combustion tube= 1150 ℃, Reduction tube= 850 ℃, Pressure= 1200 mbar, Oxygen flow= 14 mL/min, MFC flow= 200 mL/min

- Thermal Microscopy Combined with DSC

Make: Mettler Toledo.
Central processor model: FP90
TA microscopy cell model: FP84HT
Microscope: make: Olympus, model: BX51
Temperature range: room T to 375 ℃
Crucibles: glass crucibles with glass cover, diameter 7 mm

2-3- Procedures

2-3-1- Thermal study using Differential Scanning Calorimeter (DSC)

Standard Al crucibles were used for DSC experiments. A hole was made in the lid of both reference pan (an empty crucible) and sample pan using a needle to prevent pressure buildup inside the crucibles due to evaporation or decomposition. The instrument was calibrated prior to performing the experiments, using Indium and Zinc. Table 4-1 shows the result of three calibration experiments performed.

Table 4-1- Calibration of Mettler Toledo DSC1 using Indium and Zinc

Material	Test	Onset temperature (℃)			Heat flow (J/g)		
		Value	Mean	SD	Value	Mean	SD
Indium	1	156.87			28.29		
	2	156.70	156.76	0.10	28.46	28.44	0.15
	3	156.71			28.58		
Zinc	1	419.27			108.70		
	2	419.34	419.52	0.37	109.27	109.07	0.32
	3	419.94			109.23		

In Table 4-1, the recorded data were within the acceptable range of error for the calibration materials used, which is as follows (based on the information provided in the operating manual of the instrument):

- Indium: Onset temperature=156.6$\pm$0.3 $^\circ$C

                           Heat Flow= 28.45$\pm$0.6 Jg^{-1}

- Zinc: Onset temperature=419.6$\pm$0.7 $^\circ$C

                           Heat Flow= 107.5$\pm$3.2 Jg^{-1}

The recorded calibration data for indium indicated that at low temperature ranges, the bias for every recorded temperature and heat flow was respectively from 0.11 to 0.27 $^\circ$C and -0.16 to 0.13 Jg^{-1}. At high temperature ranges close to Zinc melting point, the bias for every recorded temperature and heat flow was respectively from -0.33 to 0.34 $^\circ$C and 1.20 to 1.73 Jg^{-1}.

The thermal behavior of about 5 mg of quinoline N-oxide hydrate was examined under nitrogen atmosphere. The first temperature program used is as follows: Initial T: 25 $^\circ$C, Ramp: -10 $^\circ$C/min, Final T: -35 $^\circ$C; Ramp: 10°/min, Final T: 600 $^\circ$C. Based on the resulting calorigram, several experiments with different temperature programs were performed to check the reversibility and reproducibility of each peak. The detailed temperature program for each run is shown on each DSC calorigram in section 3. The residue of each run was weighed and then, analyzed using IR spectroscopy. For mass balance studies, sealed high pressure (HP) crucibles were used just for one DSC experiment.

2-3-2- Thermal study using micro-reactor set up

The micro-reactor setup (material: Stainless steel, micro-reactor volume: 15 mL, setup total volume: 25 mL) was washed by acetone prior to experiment and then, dried using airflow. Using a sand bath, about 1 gram of quinoline N-oxide hydrate was heated to desired temperature in the micro-

reactor under nitrogen atmosphere (pressure= 500-600 kPa) for 30 minutes. Temperature and pressure were recorded every minute during the experiment. After 30 minutes, the reactor was cooled down to room temperature using airflow. The produced gases were analyzed with both gas chromatography (GC) and mass spectrometry (MS). The decomposition residue, which was partially soluble in acetone, was collected from the micro-reactor using this solvent. The insoluble part was separated from the acetone solution by a filter paper. A rotary evaporator was used to evaporate acetone from both insoluble residue and soluble residue (T=60 ℃, P= 550mbar, drying time= overnight). Figure 4-1 shows the block diagram for the thermal decomposition of quinoline N-oxide hydrate.
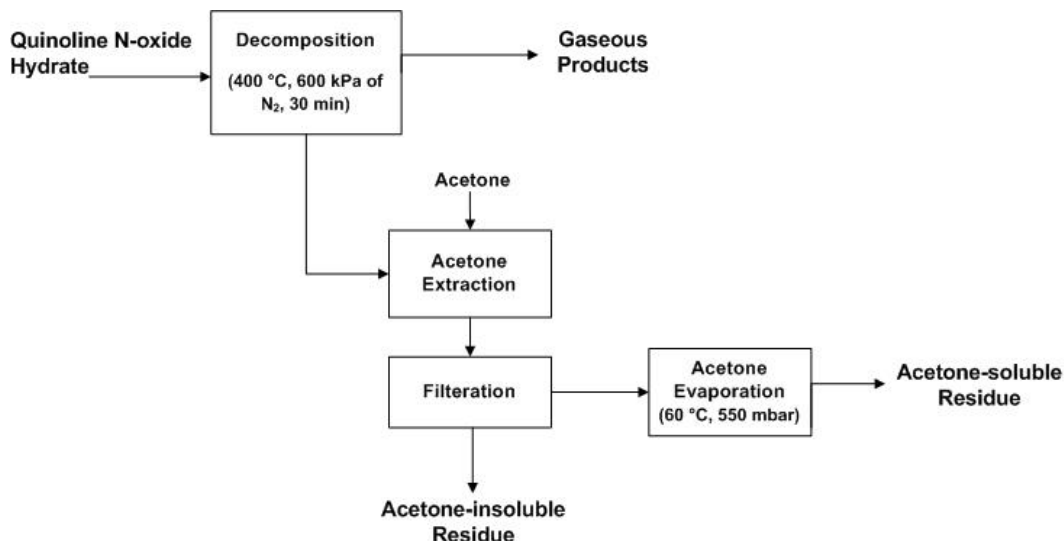
Figure 4-1- The block diagram for thermal decomposition experiment of quinoline N-oxide hydrate

Both residues were weighed and analyzed using an elemental analyzer (CHNS) and IR spectrometer with ATR attachment (IR spectrum of the acetone-insoluble residue was also measured using KBR pellets). The acetone-soluble part was also analyzed by GC-MS. Moreover, in order to obtain correct mass balance data, the collected acetone solution from the rotary evaporators was analyzed by GC-MS to check whether a part of residue was evaporated along with acetone during drying process.

3- Result and Discussion

Thermal microscopy system was used to visually see the changes in the structure of quinoline N-oxide hydrate when it was exposed to heat. About 1 mg of quinoline N-oxide hydrate is heated from room temperature to 350 ℃ by 10 ℃/min heating rate. Figure 4-2 shows the images captured by microscope camera at different temperatures.

(a)

(b)

(c)

(d)

(e)

(f)
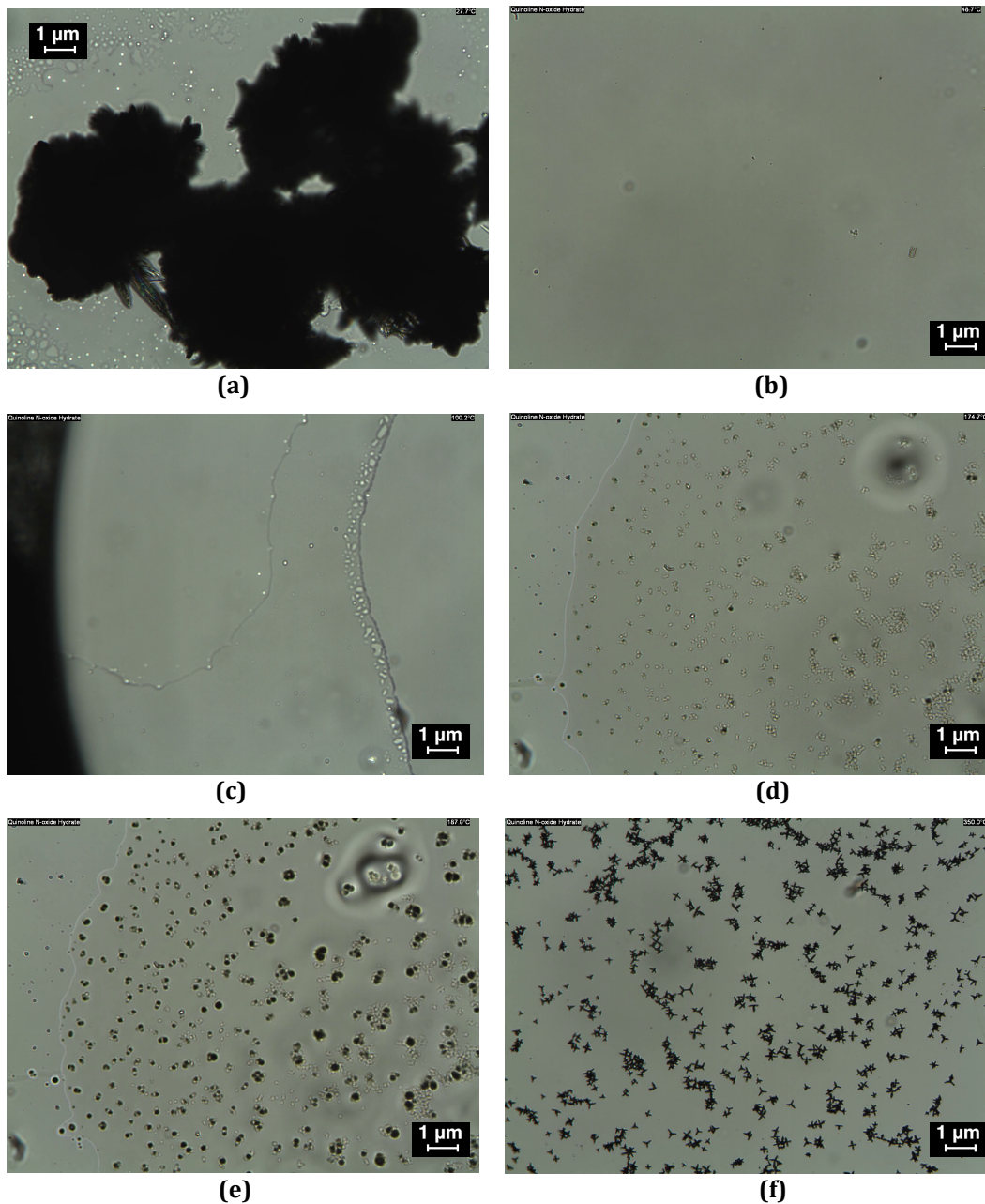
Figure 4-2- Captured images of quinoline N-oxide hydrate using thermal microscopy system at a) 27.7 ℃, b) 48.7 ℃, c) 100.2 ℃, d) 174.7 ℃, e) 187.0 ℃ and f) 350.0 ℃ 81

Image (a) was captured at room temperature. When the instrument began to heat up the sample, it started to melt at temperatures around 48 ℃ and formed a liquid phase (b), then, a part of this liquid phase evaporated from 70 ℃ to 110 ℃ (c), afterward, a decomposition event started from 170 ℃ (d and e) and ended around 220 ℃. The produced solid black residue remained unchanged till the end of experiment, at 350 ℃ (f).

It must be noted that the thermal microscopy system does not provide the same quality of information as the Mettler Toledo DSC1 and also, it cannot be operated under inert atmosphere. Therefore, the results obtained by this instrument can only be used in conjunction with other methods to correctly verify a thermal event.

To obtain more accurate thermo gravimetric data, quinoline N-oxide hydrate was heated from -35 ℃ to 600 ℃ under nitrogen environment using a cryogenic differential scanning calorimeter (DSC). Figure 4-3 shows the result and also, the temperature program used. For each observed event, the onset temperatures and the enthalpy changes are also reported in Table 4-2.
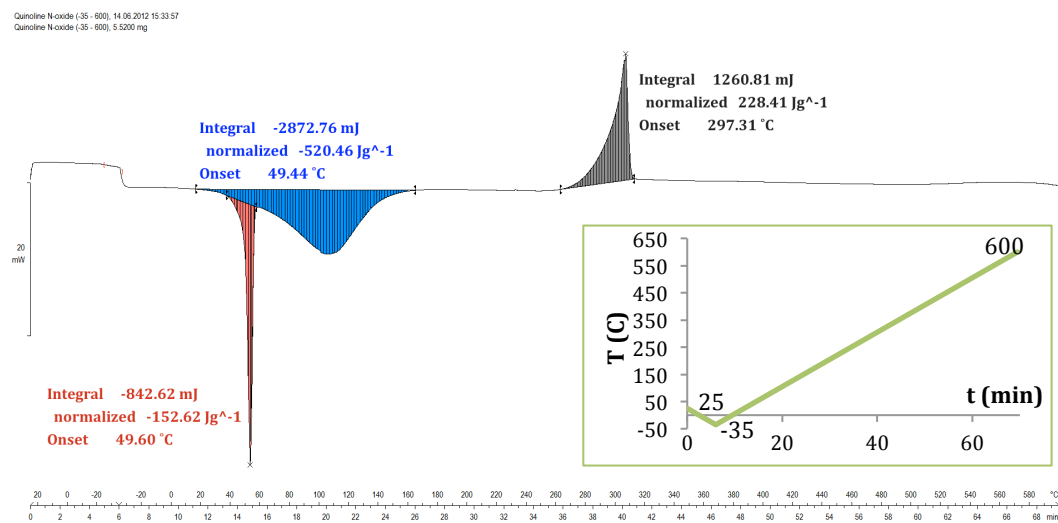
Figure 4-3- DSC graph of quinoline n-oxide hydrate from -35 to 600 ℃ under nitrogen environment

Table 4-2- Thermal events observed in DSC experiment of quinoline N-oxide hydrate from -35 to 600 ℃ under nitrogen environment

Thermal Event	Onset T (℃)	Enthalpy (Jg^{-1})
1 (red peak)	49.60	-152.62
2 (blue peak)	49.44	-520.46
3 (gray peak)	297.31	228.41

Two sets of experiments were designed to thoroughly investigate the thermal events observed in Figures 4-2 and 4-3: one using DSC with different temperature programs to separately study each one of peaks seen in Figure 4-3; and the other using a micro-reactor set up. IR spectroscopy, GC, MS, GC-MS and elemental analysis were used to characterize the products of each experiment.

The results account for 2 major thermal events happening in the studied temperature range: first, melting along with dehydration of quinoline N-oxide hydrate; and second, decomposition of quinoline N-oxide. Each step is thoroughly discussed in section 3-1 and 3-2. These sections contain the experimental results, discussions on the thermal events happening, the structure of products and also, suggested mechanisms for each event.

3-1- First step: melting along with dehydration of sample

The dehydration of quinoline N-oxide hydrate containing 2 crystallization water molecules has been studied before [3-4]. It has been reported that the water molecules are not energetically equivalent ones, since there are 2 thermal events in the DTG and DSC graphs before 150 °C. The first sharp endothermic peak at temperatures from 50 to 90 °C corresponded to the partially loss of water accompanied by melting of sample. Complete dehydration happened before 150 °C [3]. The X-ray powder analysis of quinoline N-oxide hydrate also suggested that the water molecules are nonequivalent. It is known that the N-oxides oxygen atom can interact with two proton donors to give one of the structures shown in Figure 4-4. In this

case, X-ray data indicated that the quinoline N-oxide oxygen atom was involved in hydrogen bonding with two water molecules; the length of one being 2.705 A° while the length of the other was 2,601 A° (structure A) [4].
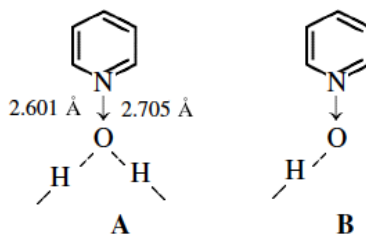
Figure 4-4- possible structures resulting from interaction of heterocyclic N-oxides with two proton donors [4]

This hypothesis is studied in the following sections (3-1-1 and 3-1-2).

3-1-1- Dehydration experiment using DSC

A DSC analysis of quinolone N-oxide hydrate was performed using multiple heating up and cooling down steps under nitrogen environment. The temperature program used is shown in Figure 4-5. At first, sample was cooled down from 25 to -35 °C and then, heated up to 195 °C. This was followed by two more sets of cooling down and heating up steps between -35 to 195 °C. To obtain a better resolution, a slower heating rate was used for the temperature ranges showing a peak (change in heat flow). Figure 4-6 and Table 4-3 present the DSC results along with information of each peak.

	First Set			Second Set				Third Set		
Heating Rate (°C/min)	-10	10	5	-10	-5	5	10	-10	-5	5
Temperature (°C)	25	-35	25	195	50	-35	100	195	50	-35	100
Time (minutes)	0	6	12	46	60.5	77.5	104.5	114	128.5	145.5	172.5
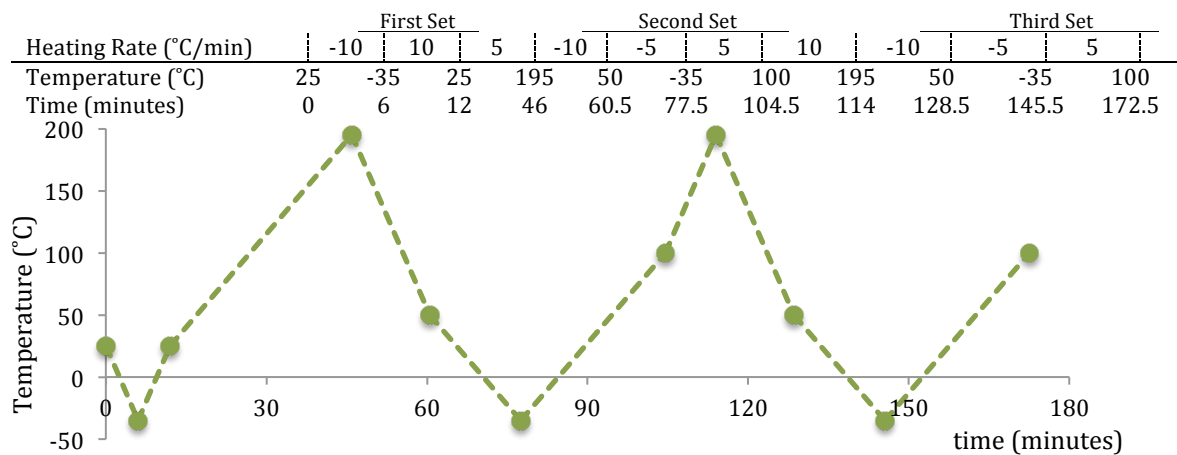
Figure 4-5- Temperature program used for DSC experiment shown in Figure 4-6

84
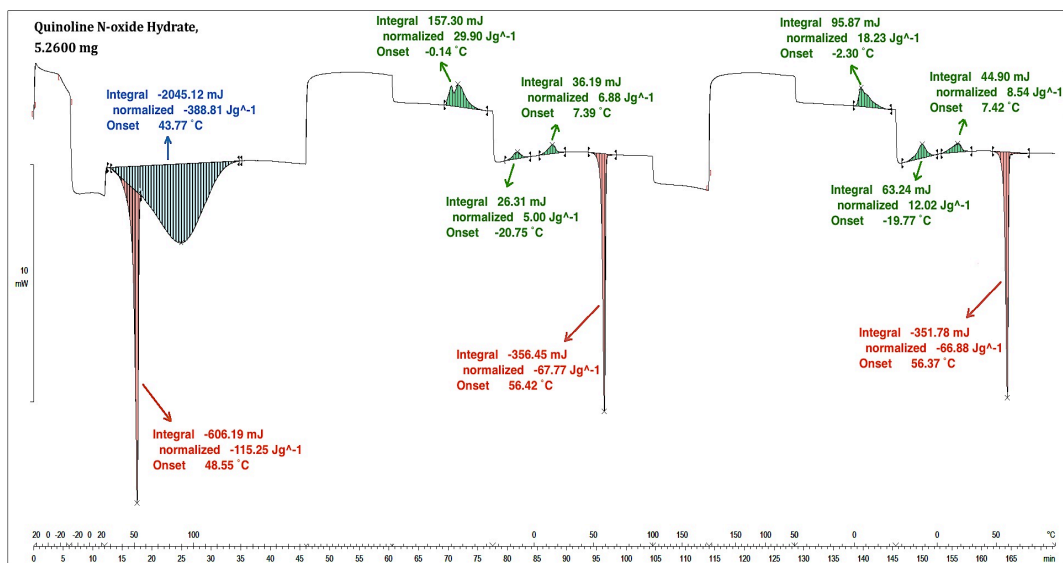
Figure 4-6- DSC graph of quinoline n-oxide hydrate from -35 to 195 °C under nitrogen environment

Table 4-3- Thermal events observed in DSC experiment of quinoline N-oxide hydrate from -35 to 195 °C under nitrogen environment

Thermal event	Onset T (°C)	Enthalpy (J/g)	Thermal event	Onset T (°C)	Enthalpy (J/g)
1	48.55	-115.25	6	56.42	-67.77
2	43.77	-388.81	7	-2.30	18.23
3	-0.14	29.90	8	-19.77	12.02
4	-20.75	5.00	9	7.42	8.54
5	7.39	6.88	10	56.37	-66.88

Considering the three red peaks in Figure 4-6, it can be seen that only a portion of the first sharp peak was repeated in the second and third heating up step which indicates that besides melting of quinoline N-oxide (melting point= 56 °C), another endothermic process has happened at temperature from 50 to 67 °C in the first heating up step. Assuming that this process and also, the endothermic process happening between 67-170 °C (blue peak) correspond to dehydration of quinolone N-oxide, the total amount of heat

absorbed for water vaporization can be calculated. The heat of fusion for the tested sample is the average of the areas of second and third red peaks:

$$Heat\ of\ fusion = \frac{356.45 + 351.78}{2} = 354.11\ mJ$$

$$\Rightarrow Heat\ of\ dehydration = 2045.12 + (606.19 - 354.11) = 2297.20\ mJ \quad (a)$$

This number can be compared with the required heat of vaporization for the water content of the sample to confirm the assumed hypothesis. The calculation of required heat of vaporization is as follows:

$$water\ content = {19.1\%\ gr\ of\ water}/{gr\ of\ quinoline\ N - oxide\ hydrate}$$

$$Initial\ sample\ weight = 5.26\ mg \Rightarrow water\ content = 0.191{\times}5.26 = 1.00mg$$

$$Enthalpy\ of\ water\ at\ 100\ kPa\ and\ 100\ °C\ [5] = \begin{cases} 418\ {}^{J}/_{g} & liquid \\ 2675\ {}^{J}/_{g} & vapour \end{cases}$$

$$\Rightarrow Enthalpy\ of\ vaporizationat\ 100\ kPa = 2257{}^{J}/_{g} = 2257\ {}^{mJ}/_{mg}$$

$$\Rightarrow Required\ heat\ for\ water\ vaporization = 2257{\times}1.00 = 2257\ mJ \quad (b)$$

The numbers (a) and (b) are close enough to each other to support the suggested hypothesis about dehydration of sample. It must be noted that quinoline N-oxide hydrate easily absorbs water from environment, and this can explain why the energy absorbed (a) is more than what's required for evaporation of original water content of sample. The final sample weight (4.23 mg) indicates 19.6 % weight loss during DSC run which is in agreement with the water content of the sample.

As it is shown in Figure 4-6, after melting and dehydration of sample in the first heating up step, there are 3 other thermal events (green peaks) happening in the second set of cooling down and heating up steps. These peaks are also repeated in the third set of cooling down and heating up steps, but the area of peak and the onset temperatures are slightly different than the second set. It must be noted that these peaks are absent in the first

cooling down step from 25 to -35 °C. In other words, they do not happen before melting and dehydration of sample. A couple of possibilities come to mind about the nature of these thermal events: recrystallization of the sample, reabsorption of water from the carrier gas, solid-solid phase transitions and so on. To further study each one of the green peaks seen in Figure 4-6, the residue of the above DSC run must be analyzed at two temperatures: one lower than the onset temperature and one higher than the endset temperature. The onset and endset temperatures of these thermal events are lower than room temperature. Therefore, a low-temperature spectroscopic instrument is required with ability to analyze samples at temperatures lower than room temperature. Due to lack of such instrument, it was not possible to further investigate these thermal events.

3-1-2- Dehydration experiment using a micro-reactor setup

To simulate the endothermic event observed in the DSC experiments, 1 gram of sample was heated up to 220 °C under 500kPa pressure of nitrogen for half an hour in the micro-reactor setup. The main difference between the micro-reactor setup and DSC experiments is the fact that unlike DSC experiments, the micro-reactor is a closed system. Therefore, the produced gases (due to evaporation or decomposition of sample) remain in the system and might condense back to the liquid/solid phase when the micro-reactor is cooled down to the room temperature, whereas, these gases leave the system along with carrier gas in the DSC experiments. As a result, the comparison between DSC and micro-reactor experiments might provide good explanation for the thermal events happening during sample heat up. Comparison of the infrared spectra of the residue of both DSC and micro-reactor setup experiments can confirm the suggested hypothesis about dehydration of sample. Figure 4-7 shows the IR spectra of distilled water, raw quinolone N-oxide hydrate, the residue of the DSC run up to 195 °C (explained in section 3-1-1) and the residue of quinolone N-oxide hydrate decomposition in a micro-reactor (sand bath T= 220 °C, P_{N2}= 500 kPa, t= 30 min).
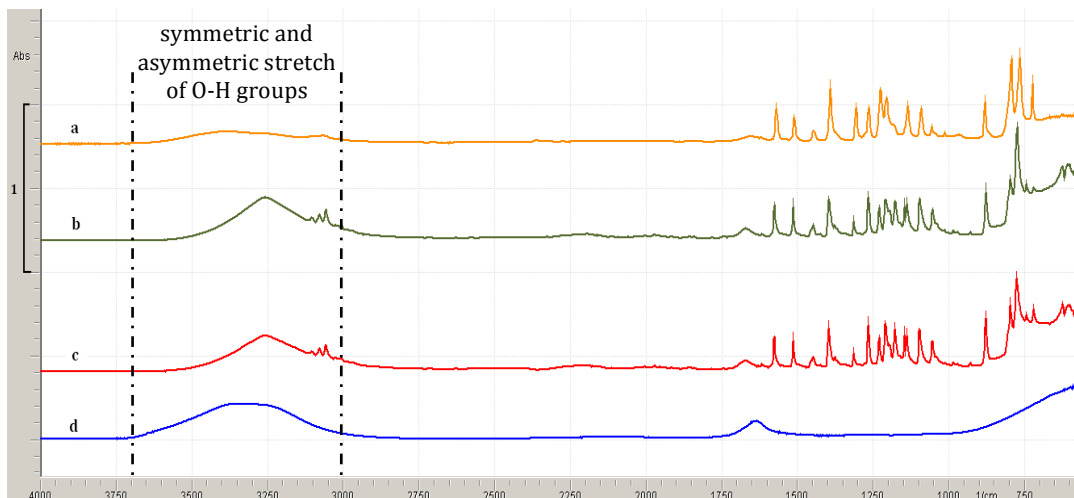
Figure 4-7- IR spectrum of a) yellow line - the decomposition residue of DSC experiment at 195 ℃, b) green line - the decomposition residue of the micro-reactor at 220 ℃ and 500 kPa of N_2, c) red line - quinoline n-oxide hydrate and d) blue line - distilled water, [using ATR attachment]

The main absorption peaks for each sample observed in Figure 4-7 are summarized in Table 4-4. For all the four studied samples, the wavenumber ranges of corresponding absorption peaks are expressed in the same line in Table 4-4 for a better comparison.

Comparing the IR spectrum of quinolone N-oxide hydrate with the one of DSC residue, it can be clearly seen that all the changes are due to the loss of OH groups, which corresponds to dehydration of sample (wavenumbers: 2900-3700 cm^{-1}). As it can be seen from IR spectra of the residue sample of the DSC experiment in this region, the sample still contains a bit of water. This can be due to ability of quinoline N-oxide to absorb water from environment during experiment, and also, during handling and analysis of sample after the DSC experiment. Moreover, assuming melting and water loss are the only events happened up to 195 ℃ and considering that the water vapor can condense back to the micro-reactor after it cools down to the room temperature, the IR spectrum of micro-reactor samples must be similar to the IR spectrum of pure quinolone N-oxide hydrate, which is correct as shown in Figure 4-7 and Table 4-4.

Table 4-4- The wavenumber range of the main absorption peaks observed in Figure 4-7

Sample			
The residue of DSC experiment at 195 °C	The residue of micro-reactor experiment (220 °C, 500 kPa of N_2)	Quinoline N-oxide hydrate	Distilled water
742-783	748-789	748-788	
783-830	789-820	788-822	
850-890	855-893	857-895	
1024-1068	1019-1065	1019-1066	
1068-1107	1065-1108	1067-1108	
1107-1160	1109-1153	1111-1154	
1160-1184	1153-1187	1165-1187	
1185-1215	1188-1220	1187-1220	
1215-1247	1220-1241	1221-1241	
1247-1287	1250-1277	1251-1277	
1287-1323	1285-1323	1286-1323	
1324-1418	1324-1412	1323-1412	
1420-1470	1430-1464	1430-1465	
1495-1530	1497-1531	1497-1527	
1549-1593	1532-1585	1540-1585	
1594-1713	1586-1716	1586-1718	1556-1725
2931-3611	2890-3586	2891-3588	2884-3722
3023-3127	3032-3067	3032-3067	
	3067-3093	3067-3093	
	3094-3116	3094-3114	

(Row label, left side, vertical:) The wavenumber range of main absorption peaks observed (cm^{-1})

Consequently, the first 2 peaks present in the DSC run of quinolone N-oxide hydrate (Figure 4-3) are melting followed by dehydration.

3-2- Second step: decomposition of sample

To study the reversibility and repeatability of the sharp exothermic peak seen in Figure 4-3, a DSC experiment was performed on quinoline N-oxide hydrate with multiple heating up (heating rate: +10 °C/min) and cooling

down (heating rate: -10 °C/min) steps between -35 to 400 °C. Figure 4-8 shows the result and the temperature program used.
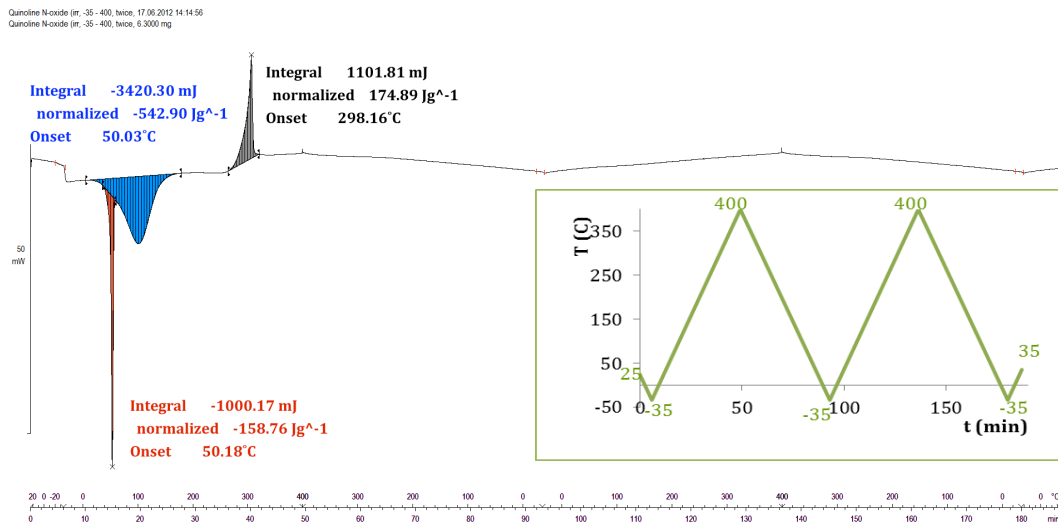
Figure 4-8- DSC graph of quinoline n-oxide hydrate decomposition from -35 to 400 ℃ versus time and T

For each observed event in Figure 4-8, the onset temperatures and the enthalpy changes are reported in Table 4-5 as well.

Table 4-5- Thermal events observed in DSC experiment of quinoline N-oxide hydrate from -35 to 400 ℃ under nitrogen environment

Thermal Event	Onset T (℃)	Enthalpy (Jg^{-1})
1 (red peak)	50.18	-158.76
2 (blue peak)	50.03	-542.90
3 (gray peak)	298.16	174.89

The absence of any peak after 43 minutes indicates that the event at about 300 °C is an irreversible event. The resulting black residue is not thermally affected at temperatures from -35 to 400 °C. However, beside the black residue, this exothermic event might also form some gaseous products, which are lost due to open system of DSC experiment. Therefore, multiple experiments were performed in the micro-reactor setup in addition to DSC experiments. In Figure 4-8, the decomposition peak starts at a temperature of about 270 ℃ and ends after about 5 minutes at 320 ℃. No other thermal

event was observed at higher temperatures up to 600 ℃ (as shown in Figure 4-3). Therefore, the thermal decomposition of quinoline N-oxide hydrate could be completed when it is heated at temperatures higher than 320 ℃ for times longer than 5 minutes. The produced residue is stable up to 600 ℃. For the performed experiments in the micro-reactor set up, 30 minutes heating at 400 ℃ was chosen as the reaction conditions. After performing the experiment, all the residues were weighed and analyzed. It was concluded that the observed exothermic event corresponds to thermal decomposition of quinoline N-oxide. The products were characterized in 3 categories: gaseous products, acetone-soluble residue and acetone-insoluble residue. The mass balance data, degree of nitrogen removal, structure of each product category and the possible mechanism of decomposition reaction are discussed in this section.

3-2-1- Temperature, pressure and mass balance data

The decomposition experiment was performed in the micro-reactor setup at 400 °C under nitrogen environment (p=600 kPa) for 30 minutes. The experiments were repeated several times to check the reproducibility of results. Temperature profile and pressure profile inside the micro-reactor setup are respectively shown in the Figures 4-9 and 4-10.
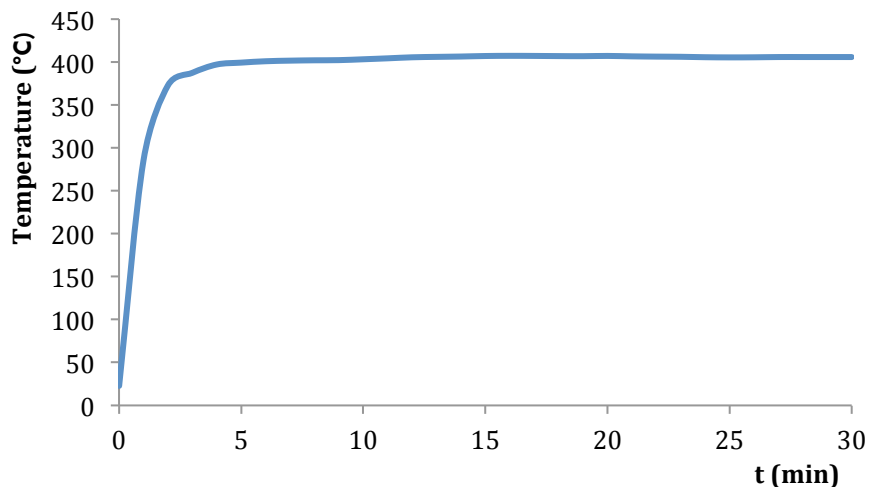
Figure 4-9- temperature profile inside micro-reactor setup during decomposition experiments

91
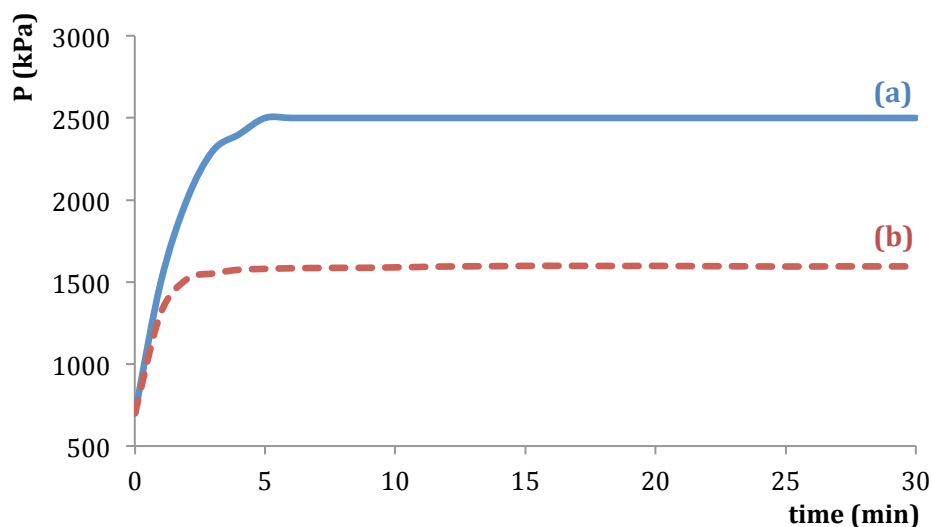
Figure 4-10- (a) Pressure profile inside micro-reactor setup during decomposition experiments (b) expected pressure inside micro-reactor due to expansion of nitrogen gas (calculated based on the initial pressure of micro-reactor setup and the recorded temperature versus time)

The dashed line in Figure 4-10 shows the expected pressure data calculated based on expansion of inert gas, i.e. nitrogen using the initial absolute pressure of micro-reactor setup (700 kPa) and the recorded temperature data versus time. The difference between these two line accounts for the formation of gaseous products inside micro-reactor set-up. It must be noted that the nitrogen gas is assumed to be 1) pure and, 2) an ideal gas. The compressibility factor for pure nitrogen gas is 0.9987 at initial conditions of reaction (25 ℃, 700 kPa) and 1.0100 at final conditions of reaction (400 ℃, 2500 kPa) [6]. Since these numbers are close to 1, the ideal gas law is good enough to approximately predict the pressure data for pure nitrogen gas at reaction conditions.

After cooling down the set-up, gaseous products were analyzed using GC and MS. The remained residue was collected from micro-reactor setup and weighed. This residue was partially soluble in acetone. Therefore, acetone extraction was used to better identify its structure. The acetone soluble part was a viscous brown liquid and the acetone insoluble part was a black residue.

Table 4-6 contains the run information and mass balance data of four experiments in micro-reactor setup and one experiment using DSC. The DSC experiment was performed using sealed HP crucibles, to simulate the same conditions as in the micro-reactor setup and to compare the results. The used temperature program is explained in Table 4-6. A fast heating step followed by an isothermal step was used to simulate the same temperature profile of micro-reactor setup. However, it was not possible to simulate the same inert environment inside sealed HP crucibles.

For the micro-reactor runs, the initial pressure is the absolute pressure of set up at room temperature, the maximum pressure is the absolute pressure recorded at 400 ℃ and the final pressure is the absolute pressure of the micro-reactor after cooling down to room temperature.

Table 4-7 shows the CHNS analysis of feed and all residues of the four micro-reactor runs listed above in Table 4-6. The oxygen amount was not measured experimentally and it is calculated based on the measured data for carbon, nitrogen, hydrogen and sulfur.

For a better comparison, the data presented in Table 4-6 are normalized for 1 gram of feed. The results along with the mean and standard deviation of data are presented Table 4-8 and also as a bar graph in Figure 4-11. Moreover, for each micro-reactor run, the nitrogen content of the residues is calculated using the mass information (Table 4-6) and the CHNS data (Table 4-7) and then, it is normalized for 1 gram of feed. The calculated data are compared with the nitrogen content of 1 gram of feed in Figure 4-12 and Table 4-9.

Table 4-6- Experimental conditions and mass balance information for thermal decomposition of quinoline N-oxide hydrate at 400 °C using the micro-reactor setup and DSC

Micro-reactor setup experiments			
1st Run			
Mass balance information (g)		**Run information**	
Feed	1.064	Initial pressure	700 kPa
Residue	0.786	Maximum pressure	2500 kPa
*Acetone soluble**	0.552	Final pressure	800 kPa
Acetone insoluble	0.234	Reaction time	30 min
2nd Run			
Mass balance information (g)		**Run information**	
Feed	0.999	Initial pressure	650 kPa
Residue	0.756	Maximum pressure	2400 kPa
Acetone soluble	0.529	Final pressure	750 kPa
Acetone insoluble	0.227	Reaction time	30 min
3rd Run			
Mass balance information (g)		**Run information**	
Feed	1.026	Initial pressure	700 kPa
Residue	0.747	Maximum pressure	2500 kPa
Acetone soluble	0.543	Final pressure	800 kPa
Acetone insoluble	0.204	Reaction time	30 min
4th Run			
Mass balance information (g)		**Run information**	
Feed	1.008	Initial pressure	700 kPa
Residue	0.770	Maximum pressure	2400 kPa
Acetone soluble	0.520	Final pressure	800 kPa
Acetone insoluble	0.250	Reaction time	30 min
DSC experiment			
Mass balance information (mg)		**Run information**	
Feed	4.72	Initial T	25 °C
Residue	4.01	Ramp	50 °C/min
Acetone soluble	2.67	Final T	400 °C
Acetone insoluble	1.34	Total run time	30 min

Data presented for acetone-soluble residue is calculated by the difference between the experimentally measured data for total residue and acetone-insoluble residue.

Table 4-7- CHNS analysis of feed, acetone-soluble residue and acetone-insoluble residue of four decomposition experiments of quinoline N-oxide hydrate using micro-reactor setup (400 ˚C, 600 kPa)

Sample	N	C	H	S	O*	C/N	C/H **
Feed							
Quinoline N-oxide hydrate	8.0	61.1	5.7	0.0	25.2	8.9	0.9
dry basis	9.8	75.1	4.5	0.0	10.6	8.9	1.4
*theoretical ***	9.7	74.5	4.8	0.0	11.0	9.0	1.3
1st Run							
Acetone-soluble residue	10.3	78.6	5.0	0.1	6.0	8.9	1.3
Acetone-insoluble residue	10.2	73.6	3.4	0.2	12.6	8.4	1.8
2nd Run							
Acetone-soluble residue	10.4	78.9	4.9	0.0	5.8	8.9	1.3
Acetone-insoluble residue	10.4	74.5	3.2	0.1	11.8	8.4	1.9
3rd Run							
Acetone-soluble residue	10.7	81.3	5.00	0.0	3.0	8.9	1.4
Acetone-insoluble residue	10.9	80.3	3.6	0.1	5.1	8.6	1.9
4th Run							
Acetone-soluble residue	10.4	77.8	4.7	0.0	7.1	8.7	1.4
Acetone-insoluble residue	10.3	73.7	3.3	0.0	12.7	8.3	1.9

Data presented for N, C, H, S, O are weight percentages.

*** Data presented for C/N and C/H are molar ratios calculated based on C, H, N (wt %).*

**** Data presented for hydrate form are measured experimentally. The dry basis values are calculated based on experimental data obtained for hydrate form, assuming that the water content is 1.9 mole/mole of quinoline N-oxide hydrate. The theoretical values are calculated based on the molecular formula of quinoline N-oxide (anhydrous).*
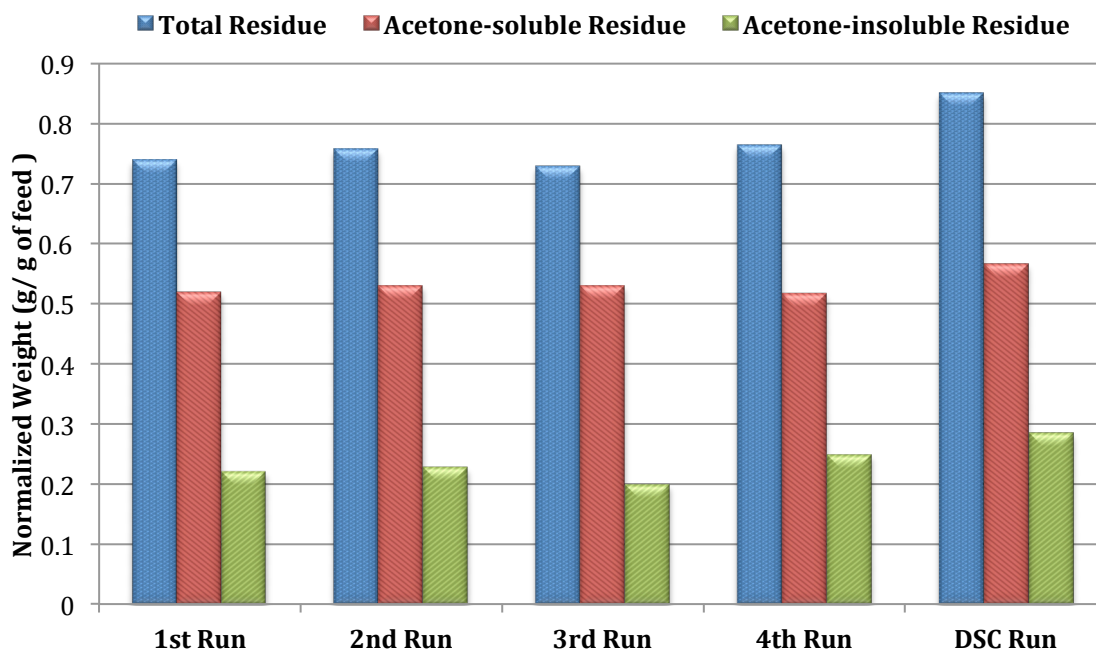
Figure 4-11- The weight of total residue, acetone-soluble residue and acetone-insoluble residue of four micro-reactor runs and one DSC experiment using HP crucibles (normalized for 1 gram of feed)
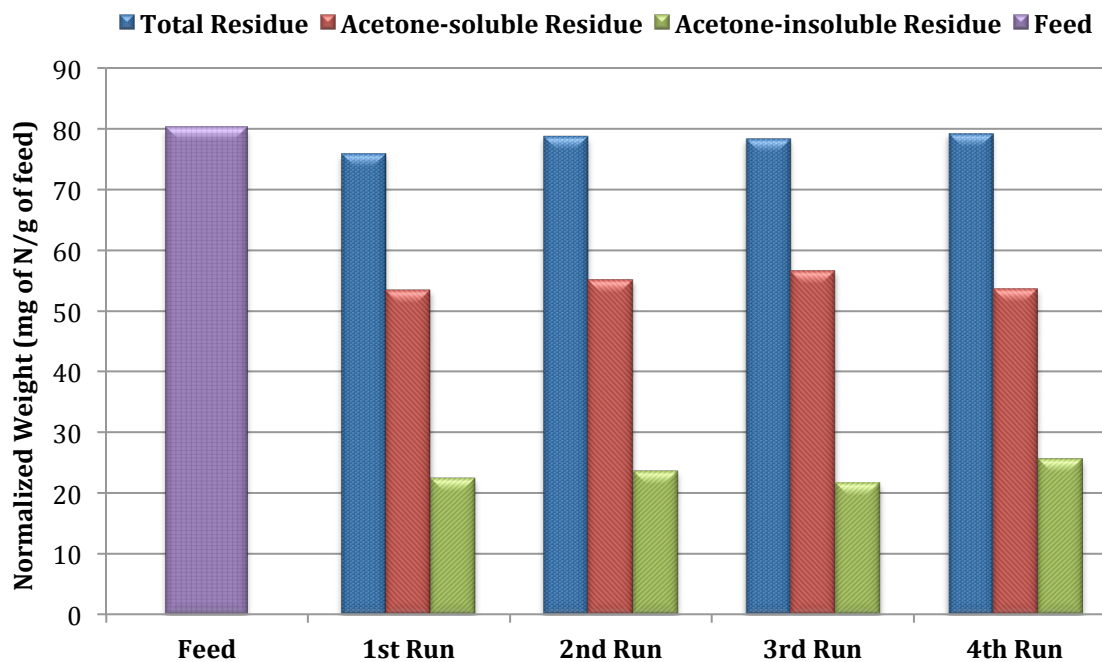
Figure 4-12- The nitrogen content of feed, total residue, acetone-soluble residue and acetone-insoluble residue of four micro-reactor runs; calculated based on CHNS data and weight of collected residues (normalized for 1 gram of feed)

Table 4-8- The weight of total residue, acetone-soluble residue and acetone-insoluble residue of four micro-reactor runs (mean and standard deviation of data are included) and one DSC experiment using HP crucibles (normalized for 1 gram of feed)

Normalized weight of Products (g/g of feed)			
Sample		Acetone-soluble residue	Acetone-insoluble residue	Total
DSC experiment		0.566	0.284	0.850
Micro-reactor experiments	1st	0.519	0.220	0.739
	2nd	0.530	0.227	0.757
	3rd	0.529	0.199	0.728
	4th	0.516	0.248	0.764
	Mean	*0.523*	*0.223*	*0.746*
	SD	*0.007*	*0.020*	*0.016*

Table 4-9- The nitrogen content of feed, total residue, acetone-soluble residue and acetone-insoluble residue of four micro-reactor runs; calculated based on CHNS data and weight of collected residues (normalized for 1 gram of feed)

Normalized nitrogen content (mg/g of feed)					Nitrogen removal (wt%)
Feed	Residue part of the products				
	Run	Acetone-soluble	Acetone-insoluble	Total	
80.2	1st	53.4	22.4	75.9	5.4
	2nd	55.1	23.6	78.7	1.9
	3rd	56.6	21.7	78.3	2.4
	4th	53.7	25.5	79.2	1.3
	Mean	*54.7*	*23.3*	*78.0*	*2.7*
	SD	*1.5*	*1.7*	*1.5*	*1.8*

In Table 4-8, the mean data of four micro-reactor runs shows that 74.6-wt% of the tested quinoline N-oxide hydrate has decomposed to a residue (of which 52.3-wt% was soluble in acetone and 22.3-wt% was insoluble in

acetone) and 25.4-wt% of it has decomposed to gaseous products. However, The DSC experiment has resulted in more amount of residue compared to micro-reactor ones. There were several differences in the experimental conditions between micro-reactor runs and DSC experiment such as differences in: pressure of experiment, the volume of sample containers, the inert versus non-inert environment, the amount of tested sample, etc. These all could have caused a difference in the amount of residue formed.

As can be seen from Figure 4-12 and Table 4-9, almost all the nitrogen content of feed was left in the residue part of the products for the four runs performed in the micro-reactor set up. A Student T-test between the data points of table 4-9 can clearly show if the nitrogen content is the same for feed (4 data points) and products (4 data points) of performed micro-reactor runs. The calculated t value is 2.95. The critical t value (ρ=0.05) for 6 degree of freedom is 2.45. Our calculated t value exceeds this number, meaning that the difference between the mean of data points for nitrogen content of feed and product is significant. This confirms that denitrogenation has happened to some extent. However, the amount of nitrogen removed is really low. The maximum nitrogen removal has happened in the 1st run where 5.4-wt% of nitrogen present in feed has gone to the gas phase of products. The amount of nitrogen removal for 2nd, 3rd and 4th runs was 1.9-wt%, 2.4-wt% and 1.3-wt%, respectively.

Therefore, thermal decomposition seems to be unable to remove most of the nitrogen available in quinoline N-oxide structure. However, it is important to understand the structure of each product category and the mechanism of its formation. These two topics are discussed in following sections.

3-2-2- Structure of products

In order to identify the structure of collected residues and also, the gaseous products, different analysis methods were used. This section

presents the analysis results and discussions on the structure of gaseous products, acetone-soluble residue and acetone-insoluble residue.

a) *Gaseous products*

Figure 4-13 shows the GC analysis of produced gases during decomposition of quinoline N-oxide hydrate at 400 °C and 600 kPa. Figure 4-14 shows the result for MS analysis of the same sample.
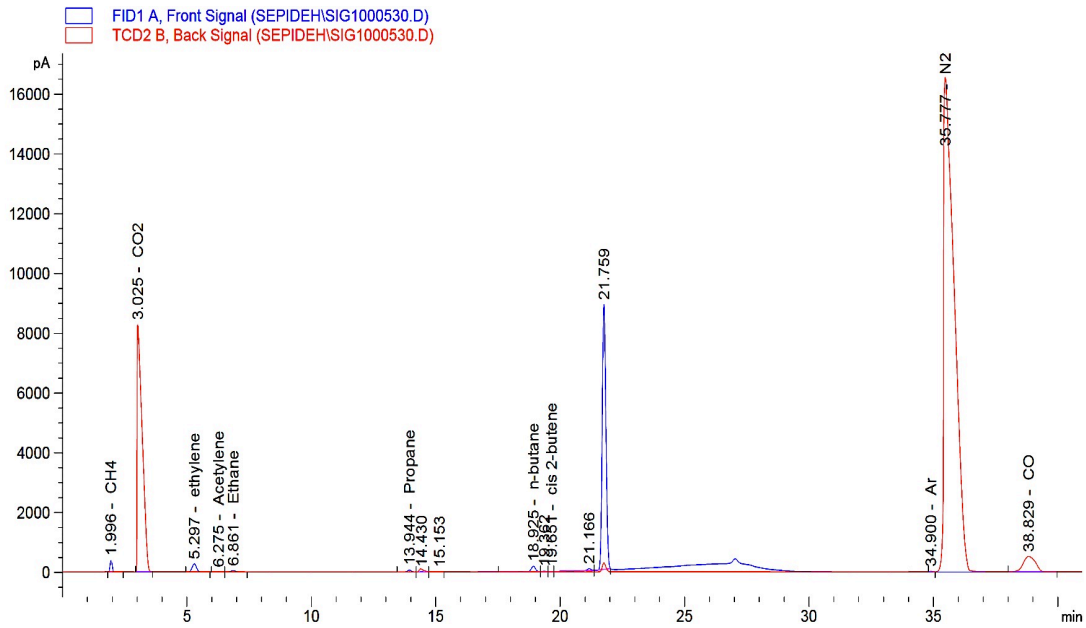
Figure 4-13- GC analysis of produced gases during decomposition of quinoline N-oxide hydrate at 400 °C and 600 kPa
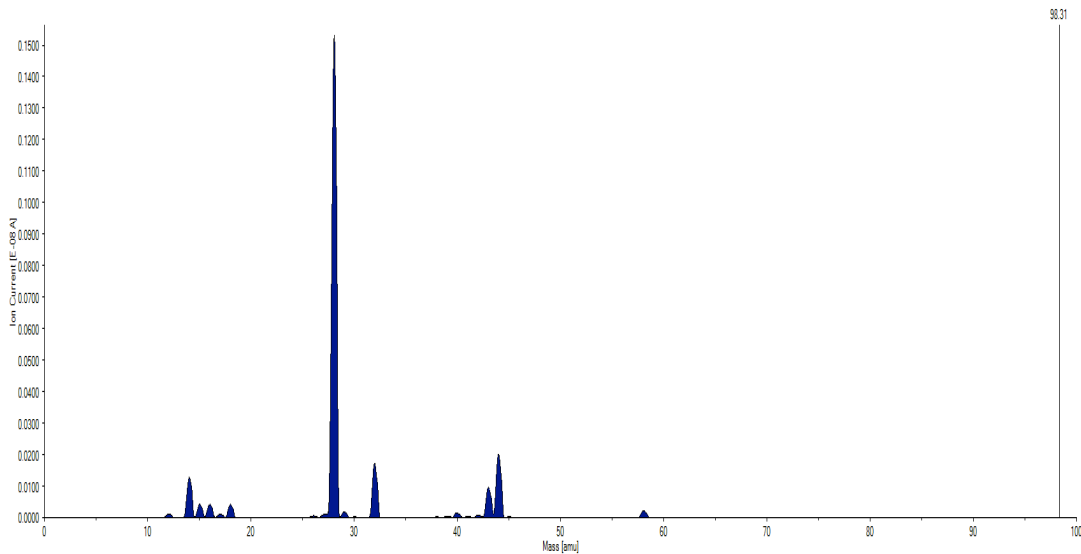
Figure 4-14- MS analysis of produced gases during decomposition of quinoline N-oxide hydrate at 400 °C and 600 kPa

GC identifies presence of CO, CO2 and N2. Small amount of methane, ethylene, acetylene, ethane, propane and n-butane are available. It must be mentioned that the peak at 14.430 min was common in all GC analysis (even in GC analysis of air or N_2) and it was probably due to a contamination in the GC setup. The only unknown compound is the one at retention time about 21.8 min. The MS result shown in Figure 4-14 can help to identify this unknown compound. The major mass peaks detected by MS are as follows (ordered based on ion current intensity): 28, 44, 32, 14, 43, 18, 16, 15, 58, 29, 27, 17, 40 and 12.

Table 4-10 shows the standard mass peaks of CO, CO_2, N_2, O_2, water and some organic compounds indicated by spectra library of Quadera™ software.

Table 4-10- The standard mass peaks in MS analysis of CO, CO_2, N_2, O_2, H_2O and some organic compounds.

Molecular Formula	Name	Main Masses
CO	Carbon monoxide	28, 12, 29, 16, 14, 30
CO_2	Carbon dioxide	44, 28, 16, 12, 45, 22, 46, 13, 29
N_2	Nitrogen	28, 14, 29
O_2	Oxygen	32, 16, 34, 33
H_2O	Water	18, 17, 16, 20, 19
CH_4	Methane	16, 15, 14, 13, 12, 17
C_2H_2	Acetylene	26, 25, 13, 24, 27, 12, 14, 28
C_2H_4	Ethylene	28, 27, 26, 25, 14, 24, 13, 29, 12
C_2H_6	Ethane	28, 27, 30, 26, 29, 15, 25, 14, 31
C_3H_8	Propane	29, 26, 28, 15, 27, 44, 14, 43, 39, 41, 42, 38, 37, 40, 30, 45, 25, 13, 12, 36
C_4H_{10}	n-Butane	43, 29, 27, 28, 41, 39, 58, 42, 26, 15, 44, 30, 59

Based on data available in Table 4-10, the following mass peaks in MS analysis of gaseous products can be explained by presence of the compounds already identified by GC (Figure 4-13):

28, 14 and 29:	Nitrogen
44, 28, 16, 12, 29:	CO and CO_2
16, 15, 14, 12:	Methane
28, 27:	Ethane, Ethylene

Since the characteristic mass peaks of gases identified by GC cannot explain the presence of mass peak at 58 amu in Figure 14-3, it must correspond to the unknown compound in the gas mixture produced by thermal decomposition of quinoline N-oxide hydrate. (GC peak at retention time about 21.8 min, Figure 4-13). Also, the mass peak at 43 amu is too big to be only the result of n-butane fragmentation (the concentration of n-butane is very low in the gas mixture). Therefore, it is possible that the compound with 58 amu loses a methyl group and gives a mass peak at 43 amu. The further fragmentation of this compound probably produces other ions which overlap on the ones resulted from materials in gaseous mixture. Based on MS analysis results, a few possible structures can be suggested. Using the same GC method used for analysis of gaseous products, these possible compounds were analyzed to confirm which one was the right compound present in gaseous mixture. It was confirmed that acetone comes out at retention time about 21.8 min which is the same as retention time of unknown compound in the gaseous products. Figure 4-15 shows the standard MS spectra of acetone [7]. In the MS spectrum of acetone, the relative intensity of the peaks at 58 amu and 43 amu matches with what was observed for the produced gaseous mixture by thermal decomposition of quinoline N-oxide hydrate (Figure 4-14).
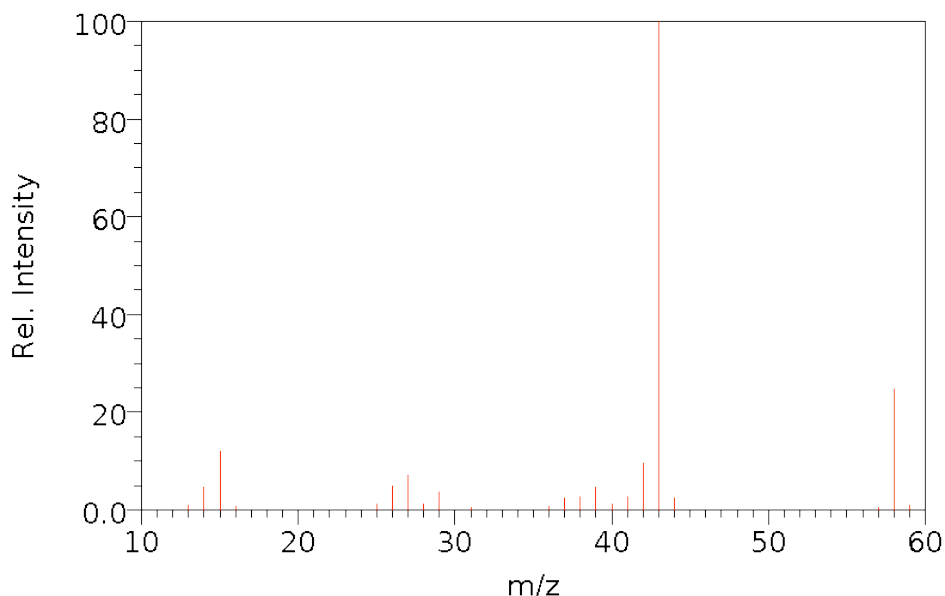
Figure 4-15- Standard MS spectra of acetone [7]

Therefore, acetone is the unknown compound in the gaseous products. However, the presence of acetone cannot be explained by any possible chemistry happening during thermal decomposition of quinoline N-oxide hydrate; but, it can be explained by the acetone-washing method used prior to thermal decomposition experiment (described in section 2-3-2). Although the micro-reactors were dried using airflow before running the experiment, some acetone could still be left in the micro-reactor setup. This has caused the presence of acetone in the gas phase at the end of experiment. This hypothesis was confirmed by doing a blank run, i.e. using the same washing method and running an experiment without a sample at 400 °C and 600kPa of N_2. The acetone peak was observed in the GC analysis of gaseous mixture confirming that it was due to washing method being used.

The MS spectrum of produced gases (Figure 4-14) also shows a mass peak at 18 amu and a mass peak at 32 amu. As it is explained in section 3-1, quinoline N-oxide hydrate undergoes dehydration at temperatures less than 190 °C. Therefore, the mass peak at 18 amu is due to presence of water in the gas mixture. Also, the mass peak at 32 amu can be explained by presence of

oxygen due to partial deoxygenation of quinoline N-oxide. This hypothesis is confirmed in the following section discussing the structure of acetone-soluble residue. It must be noted that, since GC uses a hydrogen-oxygen flame to detect compounds by FID detector, it was unable to identify oxygen.

b) *Acetone-soluble residue*

Figure 4-16 shows the IR spectrum of acetone-soluble residue in comparison with quinoline and quinoline N-oxide hydrate. Table 4-11 summarized the main absorption peaks observed for these samples. As it can bee seen, the IR spectrums of residue and quinoline almost match with each other suggesting that the acetone-soluble residue mostly consists of quinoline.
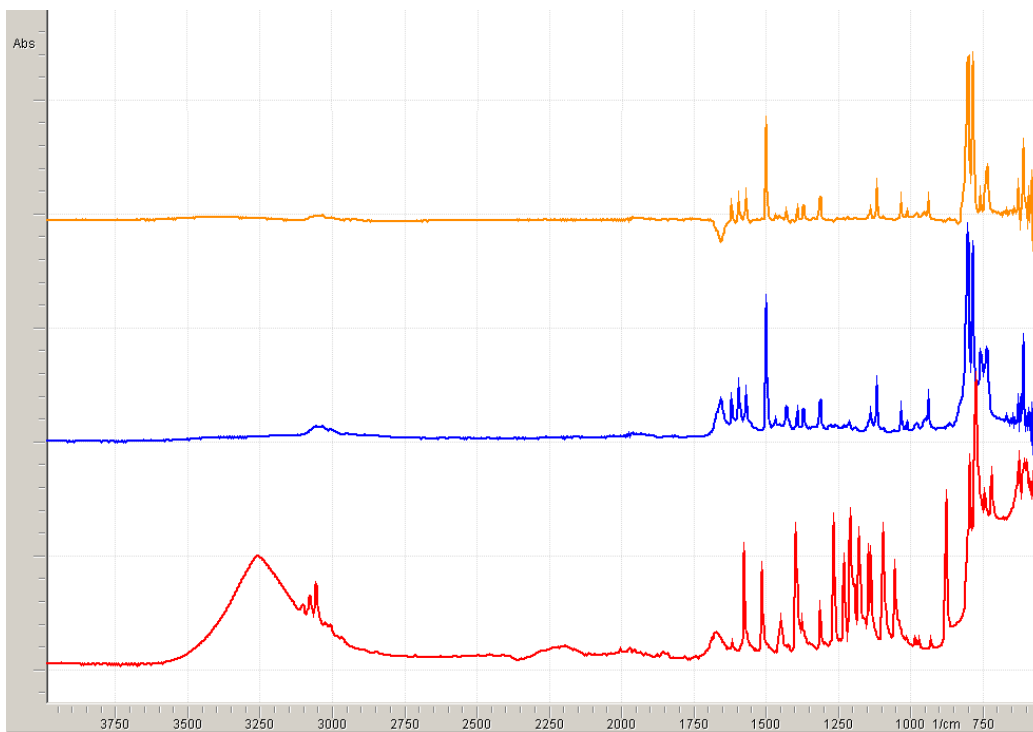
Figure 4-16- IR spectrum of 1) quinoline (yellow line), 2) acetone-soluble residue of quinoline N-oxide hydrate decomposition at 400 °C and 600 kPa N_2 (blue line), 3) quinoline N-oxide hydrate (red line), using ATR attachment

Table 4-11- The wavenumber range of the main absorption peaks observed in Figure 4-16

	Sample		
	Quinoline	Acetone-soluble residue of quinoline N-oxide decomposition (400 °C, 600 kPa of N_2)	Quinoline N-oxide hydrate
The wavenumber range of main absorption peaks observed (cm^{-1})	768-840	767-852	788-822
			857-895
	913-946	908-962	910-932
	1023-1050	1023-1051	1019-1066
	1103-1127	1101-1127	1067-1108
	1127-1170	1127-1176	1111-1154
			1165-1187
			1187-1220
			1221-1241
			1251-1277
	1294-1328	1294-1326	1286-1323
	1361-1379	1360-1378	1323-1412
	1380-1404	1378-1404	
	1416-1441	1405-1452	1430-1465
	1477-1511	1477-1512	1497-1527
	1557-1581	1521-1582	1540-1585
	1582-1606	1582-1606	
	1607-1636	1606-1635	1605-1634
		1636-1698	1586-1718
	2986-3096	2956-3114	2891-3588
			3032-3067
			3067-3093
			3094-3114

The GC/MS analysis result of acetone-soluble residue (Figure 4-17) also suggested that it mostly contained quinoline. The presence of trace amounts of bi-quinoline, 2-methyl quinoline and 3-methyl quinoline was also identified. The methyl quinolines might be the impurities present in the commercially available quinoline N-oxide, since no possible pathway was

found that could explain the formation of these compounds by thermal decomposition of quinoline N-oxide.
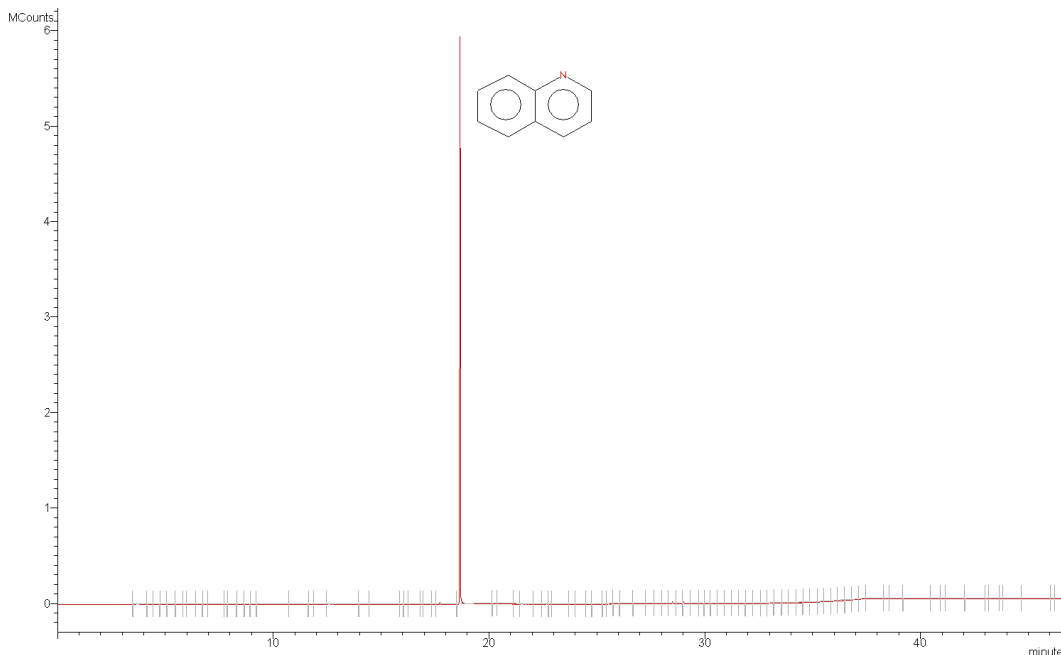
Figure 4-17- GC-MS analysis for acetone-soluble residue of quinoline N-oxide hydrate decomposition at 400 ℃ and 600 kPa of N_2

The results presented above indicate that quinoline N-oxide hydrate undergoes partial deoxygenation to produce quinoline at 400 ℃. The possible mechanism will be later explained in section 3-2-4. This deoxygenation event was the reason behind the big difference between the recorded pressure inside the micro-reactor setup and the one expected based on nitrogen expansion during setup heating time (Figure 4-10). The production of oxygen and quinoline, which were in vapor phase at reaction temperature (400 ℃), along with water production (due to dehydration of sample) and formation of CO and CO_2 were the reasons behind the pressure difference in Figure 4-10. Also, this produced quinoline vapor has left the DSC system along with carrier gas in the performed DSC experiment with standard Al crucibles (Figure 4-8). As a result, only the acetone-insoluble part of the decomposition

products (the black residue) was left in the crucible at the end of DSC experiment.

c) *Acetone-insoluble residue*

The IR spectrum of acetone-insoluble residue was obtained using both KBr pellet sampling method and also, ATR attachment for FTIR spectrometer (Figure 4-18).
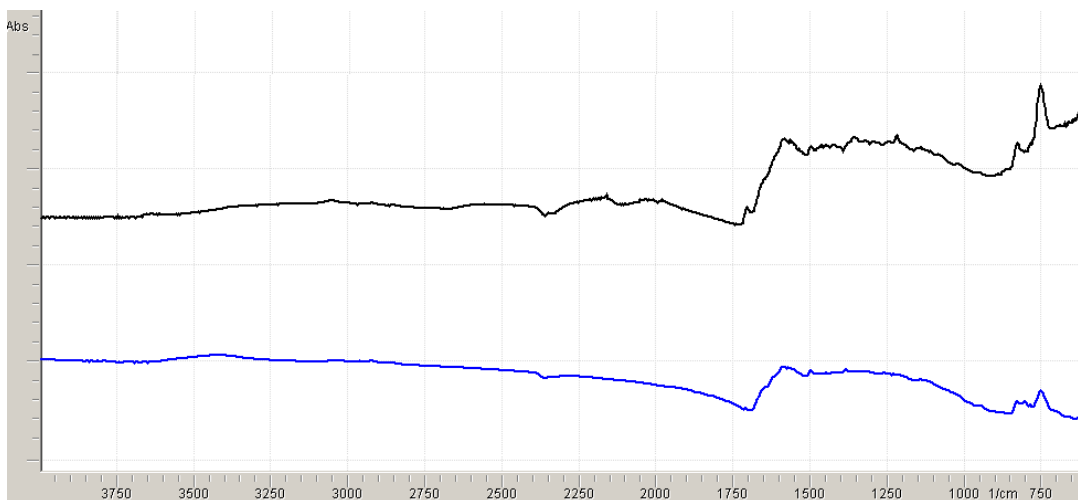
Figure 4-18- IR spectrum of acetone-insoluble residue of quinoline N-oxide hydrate decomposition at 400 °C and 600kPa of N_2: 1) using KBr pellet (blue line), 2) using ATR attachment (black line)

All N-oxides are known to show three to five strong absorption peaks in the wavenumbers from 1190 to 1350 cm^{-1} [8]. The absence of these absorption bands in the IR spectrum of acetone-insoluble residue indicates the degradation of N-oxide structure. The observed absorption bands at 750 cm^{-1} and 800-850 cm^{-1} can be assigned to polyene structures. The IR spectra of polycyclic aromatic hydrocarbons shows three main regions of absorption: C-H stretching frequencies in the region 3000-3090 cm^{-1}; C-C stretching of the aromatic structure resulting in sharp medium intensity peaks near 1600 and 1500 cm^{-1}; and the C-H out of plane bending absorptions occur in the region 650-900 cm^{-1} [9]. In condensed ring compounds, the interpretation of the 700-900 cm^{-1} helps to classify the substitution of compound in terms of adjacent hydrogen. The C-H bending vibrations in molecular regions

containing a) one adjacent hydrogen happens in the highest region of 860-900 cm^{-1}; b) two adjacent hydrogen are found from 800 to 860 cm^{-1}, c) three adjacent hydrogen occurs between 750-810 cm^{-1}; and d) 4 adjacent hydrogen happens in the lowest region of 735-770 cm^{-1} [9-10]. Therefore, in the IR spectrum of acetone-insoluble reside, the presence of three absorption bands at 750 cm^{-1} and between 800-850 cm^{-1} indicate the presence of molecular regions with two and three adjacent hydrogen atom bonded to the aromatic ring.

The elemental analysis of this black polymeric substance was presented earlier in Table 4-2. The nitrogen content is about 10.6-wt%. The carbon to hydrogen molar ratio is increased about 36% compared to quinoline N-oxide (dry basis). This confirms the formation of condensed aromatic structure. The carbon to nitrogen molar ratio is a bit less than quinoline N-oxide.

Beside acetone, this residue was found not to be soluble in water, toluene, methanol, ethanol, tetrahydrofuran (THF) and dimethyl sulphoxide at room temperature. This was found by trying to dissolve the sample in these solvents at room temperature, filtering the insoluble part and then, analyzing the solution either by GC or GC/MS or FTIR, in order to check for even a slight solubility. Further investigation on the structure of this residue was not done due to its solubility limitation. In order to identify the structure of this polymeric compound, one must try to understand the possible mechanism happening during thermal decomposition of quinoline N-oxide. This is discussed in the next section.

3-2-3- Possible mechanism of thermal decomposition reaction

The results presented in previous sections suggest that quinoline N-oxide decomposed partly to quinoline, partly to a polymeric compound at 400 °C and also, partly to a gaseous mixture of CO_2, CO, O_2, and water.

To conclude a possible mechanism for thermal decomposition of quinoline N-oxide at 400 °C, the following points must be noted:

1- Quinoline was found to be stable at reaction conditions. Quinoline has been reported to be thermally stable at 475 °C when it was heated for 30 minutes. In more severe conditions at 500 °C, 4.9-wt% of condensed heavy residue and 0.32-wt% of gases (49 mole % H_2, 47 mole % methane, 4 mole % CO) were produced [11]. Also, it was stable in liquid phase up to 510 °C and in vapor phase up to 650 °C [12].

The following experiment was performed to examine the thermal stability of quinoline. About 1 g of quinoline was heated in the micro-reactor setup under nitrogen environment (600 kPa) at 400 °C for 30 minutes. GC analysis of the gas phase revealed that no gaseous products were formed. The IR spectrum of the liquid residue matched with that of quinoline, confirming that quinoline did not decompose at the experimental conditions. Thermal decomposition of quinoline N-oxide hydrate has produced about 55-wt% quinoline. The thermal stability of quinoline suggests that neither the acetone-insoluble residue nor the gaseous products were produced by further decomposition of this produced quinoline.

2- Quinoline N-oxide hydrate undergoes dehydration from 50 °C to 170 °C (the reported amount of crystallization water is 1.91 mole/mole of quinoline N-oxide hydrate and what was observed during DSC experiments is 1.96 mole/mole of quinoline N-oxide hydrate). No evidence was found that this produced water was involved in decomposition reaction of quinoline N-oxide.

The produced quinoline from thermal decomposition of quinoline N-oxide did not react with water under experimental conditions. This was confirmed by running an experiment with about 0.8 g quinoline and 0.2 g water at 400 °C and 600 kPa of N_2 for 30 minutes and further analysis of the products by GC, MS, GC-MS and FTIR. Therefore,

reaction of quinoline with water could not be the reason behind the formation of quinoline N-oxide decomposition products.

To eliminate water role in decomposition reaction, a new experiment was designed. About 1 g of quinoline N-oxide hydrate was first heated in the micro-reactor setup under nitrogen environment (600 kPa) up to 170 ℃ for 15 minutes. Then, the produced gases, due to dehydration of the quinoline N-oxide hydrate, were released while the micro-reactor set up was kept at 170 ℃. The micro-reactor was then cooled down to room temperature, pressurized with N_2 (600 kPa) and then, heated to 400 ℃ for 30 minutes. The gaseous products, acetone-soluble residue and acetone-insoluble residue were analyzed using GC, MS, GC-MS and IR spectroscopy. The results were the same as what is presented in previous sections (Figures 4-13 – 4-18), confirming that water did not play a role in thermal decomposition of quinoline N-oxide at 400 ℃.

Presence of quinoline in the acetone-soluble residue can be easily explained by deoxygenation of quinoline N-oxide. Many reduction reactions of heterocyclic N-oxides lead to loss of the oxygen atom and production of parent heterocycle. Compared to aliphatic or alicyclic N-oxides, in heteroaromatic N-oxides, the N-oxide group is considerably more resistant toward reduction. However, quinoline N-oxides are significantly less stable toward reduction compared to their pyridine analogues. Thermal deoxygenation is the simplest method without an added reagent for incomplete deoxygenation of quinoline N-oxides [13]. Quinoline N-oxide loses its oxygen in the heated inlet of an analyzing instrument [8] such as a gas chromatograph. It is reported that the decomposition of quinoline N-oxide starts at 160°C and becomes rapid at 190-200°C. The experiment was simply performed by heating the sample in a distillation flask. The products contained 13% quinoline when quinoline N-oxide was heated alone, 26% quinoline when it was heated with PhNO2 as catalyst, and 35% quinoline

109

when it was heated with Cu dust as catalyst [14]. In the studied experiments in previous sections, the thermal decomposition started at 170 ℃ when the experiment is performed under atmospheric air using Mettler Toledo thermal microscopy system and it started at 270℃ when the experiment is performed under inert environment using Mettler Toledo DSC1.

Many N-oxides lose their oxygen if heated more strongly, either alone or using various solid catalysts. Pyridine N-oxide is reported to give some pyridine at 220 ℃. Copper or zinc powder could catalyze this reaction [13]. In another study, pyridine N-oxide was decomposed partially to pyridine from 210 ℃ to 260 ℃ [14-15]. The rate of reaction was increased in the presence of hydrogen halides. The following mechanism is suggested for thermal decomposition of pyridine N-oxide (Figure 4-19). The products are identified as: pyridine, bipyridine N-oxide, hydroxypyridine, CO, CO_2, N_2, H_2O and a black polymeric compound containing 16.8% nitrogen [15].
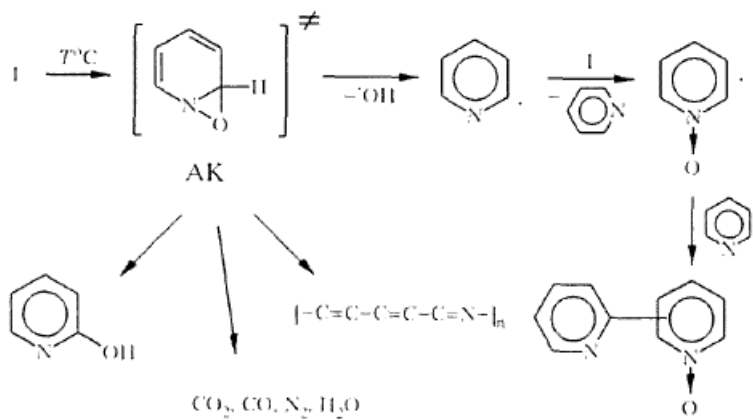
Figure 4-19- The mechanism of thermal decomposition of pyridine N-oxide [15]

Although there are some similarities between the products identified for pyridine N-oxide decomposition and the products of quinoline N-oxide decomposition, the absence of a compound containing OH group in the latter one suggest that not all of the suggested decomposition pathways are valid for quinoline N-oxide decomposition. However, the formation of an oxaziridine complex (a more active and more ordered cyclic intermediate) is

110

repeatedly suggested as the initial step in the thermolysis of pyridine N-oxides (either in gas phase or liquid phase). This mechanism suggests that the reactive center for the first step in thermolysis of pyridine N-oxides is the N-O bond (Figure 4-20) [16].
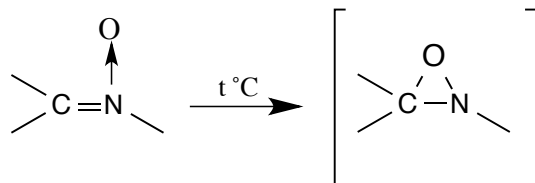
Figure 4-20- Formation of an oxaziridine complex as the initial step in the thermolysis of pyridine N-oxides [16]

The production of quinoline present in acetone-soluble reside can be explained by deoxygenation of this oxaziridine intermediate. Also, there must be another pathway available leading to production of heavier products classified as acetone-insoluble residue

Figure 4-21 shows the mechanism suggested for photochemical reaction of phenylquinoline N-oxide leading to indole production.
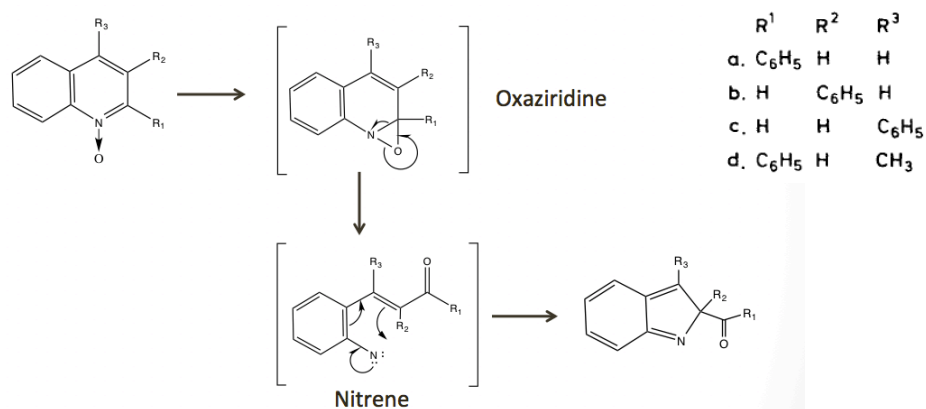
Figure 4-21- One of the suggested mechanisms for photochemical reaction of some phenylquinoline N-oxides [17]

The nitrene XX intermediate can be formed from the oxaziridine XII using a thermal or photochemical process [17]. This mechanism can perfectly explain the presence of CO and CO_2 in the gaseous products of quinoline N-oxide decomposition. The CO bond, formed in the nitrene structure, can

break from the rest of structure leading to production of CO. Decarbonylation of aromatic aldehydes is reported to proceed through aromatic electrophilic substitution leading to formation of carbon monoxide [18]. Further oxidation of nitrene structure with present oxygen (from deoxygenation of quinoline N-oxide) or with quinoline N-oxide can form CO_2 functionality. Assuming that this mechanism is valid for thermal decomposition of quinoline N-oxide, two possibilities can explain the formation of the condensed polymeric structure:

1- Before the reaction shown in Figure 4-21 goes to completion, the formed nitrene compound can react with other compounds (like quinoline N-oxide) to form heavier products.

2- After the completion of the reaction sequence shown in Figure 4-21, the produced indole polymerizes to form heavier products. Several pathways were proposed for indole dimerization, trimerization and polymerization [19-20]. The polymer has a 2,3 couplings structure and nitrogen atom does not participate in the bonding between indole units as shown in Figure 4-22 [20-21].
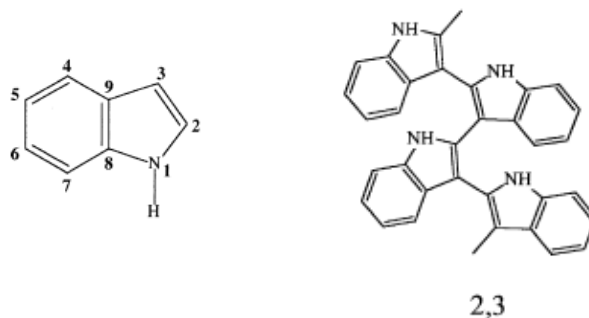
Figure 4-22- Structure of indole and its polymer with 2,3 couplings between carbon atoms [21]

Assuming that the formation of the polymeric structure is due to the second possibility, some indole must be present in the acetone-soluble residue, since it is unlikely for the polymerization reaction to have a 100% conversion. The GC-MS analysis results for a solution of indole in acetone and the acetone-soluble residue are shown in Figures 4-23 and 4-24, respectively.

112

For a better comparison, the graph presented in Figure 4-24 is also zoomed at retention times from 18.5 min to 19.6 min. Comparing these two Figures, it can be easily seen that no amount of indole is found in the acetone-soluble residue. This indicated that the second possibility is unlikely.
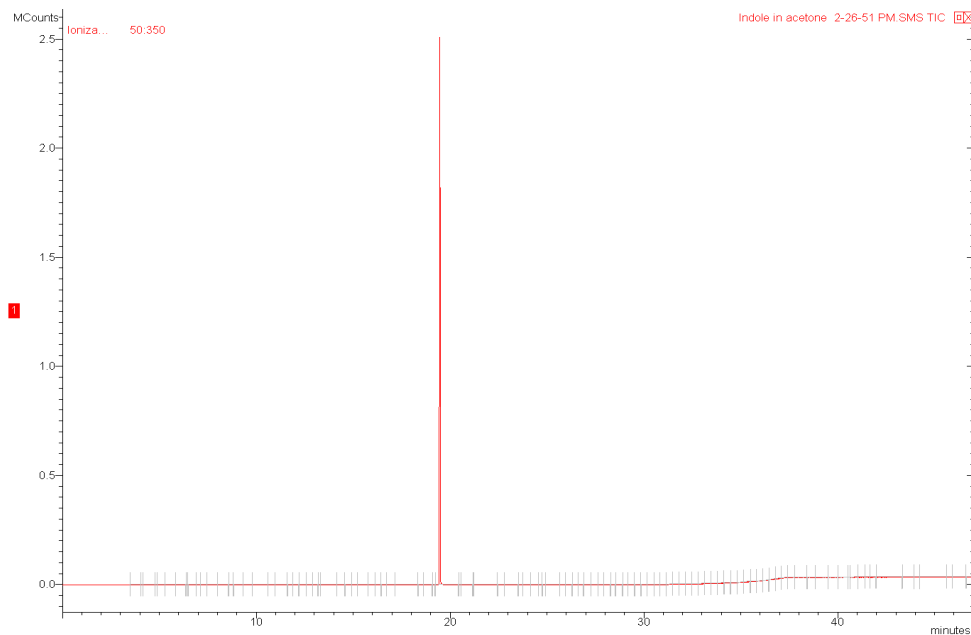
Figure 4-23- GC-MS analysis for solution of indole in acetone
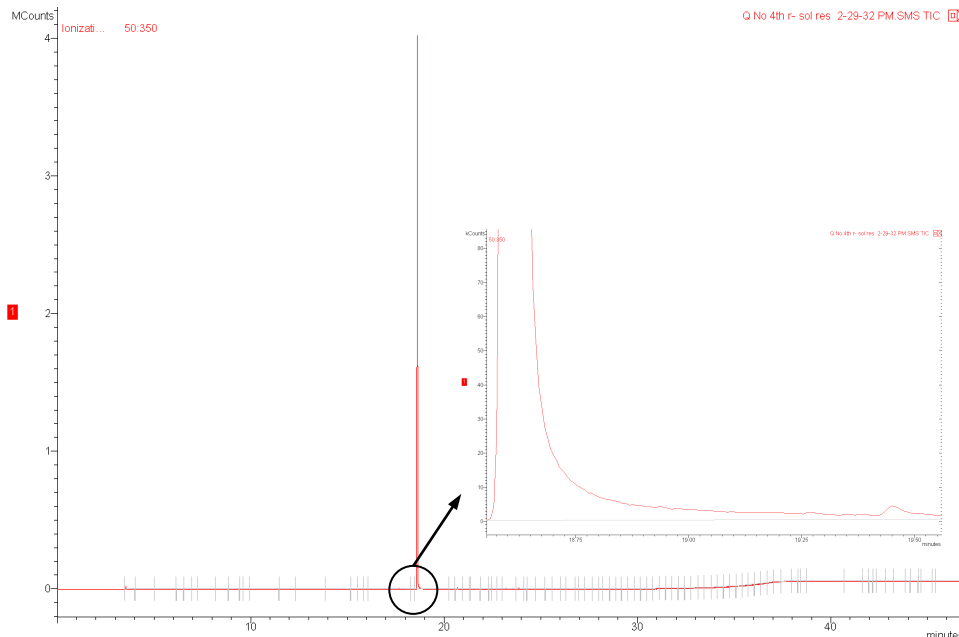
Figure 4-24- GC-MS analysis for acetone-soluble residue of quinoline N-oxide hydrate decomposition at 400 °C and 600 kPa of N_2 (zoomed at 18.5 - 19.6 min)

Therefore, the formation of nitrene structure from the oxaziridine intermediate and further reaction of this compound is the best hypothesis found that can explain how the thermal decomposition of quinoline N-oxide might lead to formation of the acetone-insoluble residue and the gaseous products (identified in section 3-2). Based on this hypothesis, the decomposition pathway of quinoline N-oxide at 400 °C can be explained as follows: At first, quinoline N-oxide forms the oxaziridine intermediate. This intermediate partially deoxidizes to form quinoline and oxygen and also, partially rearranges to form the nitrene intermediate (as shown in Figure 4-21). Before formation of indole, the nitrene intermediate reacts with other compounds such as quinoline or quinoline N-oxide (it must be noted that quinoline N-oxide can act as a electrophile agent as well as a nucleophile agent, due to the formation of its different resonance structures). This leads to production of a poly-aromatic structure and also, CO and CO_2. This mechanism is shown in Figure 4-25.
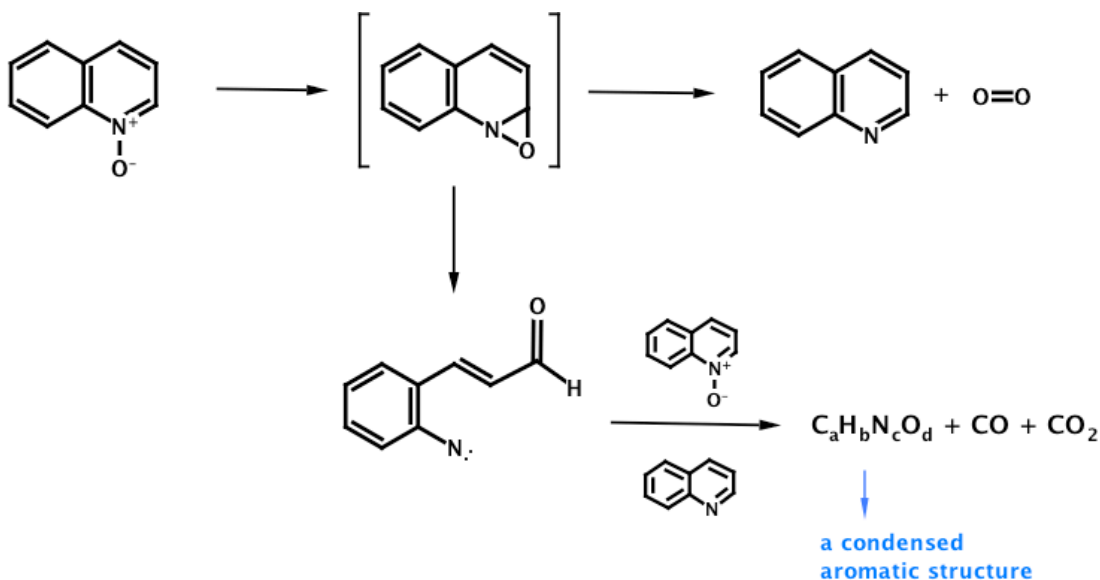
Figure 4-25- The suggested reaction pathway for thermal decomposition of quinoline N-oxide at 400 °C and 600 kPa

It must be noted that, due to the solubility limitation of the acetone-insoluble residue, it is not feasible to verify the suggested hypothesis using standard analytical instruments. Further investigation is necessary to properly understand the mechanism happening during thermal decomposition of quinoline N-oxide.

4- Conclusion

Quinoline N-oxide hydrate was found to lose its crystallization water when heated under nitrogen environment. The water molecules were not energetically equivalent, since dehydration has happened in 2 steps, 1 in conjugation with melting from 50 to 70 °C and the other one from 70 to 170 °C.

Thermal decomposition of quinoline N-oxide starts at temperatures around 270 °C. The products of thermal decomposition of quinoline N-oxide hydrate at 400 °C and 600 kPa of N_2 (reaction time: 30 minutes) were identified as: 52-wt% of quinoline:, 22-wt% of a black nitrogen-containing polymeric compound and 26-wt% of gaseous products. The main gaseous products identified were CO_2, CO, O_2, water, CH_4, butane and ethylene. Trace amount of biquinoline was also present in the acetone-soluble part of the residue. The produced quinoline was found to be stable under experimental condition and the crystallization water was found not to participate in thermal decomposition reaction. The production of an oxaziridine intermediate is suggested as the initial step in the mechanism of thermal decomposition. This intermediate partially undergoes deoxygenation to produce oxygen and quinoline present in acetone-soluble reside and partially forms a nitrene compound. Further reaction of the nitrene leads to formation of CO, CO_2, a poly-aromatic structure and also, traces amount of other organic materials.

Almost all the nitrogen content of feed was remained in the residue part of the products. This proves that not only thermal decomposition was ineffective for denitrogenation of quinoline N-oxide, but it also has caused the production of a more complex aromatic structure with 10-wt% nitrogen content.

5- References

[1] Cooper, C. D.; Alley F. C. *Air Pollution Control- A Design Approach,* 3rd ed; Waveland Press Inc.: Illinois, 2002; pp 2-3 & 51-52.

[2] Borah D.; Baruah M. I. Oxidation of High Sulphur Coal. 3. Desulfurization of Organic Sulphur by Peroxyacetic Acid (Produced in situ) in Presence of Metal Ions, *Fuel Processing Technology* **2005**, *86*, 959-976.

[3] Gubarev Yu. A.; Lebedeva N. Sh.; Andreev V. P.; Girichev G. V. Thermal Behavior of Quinoline N-Oxide Hydrates and Deuterohydrate, *Russian Journal of General Chemistry* **2009**, *79*, 1183-1190.

[4] Gubarev Yu. A.; Lebedeva N. Sh.; Andreev V. P.; Nizhnik Ya. P.; V'yugin A. I. Thermooxidative Decomposition of Heterocyclic *N*-Oxides, *Russian Journal of General Chemistry* **2007**, *77*, 1093-1099.

[5] Lide, D. R.; Properties of Water and Steam as a Function of Temperature and Pressure, in *CRC Handbook of Chemistry and Physics*, *Internet Version 2005*; http://www.hbcpnetbase.com; CRC Press: Florida, 2005; section 3.

[6] Perry, R. H.; Green, D. W.; Maloney J. O. *Perry's Chemical Engineers' Handbook*, 7th ed.; McGraw-Hill Companied Inc.: New york, 1997; p 2-145.

[7] National Institute of Standards and Technology (NIST), http://webbook.nist.gov/cgi/cbook.cgi?ID=C67641&Mask=200 (accessed Nov 9, 2012).

[8] *The Chemistry of Heterocyclic Compounds: Quinolines, Part II;* Jones, G.; John Wiley and Sons Ltd: New York, 1982; Vol. 32, pp 414 & 424.

[9] Harvey, R. G. *Polycyclic Aromatic Hydrocarbons: Chemistry and Carcinogenicity;* Cambridge University Press: Cambridge, 1991; pp 109-110.

[10] Colthup, N. B.; Daly, L. H.; Wiberley, S. E. *Introduction to Infrared and RamanSpectroscopy,* 2nd ed; Academic Press: London, 1975; pp 270-271.

[11] Madison, J. J.; Roberts, R. M. Pyrolysis of Aromatics and Related Heterocyclics, *Industrial & Engineering Chemistry* **1958**, *50*, 2, 237-250.

[12] Johns, I. B.; McElhill, E. A.; Smith, J. O. Thermal Stability of Some Organic Compounds, *Journal of Chemical & Engineering Data* **1962**, *7*, 2, 277-281.

[13] Katritzky, A. R.; Lagowski, J. M. *Chemistry of the Heterocyclic N-oxides;* Academic Press: London, 1971; pp 168 & 229.

[14] Katada, M. Polarization of Aromatic Heterocyclic Compounds. LIII. Deoxidation of Pyridine and Quinoline 1-oxides by Thermal Decomposition; *Yakugaku Zasshi* **1947***, 67,* 53-55.

[15] Klyunchnikov, O. R.; Saifullin, I. Sh.; Nikishev, Yu. Yu. Structural Kinetic Rules Governing the Thermal Decomposition of Pyridine N-oxides, *Chemistry of Heterocyclic Compounds* **1994**, *30,* 5, 564-566.

[16] Klyuchnikov, O. R.; Nikishev Yu. Yu. Thermal Stability and Thermal Decomposition of N-oxides, *Chemistry of Heterocyclic Compounds* **1995**, *31*, 11, 1367-1369.

[17] Buchardt, O.; Kumler, Ph. L.; Lohse, Ch. Photochemical Studies. XVI. Photolysis of Phenylquinoline N-Oxides in Solution. A Novel Light-Induced Reaction. Solvent Influence on the Product Distribution. *Acta Chemica Scandinavica* **1969**, *23*, 2149-2157.

[18] *The Chemistry of Functional Groups: The Carbonyl Group* [Online]; Patai, S.; John Wiley and Sons Ltd, 1966; Vol. 1, pp 697. http://onlinelibrary.wiley.com.login.ezproxy.library.ualberta.ca/book/10.10 02/9780470771051

[19] *The Chemistry of Heterocyclic Compounds: Indoles, Part I;* Houlihan, W. J.; Remers, W. A.; Brown, R. K.; Wiley-Interscience: New York, 1972; Vol. 25, pp 66-69.

[20] Sarac, A. S.; Ozkara, S. In-situ Spectroelectrochemical Investigation of Indole polymerization, *International Jourmal of Polymeric Materials* **2004**, *59*, 587-599.

[21] Talbi, H.; Monard, G.; Loos, M.; Billaud D. Theoretical Study of Indole Polymerization, *Journal of Molecular Structure (Theochem)* **1998**, *434*, 129-134.

Chapter 5

Thermodynamic Study

1- Introduction

Gibbs free energy is a measure of the driving force for a reaction to Proceed. In other words, any spontaneous reaction will minimize the Gibbs free energy of a system. A reaction is spontaneous when its Gibbs energy is negative. At constant conditions, calculating the Gibbs energy of a reaction could indicate whether it is thermodynamically favored by nature [1].

In this chapter, the Gibbs free energy of reactions involved in oxidative denitrogenation of quinoline is studied. The studied reactions include both hypothetical reactions for a successful denitrogenation and also, the observed reactions based on the experimental results presented in previous chapters.

2- Thermodynamic Studies

For a reaction, the Gibbs free energy is defined as [1]:

$$\Delta_r G^\circ = G_{Products} - G_{Reactants} \qquad (5\text{-}1)$$

At standard conditions (25 ℃, 1 atm), $G_{Products}$ or $G_{Reactants}$ is the sum of standard Gibbs free energy of formation for each compound. This energy can be estimated from the molecular structure of the compound [1]. The estimation method used is explained in section 2-1. Section 2-2 presents the scheme of the studied reactions and section 2-3 discusses the result drived from the calculated Gibbs free energy of reactions.

2-1- Joback method

In the Joback method, the standard Gibbs free energy of formation for a compound is estimated based on its molecular structure. This method assigns contributions to molecular groupings. The numbers are simply added to calculate the Gibbs free energy of formation, as shown in Formula 5-2 [1].

$$\Delta G_f^{\circ} = 53.88 + \sum_k N_k \Delta g_{fk} \qquad (5\text{-}2)$$

Table 5-1 presents the contribution of some common molecular grouping in the Joback method [1]. These are the molecular groupings that are used in section 2-3 to calculate the Gibbs free energy of studied reactions.

Table 5-1- The contribution of some molecular groupings to Gibbs free energy of formation in Joback method [1]

Ring Structures	Molecular Group	=CH-	=C<	-CH$_2$-	=N-	ANO*	
	Contribution (kJmole^{-1})	11.3	54.05	-3.68	79.93	-22.48	
Non-ring Structures	Molecular Group	-CH$_3$	-CH$_2$-	-CH-	-CH=O	ACO$_2$H	ACO$_3$H**
	Contribution (kJmole^{-1})	-43.96	8.42	58.36	-143.48	-387.87	-31.53

In Table 5-1, the numbers for ANO (the N=O group in the structure of pyridinic N-oxides) and ACO$_3$H (the peroxide group in the structure of peracids) are not available by Joback method. The contribution of ANO was back calculated from the Gibbs free energy of formation for pyridine N-oxide, i.e. 87.9 kJmole^{-1} [2]. The number for the ANO group is later used to calculate the Gibbs free energy of formation for quinoline N-oxide. In the same manner, the contribution of ACO$_3$H was back calculated from the structure of peroxy tridecanoic acid [3].

2-2- Studied reactions

The oxidative denitrogenation of quinoline, if being successful, should happen in two steps: In the first step quinoline is converted to the partially oxidized form, i.e. quinoline N-oxide; In the second step, thermal decomposition of this partially oxidized form removes nitrogen as the respective nitrogen oxides. However, the experimental results (presented in chapters 3 and 4) show that, although oxidation of quinoline by perdecanoic acid leads to formation of quinoline N-oxide, the thermal decomposition of this oxide form produces quinoline, a condensed aromatic structure and some gaseous products other than nitrogen oxides. Therefore, the thermodynamics of four reactions are studied in this chapter: one oxidation reaction, one hypothetical denitrogenation reaction and two experimentally observed thermal decomposition reactions.

a) Oxidation of quinoline

As it's earlier discussed in chapter 3, the oxidation of quinoline by perdecanoic acid leads to formation of quinoline N-oxide and decanoic acid, as shown in Figure 5-1.
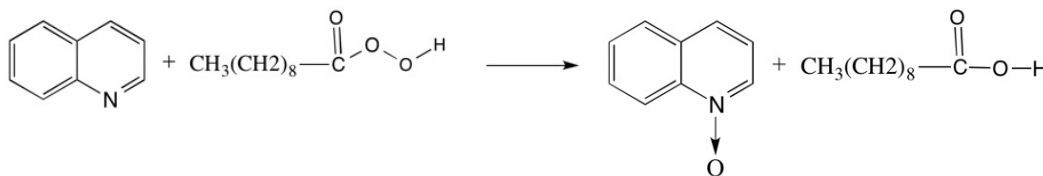

Figure 5-1- Reaction scheme for oxidation of quinoline by perdecanoic acid

b) Hypothetical denitrogenation of quinoline N-oxide

For a successful denitrogenation, the nitrogen-containing aromatic ring of quinoline N-oxide must be opened by thermal decomposition in order to release nitrogen as respective nitrogen oxides. This reaction is shown in

Figure 5-2. Tetralin is added to the reaction scheme in order to balance out the structure of opened aromatic ring.
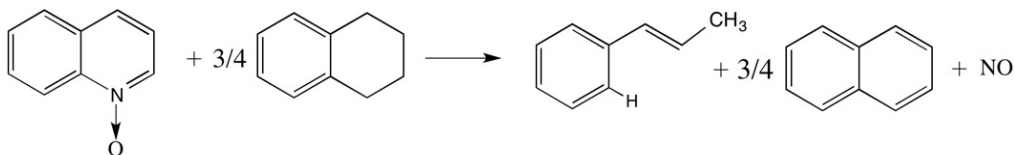

Figure 5-2- Reaction scheme for hypothetical denitrogenation of quinoline N-oxide

c) Deoxygenation of quinoline N-oxide

The results presented in chapter 4 indicate that thermal decomposition of quinoline N-oxide hydrate leads to the formation of quinoline and a condensed aromatic structure. The reaction pathway for deoxygenation of quinoline N-oxide is shown in Figure 5-3.
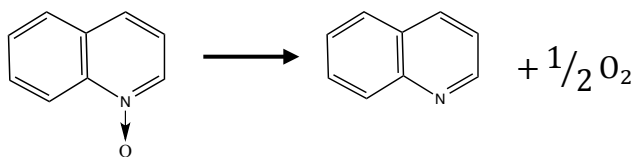
Figure 5-3- Reaction scheme for deoxygenation of quinoline N-oxide

d) Formation of a poly-aromatic structure

The elemental analysis of the produced condensed aromatic structure is earlier presented in Table 4-7. The molar ratios of carbon to hydrogen, carbon to nitrogen and carbon to oxygen is about 1.9, 8.4 and 8.4. This gives a structure close to $C_{17}H_9N_2O_2$. Also, a possible reaction pathway is proposed for the studied thermal decomposition experiments in chapter 4, section 3-2-3. It is stated that thermal decomposition of quinoline N-oxide might result in formation of a nitrene intermediate which could further react with quinoline or quinoline N-oxide to form a condensed aromatic structure. It must be noted that quinoline N-oxide can act as an electrophile as well as a

123

nucleophile, due to the formation of its different resonance structures. Considering this mechanism and also, the elemental analysis results, it is possible to propose a hypothetical structure for the produced poly-aromatic compound. This hypothetical structure and the reaction scheme are shown in Figure 5-4.

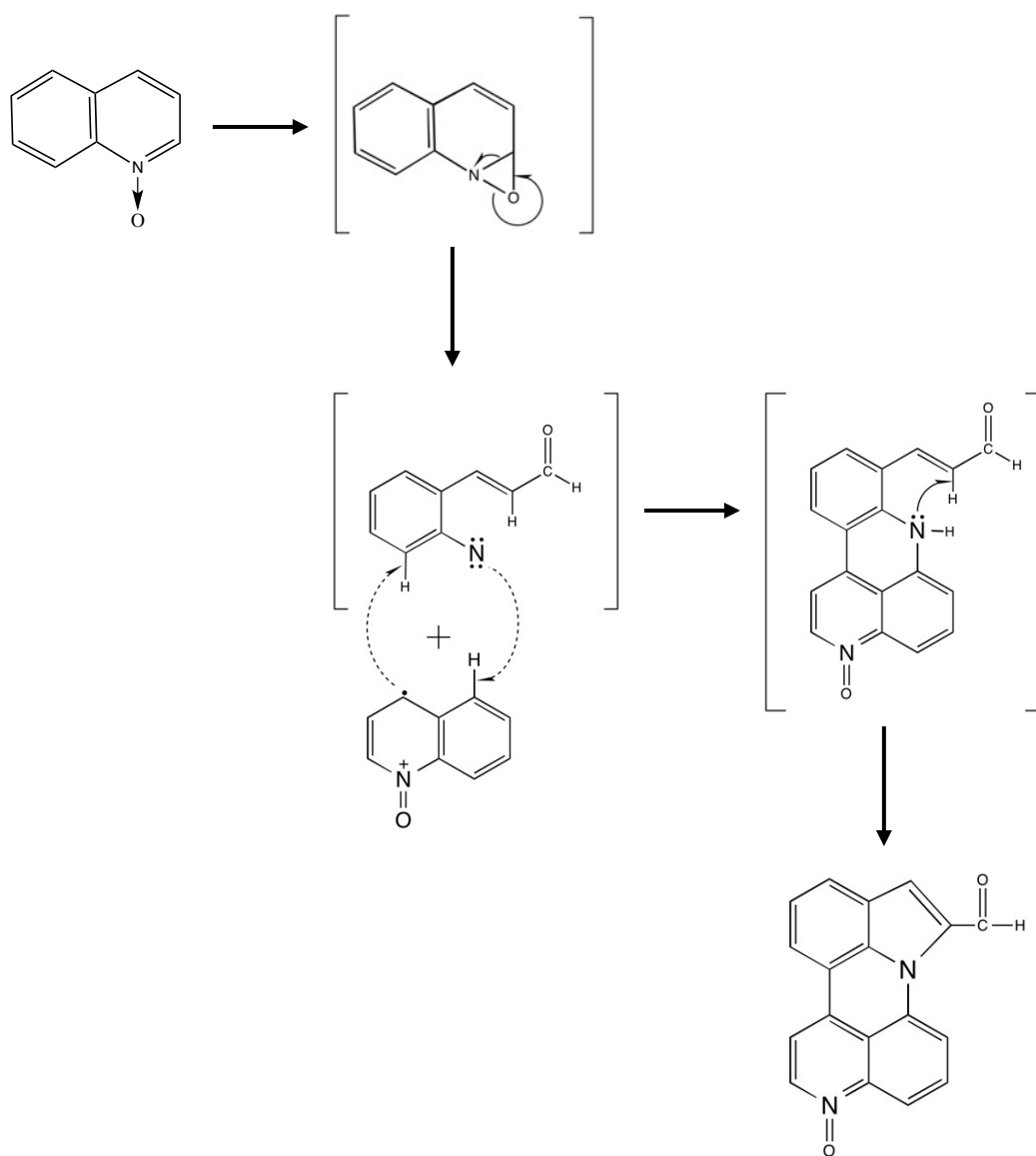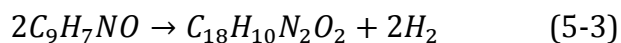**Figure 5-4-** Reaction scheme for condensation of quinoline N-oxide

The reaction pathway shown in Figure 5-4 can be summarized as:

124

$$2C_9H_7NO \rightarrow C_{18}H_{10}N_2O_2 + 2H_2 \qquad (5\text{-}3)$$

In Formula 5-3, the molar ratios of carbon to hydrogen, carbon to nitrogen and carbon to oxygen for the condensed structure is 1.8, 9 and 9 respectively. These numbers are close to what has been measured using elemental analyzer. It is also likely that the H_2 will not be produced as molecular hydrogen, but rather as water through reaction with the oxygen derived from N-oxides.

2-3- Results and discussions

Table 5-2 shows the number of molecular group for all the compounds involved in the reactions presented in section 2-2. Using the Joback method, the Gibbs free energy of formation is calculated for each compound and is compared with data available from VMGSim software database [3] in Table 5-3.

Table 5-2- The number of molecular groups for all the compounds involved in the reactions presented in section 2-2

| Compound | Number of Molecular Groups | | | | | | | | | | |
| | Ring Structures | | | | | Non-ring Structures | | | | | |
	=CH-	=C<	-CH$_2$-	=N-	ANO	-CH$_3$	-CH$_2$-	-CH-	-CH=O	ACO$_2$H	ACO$_3$H
Quinoline	7	2		1							
Quinoline N-oxide	7	2			1						
Perdecanoic Acid						1	8				1
Decanoic acid						1	8			1	
Tetralin	4	2	4								
Naphthalene	8	2									
cis- Propenyl benzene	5	1				1		2			
C$_{18}$H$_{10}$N$_2$O$_2$	9	8		1	1				1		

Table 5-3- Calculated Gibbs free energy of formation for the compounds presented in Table 5-2 using Joback method compared with data from VMG software database [3]

Compound	Joback Method (kJmole^{-1})	VMGSim software (kJmole^{-1})
Quinoline	321.0	293.6
Quinoline N-oxide	218.6	-
Perdecanoic Acid	45.8	14.0
Decanoic acid	-310.6	-305.1
Tetralin	192.5	167.7
Naphthalene	252.4	224.1
Nitric Oxide (NO)	-	53.9
cis- Propenyl benzene	237.2	216.7
$C_{18}H_{10}N_2O_2$	506.4	-

As it can be seen, there are some differences in the calculated numbers compared to available data from VMGSim database. However, in order to have the same type of error for all data, the calculated numbers by Joback method are further used. Using the standard Gibbs free energy of formation for each compound, the Gibbs free energy of the reactions (explained in section 2-2) are calculated and presented in Table 5-4.

Table 5-4- Calculated Gibbs free energy of reaction using data in Table 5-3

Reaction	Gibbs Energy (kJmole^{-1})
a) Oxidation of quinoline	-458.8
b) Hypothetical denitrogenation of quinoline N-oxide	117.4
c) Deoxygenation of quinoline N-oxide	102.4
d) Formation of a poly-aromatic structure	69.2

A few conclusions can be drawn from the data presented in Table 5-4:

1. It is reported that the oxidation of quinoline by perdecanoic acid involves the formation of a quinoline-perdecanoic acid intermediate, which further decomposes to produce quinoline and decanoic acid. The formation of this intermediate is a non-spontaneous reaction which requires high amount of activation energy [4]. In Table 5-4, the overall Gibbs energy of reaction shows that this oxidation is not thermodynamically restricted at room temperatures. However, higher temperatures are required to overcome the activation energy of intermediate formation.

2. Deoxygenation of quinoline N-oxide is a non-spontaneous reaction at standard condition. This explains the stability of quinoline N-oxide at room temperature and also, its deoxygenation upon heating. The reverse reaction, i.e. oxidation of quinoline by oxygen, seems to be a spontaneous reaction at standard condition. However, the inability of oxygen to oxidize quinoline indicates that this reaction is mechanistically unfavoured.

3. Both the condensation and hypothetical denitrogenation reactions are non-spontaneous at standard conditions. However, the lower amount of Gibbs energy for the condensation reaction can explain why it is thermodynamically more favoured at the studied thermal decomposition conditions (400°C, 600 kPa of N_2) compared to the denitrogenation reaction. Also, in case that water (Gibbs free energy of formation= -228.7 kJmole^{-1} [3]) is produced instead of molecular hydrogen, the Gibbs free energy of condensation reaction is a negative number, which makes it a spontaneous reaction at standard condition.

3- References

[1] Poling, B. E.; Prausnitz, J. M.; O'Connell J. P. *The Properties of Gases and Liquids*, 5th ed.; McGraw-Hill: New York, 2001, pp 3-1 – 3-15.

[2] National Institute of Standards and Technology (NIST), http://webbook.nist.gov/cgi/cbook.cgi?ID=C694597&Mask=8 (accessed June 2013)

[3] *VMGSim*, version 7.0; Virtual Materials Group Inc.: Calgary (accessed June 2013)

[4] Dutka, V.S.; Matsyuk, N.V.; Dutka, Yu.V. Influence of a Reaction Medium on the Oxidation of Aromatic Nitrogen-Containing Compounds by Peroxyacids, *Russian Journal of Physical Chemistry A* **2011**, *85*, 45-50.

Chapter 6

Conclusion and Future work

1- Conclusion and Future Work

The oxidative denitrogenation has been evaluated as method to remove the nitrogen from the structure of quinoline (as a model compound representing the pyridinic type of compounds in coal liquids) in 2 steps:

1- Oxidation of quinoline to produce quinoline N-oxide and therefore, decrease the strength of the N-C bond. Synthesized perdecanoic acid was used as the oxidizing agent. 83 mole % of quinoline has been converted to quinoline N-oxide when the reaction was performed at 50 ℃ for 30 minutes. The results were reproducible and the produced quinoline N-oxide was stable while kept in the freezer for 1 week.

2- Thermal decomposition of the partially oxidized nitrogen structure. The commercially available quinoline N-oxide hydrate was heated from room temperature to 400 ℃ under inert environment. At first, this molecule lost its crystallization water in two steps, one in conjugation with melting from 50 ℃ to 70 ℃ and the other one from 70 ℃ to 170 ℃. Thermal decomposition started at temperatures around 270 ℃. The thermal decomposition of quinoline N-oxide at 400 ℃ and 600 kPa of N_2 for 30 minutes produced 52-wt% quinoline, 22-wt% a black nitrogen-containing polymeric compound and 26-wt% gaseous products. The main gaseous products identified were CO_2, CO, O_2, water, CH_4, butane and ethylene. Trace amounts of biquinoline was also present in the acetone-soluble part of the residue. The production of an oxaziridine intermediate is suggested as the initial step in the mechanism of thermal

decomposition. This intermediate partially undergoes deoxygenation to produce oxygen and quinoline, and partially forms a nitrene compound which upon further reaction leads to formation of CO, CO_2, a poly-aromatic structure and also, traces of other organic materials.

Although the oxidation step is able to produce the partially oxidized nitrogen compound, thermal decomposition not only fails to remove the nitrogen from the structure of the oxidized molecule, but it also leads to the production of a more complex aromatic structure with 10-wt% nitrogen content.

This proves that thermal decomposition is not a suitable method for nitrogen removal of the N-oxides of pyridinic type of compounds. However, the oxidation step increases the polarity of the nitrogen compound. Therefore, solvent extraction might be a suitable substitute for the second step to remove the partially oxidized nitrogen compounds from the coal liquid mixture. To test the suitability of this proposed method, different polar solvents should be tried on both model compounds (representing the coal liquid structure) and actual coal liquid mixtures. Also, the oxidation step should be tried on the coal liquids. The following criteria must be considered to evaluate the proposed method in comparison with other available denitrogenation methods:

- The degree of oxidation of nitrogen in nitrogen containing compounds in competition with carbon
- The ability of the solvent in extracting the nitrogen compounds versus other available structures
- The amount of nitrogen removal and the possible methods to increase conversion
- The effect of the whole process on heating value and the composition of coal liquid mixture
- The methods to recover the solvent